USGS
science for a changing world

Prepared in cooperation with the Alaska Division of Geological & Geophysical Surveys

GIS-Based Identification of Areas that have Resource Potential for Critical Minerals in Six Selected Groups of Deposit Types in Alaska

Edited by Susan M. Karl, James V. Jones, III, and Timothy S. Hayes

With contributions from Matthew Granitto, Timothy S. Hayes, James V. Jones, III, Susan M. Karl, Keith A. Labay, Jeffrey L. Mauk, Jeanine M. Schmidt, Nora B. Shew, Erin Todd, Bronwen Wang, Melanie B. Werdon, and Douglas B. Yager

Open-File Report 2016–1191

2016

U.S. Department of the Interior
U.S. Geological Survey

U.S. Department of the Interior
Sally Jewell, Secretary

U.S. Geological Survey
Suzette Kimball, Director

U.S. Geological Survey, Reston, Virginia: 2016

Suggested citation:
Karl, S.M., Jones, J.V., III, and Hayes, T.S., eds., 2016, GIS-based identification of areas that have resource potential for critical minerals in six selected groups of deposit types in Alaska: U.S. Geological Survey Open-File Report 2016–1191, 99 p., 5 appendixes, 12 plates, scale 1:10,500,000, http://dx.doi.org/10.3133/ofr20161191.

ISSN 2331-1258 (online)

COVER:
Mineralized and altered alkaline granitic rocks near the western margin of the Paleocene Tired Pup pluton, in the western Alaska Range. The pluton includes both alkaline and peraluminous granitic rocks of the same age; the alkaline granitic rocks commonly contain fluorite, allanite, monazite, and xenotime, and the peraluminous granitic rocks contain fluorite, tourmaline, molybdenite, and cassiterite. Sediments in adjacent streams contain high levels of rare earth elements, tin, and molybdenum. Photograph by S.M. Karl, 2013.

Contents

Figures

Tables

Plates

[Available online at http://dx.doi.org/10.3133/ofr20161191]

Appendixes

[Available online at http://dx.doi.org/10.3133/ofr20161191]

Conversion Factors

[inch/pound to International System of Units]

Multiply	By	To obtain
	Length	
foot (ft)	0.3048	meter (m)
mile (mi)	1.609	kilometer (km)
	Area	
acre	4,047	square meter (m^2)
acre	0.004047	square kilometer (km^2)
square foot (ft^2)	0.09290	square meter (m^2)
square mile (mi^2)	2.590	square kilometer (km^2)
	Mass	
ounce, avoirdupois (oz)	28.35	gram (g)
pound, avoirdupois (lb)	0.4536	kilogram (kg)
ton, short (2,000 lb)	0.9072	megagram (Mg)
ton, long (2,240 lb)	1.016	megagram (Mg)
ton, short (2,000 lb)	0.9072	metric ton (t)
ton, long (2,240 lb)	1.016	metric ton (t)

Abbreviations

ADGGS	Alaska Division of Geological & Geophysical Surveys
AGDB2	Alaska Geochemical Database, Version 2.0
AM	analytical method
AMRAP	Alaska Mineral Resource Assessment Program
ANK	molar Al/[Na+K]
ARDF	Alaska Resource Data File
ASI	aluminum saturation index
eK	equivalent potassium
ES_SQ	semiquantitative emission spectroscopy
eTh	equivalent thorium
eU	equivalent uranium
GIS	geographic information system
g/t	grams per metric ton
ICP-MS	inductively coupled plasma mass spectrometry
HFSE	high field strength elements
HMC	heavy-mineral concentrate
HREE	heavy rare earth elements
HUC	hydrologic unit code
LREE	light rare earth elements
MALI	modified alkali-lime index
Mt	million metric tons
MUM	mafic to ultramafic
NHD	National Hydrography Dataset
NURE	National Uranium Resource Evaluation
NURE-HSSR	NURE-Hydrogeochemical and Stream Sediment Reconnaissance
pct	weight percent
PGE	platinum group elements
ppm	parts per million
REE	rare earth elements
sedex	sedimentary exhalative
ssU	sandstone-hosted uranium
USGS	U.S. Geological Survey
WBD	Watershed Boundary Dataset
XRF	x-ray fluorescence

GIS-Based Identification of Areas that have Resource Potential for Critical Minerals in Six Selected Deposit Groups in Alaska

By Susan M. Karl,[1] James V. Jones, III,[1] and Timothy S. Hayes,[1] editors

With contributions from Matthew Granitto,[1] Timothy S. Hayes,[1] James V. Jones, III,[1] Susan M. Karl,[1] Keith A. Labay,[1] Jeffrey L. Mauk,[1] Jeanine M. Schmidt,[1] Nora B. Shew,[1] Erin Todd,[1] Bronwen Wang,[1] Melanie B. Werdon,[2] and Douglas B. Yager[1]

Abstract

Alaska has considerable potential for undiscovered critical mineral resources. Critical minerals are those for which the United States imports more than half of its total supply and which are largely derived from nations that cannot be considered reliable trading partners. In this report, estimated mineral resource *potential* and *certainty* for the state of Alaska are analyzed and mapped for the following six selected groups of mineral deposit types that may each contain one or more critical minerals: (1) rare earth element (REE) deposits with or without thorium (Th), yttrium (Y), niobium (Nb), uranium (U), and zirconium (Zr), associated with peralkaline to carbonatitic intrusive rocks; (2) placer and paleoplacer gold (Au) deposits that in some places might also produce platinum group elements (PGE), chromium (Cr), tin (Sn), tungsten (W), silver (Ag), or titanium (Ti); (3) platinum group element (PGE) deposits with or without cobalt (Co), chromium (Cr), nickel (Ni), titanium (Ti), and vanadium (V), associated with mafic to ultramafic intrusive rocks; (4) carbonate-hosted copper (Cu) deposits with Ag, and possibly cobalt (Co), germanium (Ge), and gallium (Ga); (5) sandstone-hosted uranium (U) deposits that in some deposits might also produce V or Cu; and (6) tin (Sn)-tungsten (W)-molybdenum (Mo) deposits, possibly with indium (In), and (or) fluorspar associated with specialized granites.

This study used a data-driven, geographic information system (GIS)-implemented method to identify areas with mineral resource potential in Alaska. This method systematically and simultaneously analyzes geoscience data from multiple geospatially referenced datasets and uses individual subwatersheds (12-digit hydrologic units [or HUCs]) as the spatial unit of classification. The final map output uses a red, yellow, and green color scheme to portray estimated relative *potential* (High, Medium, Low, Unknown [shown in gray]) for each of the six groups of mineral deposit types, and it indicates the *certainty* (High, Medium, Low,) of that estimate for any given HUC using dark, medium, and light shades of those colors, respectively. Accompanying tables describe the data layers employed to the score favorability for the presence of each mineral deposit group, the values assigned for specific analysis parameters, and the relative weighting of each data layer that contributes to estimated measures of *potential* and *certainty*. Core datasets used include the Alaska Geochemical Database, Version 2.0 (AGDB2), the Alaska Division of Geological & Geophysical Surveys (ADGGS) web-based geochemical database, the digital "Geologic Map of Alaska" (Wilson and others, 2015), and the Alaska

[1] U.S. Geological Survey
[2] Alaska Division of Geological & Geophysical Surveys

Resource Data File (ARDF). Maps accompanying this report illustrate the scores for estimated mineral resource potential for the six deposit groups on a statewide basis.

Numerous areas in Alaska, some of them large, have high potential for one or more of the selected groups of deposit types within Alaska; selected examples of areas with high potential for critical minerals are described in the following paragraphs.

Areas in Alaska that have noteworthy potential for associated REE deposits include the Darby-Hogatza igneous belt and parts of the Ruby batholith in the Kokrines-Hodzana belt. Other areas that have high potential for REE deposits include the area surrounding a known carbonatite occurrence near Tofty in the Hot Springs placer district, the Roy Creek area in east-central Alaska, and the Bokan Mountain to Dora Bay area in the southern part of southeastern Alaska. REE prospects at Bokan Mountain may have the greatest immediate potential for development of an REE resource in the state.

Placer gold potential is relatively high in many drainages widely scattered across the state. Prospecting for, and production from, placer gold deposits such as the Fairbanks, Circle, and Fortymile districts in east-central Alaska, the Aniak and Innoko districts in southwestern Alaska, the Nome district on the Seward Peninsula, and the Valdez Creek district in south-central Alaska, were significant in the past, and continue at a reduced level in the present. The western part of the Alaska Range might have additional untested and undeveloped placer gold potential.

Areas that have high potential for PGE deposits associated with mafic to ultramafic intrusive rocks include the Angayucham terrane in the northwestern and south-central Brooks Range, the Goodnews Bay area of southwestern Alaska; the Border Ranges belt in south-central Alaska, and the belt that includes Klukwan to Duke Island in southeastern Alaska. The areas most deserving of additional investigation appear to be on the north flank of the central Brooks Range.

Discrete belts that have high potential for carbonate-hosted copper deposits include the northeastern Brooks Range, the northern foreland of the Brooks Range, the Cosmos and Jade Hills areas, the central Brooks Range, the central Seward Peninsula, and the Kennecott district in the Wrangell Mountains in south-central Alaska. Prospects in the northeastern Brooks Range are within the Arctic National Wildlife Refuge where prospecting and development are prohibited, but areas in east-central Alaska and on the north flank of the Alaska Range are worthy of additional investigation to potentially distinguish them as basalt- or hydrothermal-related Cu deposits rather than Cu-skarn deposits.

Areas that have the highest potential for sandstone-hosted uranium potential are widely scattered across the state. Sandstone-hosted uranium in Alaska is mostly associated with areas proximal to felsic plutonic complexes, such as the Death Valley deposit adjacent to the Darby pluton on the eastern Seward Peninsula. Other areas in Alaska that show high potential for sandstone-hosted uranium deposits tend to be located in areas that also have potential for REE deposits associated with alkaline igneous rocks, such as in the Darby-Hogatza and Kokrines-Hodzana belts in central Alaska, and felsic plutons in the western Alaska Range.

In addition to the known tin province in the Lost River–Kougarok belt of intrusive rocks on the Seward Peninsula, areas that have high potential for tin-tungsten-molybdenum-tantalum-indium-fluorspar deposits associated with ‘specialized’ granites also are widely scattered across Alaska. The main additional areas recognized for tin-tungsten and molybdenum potential include the central and northeastern Brooks Range, the Porcupine area southeast of the Brooks Range, the Hogatza and Kokrines-Hodzana intrusive belts that rim the Yukon-Koyukuk basin in central Alaska, the White Mountains and Yukon-Tanana uplands area in east-central Alaska, and the Coast Mountains, which include Groundhog Basin (Sn) and Quartz Hill (Mo) in southeastern Alaska. Felsic intrusive rocks in the western Alaska Range appear to have greater tin and molybdenum potential than has previously been recognized. Few areas in the United States have greater potential than Alaska for tin, tungsten, and molybdenum deposits, with or without indium and fluorspar, in association with specialized, highly fractionated granitic intrusions.

Introduction

Purpose and Scope

The Alaska Division of Geological & Geophysical Surveys (ADGGS) and the U.S. Geological Survey (USGS) collaborated to identify areas in Alaska that have mineral resource potential for six selected groups of critical-mineral-containing deposit types. As defined here, critical minerals are those classified as a strategic and critical material by the Strategic Materials Protection Board of the U.S. Department of Defense because they are used in products that are vital to national security (National Research Council, 2008), as well as those mineral commodities for which the United States imports more than half of its total supply and which are largely derived from nations that cannot be considered reliable trading partners (U.S. Department of Energy, 2010). Using these criteria, the following list of commodities were considered for this study: antimony (Sb); barite or barium (Ba); beryllium (Be); cobalt (Co); fluorite or fluorine (F); germanium (Ge) and its elemental associate, indium (In); gallium (Ga); graphite; lithium (Li); manganese (Mn); niobium (Nb) and its elemental associate, tantalum (Ta); the six platinum group elements (PGEs); the fifteen rare earth elements (REEs); rhenium (Re); selenium (Se); tellurium (Te); tin (Sn); titanium (Ti); tungsten (W); vanadium (V); and zirconium (Zr) and its elemental associate hafnium (Hf).

The work here attempts to identify areas that have geologic potential for selected types of as-yet-undiscovered critical mineral resources in Alaska. It is not a comprehensive review of known mines, prospects, occurrences, or mineral deposit types that are found in the state. Instead, it is an evaluation of where in Alaska mineral deposits within several specific deposit groups might be found on the basis of geoscientific data and (or) features such as geology (for example, lithology, mineralogy, known prospects), geochemistry (of rock and stream sediment samples), and (or) geophysical properties.

For this study, mineral "deposits" are localities that have reported inventory or past production, whereas mineral "prospects" and "occurrences" describe localities where minerals of the commodity are known but have no reported inventory. Mineral deposit "types" are recognized styles of mineralization described in published deposit models, and mineral deposit "groups" contain two or more mineral deposit types that have similar commodities that occur in broadly similar geological settings. For example, this report's platinum group element (PGE) deposit group contains no fewer than 20 deposit types; however, only four main deposit types in which PGEs are spatially associated with mafic to ultramafic intrusive rocks worldwide (table 1) are addressed here. These four types are expanded to nine variations (table 6), which are judged to have the greatest probability to contain concentrations of PGE in Alaska.

The six groups of mineral deposit types that are considered in this study (table 1) are (1) rare earth elements-thorium-yttrium-niobium(-uranium-zirconium) [REE-Th-Y-Nb(-U-Zr)] deposits associated with peralkaline to carbonatitic igneous intrusive rocks; (2) placer and paleoplacer gold (Au) deposits that in some places might also produce platinum group elements (PGE), chromium (Cr), tin (Sn), tungsten (W), silver (Ag), or titanium (Ti); (3) platinum group elements(-cobalt-chromium-nickel-titanium-vanadium) [PGE(-Co-Cr-Ni-Ti-V)] deposits associated with mafic to ultramafic intrusive rocks; (4) carbonate-hosted copper(-cobalt-silver-germanium-gallium) [Cu(-Co-Ag-Ge-Ga)] deposits; (5) sandstone-hosted uranium(-vanadium-copper) [U(-V-Cu)] deposits; and (6) tin-tungsten-molybdenum(-tantalum-indium-fluorspar) [Sn-W-Mo(-Ta-In-fluorspar)] deposits associated with specialized granites.

The study is not a three-part probabilistic mineral resource potential assessment (Singer, 1993, 2007; Singer and Menzie, 2010), as has been conducted by the USGS for many areas in recent years (for example, Zientek and others, 2014). Instead, the work here identifies areas that have potential for each of the six deposit groups, with the objective of identifying areas (on the basis of available data) that have resource potential and that might not have been recognized previously. The boundaries of the evaluated

areas are the boundaries of subwatersheds (identified by 12-digit hydrologic unit codes [HUCs]), for each of which scores from geology, geochemistry, mineralogy, geophysics, and mineral occurrences are summed. A geographic information system (GIS) analysis was then used to systematically and simultaneously consider disparate types of geological, mineralogical, geochemical, mineral occurrence, and geophysical data as tools for prospectivity mapping for these six deposit groups across the state.

In this GIS process, key quantifiable characteristics of the six deposit groups were identified in available datasets and scored in terms of importance for indicating potential for resource occurrence. Herein, and in agreement with previous workers (Goudarzi, 1984; Taylor and Steven, 1983), "potential mineral resource" is defined as the potential for the occurrence of a concentration of a mineral resource, and it does not imply potential for economically viable development or extraction of the mineral resource. This study separates four levels of mineral resource potential, qualified by certainty of the analysis based on the presence and abundance of favorable attributes for each deposit group. The product of the analysis is a map for each deposit group that indicates the relative level (High, Medium, Low, Unknown) of *potential*, as well as the relative level (High, Medium, Low) of *certainty*, of the specific deposit group for all of the subwatersheds (as indicated by 12-digit HUCs) within Alaska (plates 1–12; see discussion below regarding 12-digit HUCs).

In this GIS analysis, a data scoring and ranking process was tailored to critical parameters for each of the six deposit groups. Associated tables indicate which datasets were used in the analysis for each deposit group, which parameters in the datasets were queried, and the amount that each parameter contributed to the estimate of deposit group prospectivity in each HUC (tables 2–14). Data tables (appendixes A, C, D), additional data sources (appendix B), and geospatial data file sources (see Data Resources section) provide the scoring results (appendix E) for each deposit group, and they permit the user to analyze and query the findings in a spatial context on each of the final digital map products.

In accordance with previous work (Goudarzi, 1984; Taylor and Steven, 1983) and also as defined below, the four levels (High, Medium, Low, Unknown) of resource *potential* are assigned in our analyses as follows:

(1) High mineral resource *potential* is assigned to areas where geological, mineralogical, geochemical, mineral occurrence, and geophysical characteristics indicate a geologic environment that is favorable for resource occurrence, where interpretations of data indicate a high degree of likelihood for resource accumulation, where data indicating presence of resources support mineral deposit models, and where evidence indicates that mineral concentration has taken place. Resources or deposits need not be identified for an area to be assigned high resource potential.

(2) Medium mineral resource *potential* is assigned to areas where geological, mineralogical, geochemical, mineral occurrence, and geophysical characteristics indicate a geologic environment that is favorable for resource occurrence, where interpretations of data indicate a reasonable likelihood of resource accumulation, and where an application of mineral deposit models indicates favorable ground for concentration of the specified type(s) of minerals.

(3) Low mineral resource *potential* is assigned to areas where geological, mineralogical, geochemical, mineral occurrence, and geophysical characteristics indicate a geologic environment in which the existence of the specific resource is unlikely.

(4) Unknown mineral resource *potential* is assigned where information is inadequate to assign low, medium, or high levels of resource potential to the area.

In accordance with previous work (Goudarzi, 1984; Taylor and Steven, 1983), the three levels (High, Medium, Low) of *certainty* are assigned herein as follows:

(1) High *certainty* is assigned to areas for which available information from multiple sources provides a robust indication of the level of mineral resource *potential*.

(2) Medium *certainty* is assigned to areas for which available information is sufficient to give a reasonable indication of the level of mineral resource *potential*.

(3) Low *certainty* is assigned to areas for which available information is limited and only suggests a level of mineral resource *potential*.

For the GIS analyses in this report, *certainty* for each HUC is quantified by the number of geoscientific data layers that contribute to the resource *potential* score of that HUC (see tables 3, 5, 7, 9, 11, 13). There is no certainty assignment for areas of unknown potential because unknown potential is based on a lack of data, and no certainty can be assigned to an absence of data.

The methods used here can be applied to other groups of deposit types. Some appropriate publicly available digital datasets can contain information to apply attributes to most deposit groups, although available data may not be adequate to discriminate between all deposit types within a deposit group. The limitation to evaluation of deposit groups arises because the reconnaissance level of regional-scale geologic mapping and geochemical and geophysical data collection typically provide insufficient detail to target specific deposit types within a group of related deposits. The groups of deposit types selected here were chosen with principal attention to their association with specific critical minerals. For this reason, some of the economically most important deposit types in Alaska, including sedimentary exhalative zinc-lead-silver-barite deposits such as Red Dog and porphyry copper-gold deposits such as Pebble, were not addressed in this report, but they are candidates for future GIS analysis. Also, this type of GIS analysis could alternatively be applied to a different areal unit of evaluation such as a square-mile grid. However, data density that is sufficient to evaluate by a square-mile grid is rarely available outside of private exploration companies and is typically available only for selected, relatively small, areas of interest, which could bias certain areas in a regional analysis.

Deposit-Group Characteristics

The six deposit groups evaluated in this study and summarized below do not include all of the mineral deposit types that are known, or are likely, to occur in Alaska. They were selected because they both contain one or more strategic and critical elements (National Research Council, 2008) and are known to occur in the state. Principal characteristics of the six deposit groups, their major and associated commodities, premier examples worldwide and in Alaska, and key references are summarized in table 1.

REE-Th-Y-Nb(-U-Zr) Deposits Associated with Peralkaline to Carbonatitic Intrusive Rocks

Economic deposits of REE and related high field strength elements (HFSE) worldwide are primarily associated with carbonatitic and peralkaline igneous rocks and their weathering products (Pollard, 1995; Richardson and Birkett, 1996; Long and others, 2010; Verplanck and others, 2014). Carbonatites are particularly REE-enriched (Notholt and others, 1990; Rankin, 2005), although they are rare among igneous rocks worldwide. The petrogenesis of carbonatitic magmas is unclear, but these igneous rocks are mainly found as intrusive dikes or complexes in stable cratonic environments (Bell, 1989); in addition, they are spatially associated with prominent structural features and are likely derived from sublithospheric mantle (Yuan and others, 1992; Bell and Simonetti, 2010). Peralkaline intrusive complexes are typically derived from fractional crystallization of alkaline, silica-undersaturated magmas derived from low-degree partial melts of mantle material in rift or within-plate settings (Eby, 1990: Frost and Frost, 2011). Most carbonatite-associated deposits are light REE (LREE; lanthanum to europium, atomic numbers 57 through 63) enriched. REE (±HFSE) deposits associated with peralkaline intrusive complexes are rarely as LREE-enriched as carbonatites, and they are commonly more enriched in heavy REE (HREE; gadolinium to lutetium, atomic numbers 64 through 71) relative to LREE. Economic concentrations of REE (±HFSE) form in alkaline and carbonatitic magmas derived from partial melting of metasomatized mantle; initial enrichments of these incompatible elements are further enriched by fractional crystallization of the magmas (Pilet and others, 2008; Bell and Simonetti, 2010; Verplanck and others, 2014). Although alkaline igneous REE (±HFSE) mineralization may result from primary igneous processes or reflect precipitation from late-stage orthomagmatic fluids, the effects of late-stage

hydrothermal alteration may make it difficult to distinguish between the two processes. Globally, the two REE mines that have the largest production are Mountain Pass, California (Castor, 2008), and Bayan Obo, China (Yang and others, 2011), both of which are associated with carbonatite. Bastnäesite [hexagonal $(Y,REE)CO_3(F,OH)$], the main ore mineral at each deposit (Le Bas and others, 1992; Castor, 2008), and may reflect hydrothermal processes associated with the carbonatite at both deposits (Chao and others, 1997; Castor, 2008). REE ore minerals in carbonatite-associated deposits are either fluorocarbonates, including bastnäesite, synchysite [orthorhombic $Ca(REE,Y)(CO_3)_2F$], and parisite [rhombohedral $Ca(REE)_2(CO_3)_3F_2$], or phosphate minerals such as monazite [monoclinic $(Th,REE)PO_4$] and xenotime [tetragonal $(Y,REE)PO_4$] (Lottermoser, 1990; Long and others, 2010). Rarely, hydrated carbonates, including ancylite [orthorhombic $Sr(Ce,La)(CO_3)_2(OH)\cdot H_2O$], are principal REE carriers in carbonatite-associated deposits (for example, Dahlberg, 2014). In higher temperature, less silica-undersaturated systems, including those associated with peralkaline granite, the REE minerals are mainly oxides such as fergusonite [tetragonal $(REE,Y)(Nb,Ti)O_4$] and silicates, including allanite [monoclinic $(Ca, REE)_2(Al,Fe)_3(SiO_4)_3(OH)$] (Sheard and others, 2012). REE-hosting minerals associated with syenitic to ultra-alkaline and carbonatitic rocks (for example, aeschynite [orthorhombic $(Ca,Ce,Nd,Fe,Th)(Ti,Nb)_2(O,OH)_6$], pyrochlore [isometric $(Na,Ca)2Nb_2O_5(OH,F)$], fergusonite [tetragonal $(Ce,Nd, La, Y)(Nb,Ti)O_4$], and loparite [tetragonal or orthorhombic $(Ce,Na,Ca)(Nb,Ti)O_3$]; Long and others, 2010) commonly contain Nb, Th, and Y. Other REE-hosting minerals associated with peralkaline granite and syenite (for example, brannerite [monoclinic $(U,Ca,Y,Ce)(Ti,Fe)_2O_6$] and betafite [isometric $(Ca,U)_2(Ti,Nb,Ta)_2O_6(OH)$]) also commonly contain HFSE (Sheard and others, 2012). Uranium may occur in oxides (for example, samarskite [orthorhombic $(Y,Ce,U,Fe)_3(Nb,Ta,Ti)_5O_{16}$]), with or without Nb, REE, Y, Th, or Ta, in these deposits. Zirconium occurs in igneous and (or) hydrothermal zircon (tetragonal $ZrSiO_4$) and eudialyte [rhombohedral $Na_{16}Ca_6Fe_3Zr_3(Si_3O_9)(Si_9O_{27})_2(OH,Cl)$] (Verplanck and others, 2014).

REE-bearing minerals can be concentrated in placer deposits as a result of mechanical weathering, and they also can accumulate in clays (for example, Fe- and Al-oxyhydroxides in lateritic soils) as a result of chemical weathering of peralkaline and carbonatitic igneous rocks in tropical and subtropical settings (Mariano, 1989). Although climatic conditions in Alaska are not generally conducive to formation of laterites by chemical weathering, supergene enrichment of uranium is documented at Death Valley on the Seward Peninsula (see chapter 5, this report, on sandstone-hosted U). Our focus is on the association of REE (±HFSE) with igneous rocks, as the primary resource for REE and the source of REE-bearing minerals in placer and chemical-weathering deposits. Alaska currently contains one significant REE deposit, which is associated with the Jurassic Bokan Mountain peralkaline granite on Prince of Wales Island (fig. 1; plate 2). The Bokan Mountain deposit includes a 5.2-Mt inferred resource that contains 0.548 percent total REE (Bentzen and others, 2013) in a band of structurally controlled, pegmatitic to aplitic veins and dikes that extends northwestward and southeastward for about 3 km from the pluton.

Placer and Paleoplacer Gold (Au) Deposits

Placer deposits are concentrations of high-density minerals formed by gravitational sorting during sedimentary processes. Heavy minerals are liberated from their primary host rocks during weathering and erosion and then transported and concentrated in surficial deposits. Placer deposits exhibit a wide range of textures, form in many different environments, and host a variety of minerals, including gold, titanium, tin, PGE, REE, and iron (Slingerland and Smith, 1986; Garnett and Bassett, 2005). Gold in placer deposits was initially derived from bedrock that contains gold-quartz veins, disseminated gold, or other gold-bearing mineral deposits such as porphyry Cu, Cu-skarn, and polymetallic-replacement deposits (Yeend, 1986). Primary gold-bearing deposits typically occur in igneous (Baker, 2002; Seedorff and others, 2005; Hart, 2007; Sinclair, 2007; Taylor, 2007) or

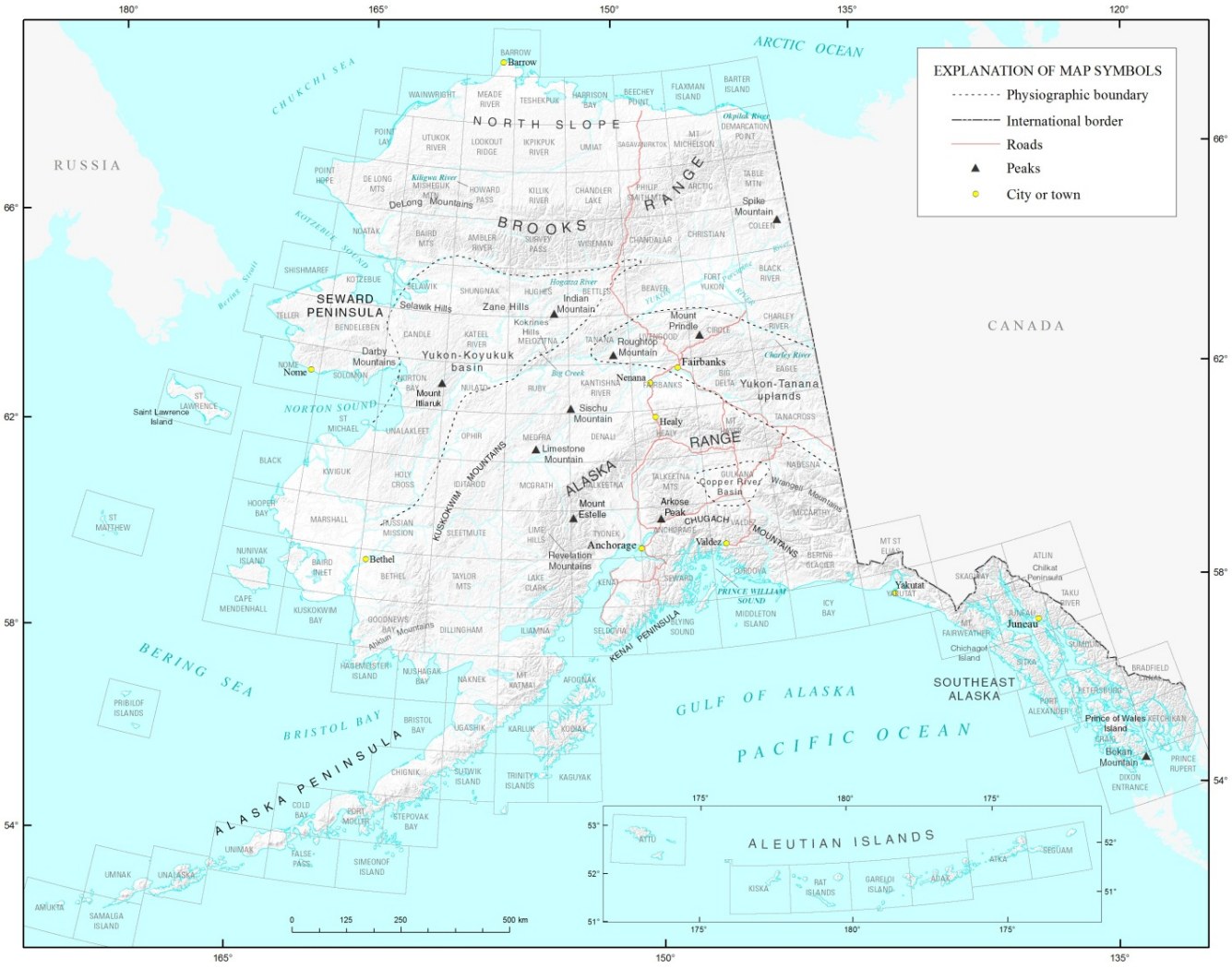

Figure 1. Physiographic map of Alaska, showing 1:250,000-scale quadrangles in Alaska and locations mentioned in text.

metamorphic rocks (Berger and Henley, 1989; Groves and others, 1998; Goldfarb and others, 2005), although occurrences in sedimentary deposits such as paleoplacers and modified paleoplacers (Pretorius, 1981; Minter, 2006) are also documented.

Alluvial placer deposits, which form in rivers and streams, represent the initial concentration of heavy minerals relative to source rocks within a drainage network. Heavy-mineral deposition and concentration occurs where gradients flatten or diminish and (or) where transport velocities decrease; these depositional regimes form at the inside of meanders, below rapids and falls, beneath boulders, and in vegetation mats (Yeend, 1986). Placer gold deposits typically form in alluvial gravel and conglomerate. Gold grains and, more rarely, nuggets are mostly concentrated at the base of gravel deposits where natural traps such as riffles, fractures, bedding planes, or other features are oriented transverse to water flow. Additional ore-mineral concentration can take place as sediment moves downstream and as older alluvial deposits are reworked by younger systems. Sediment reworking is most likely to occur in geomorphically stable areas where multiple generations of sediment and (or) sedimentary rocks were recycled into potentially multiple stages of terrace and streambed gravels (Yeend, 1986) during protracted erosional episodes.

Coastal placer and paleoplacer deposits, mainly beach placers, form in a variety of coastal sedimentary environments that are typically dominated by eolian, wave, and tidal processes (Hamilton, 1995). Heavy minerals in coastal environments are derived from sources that could include deeply weathered local bedrock exposures, sediment deposited at river deltas, or offshore sand bars or deposits scoured from the seafloor during storm events. Along wave-dominated coastlines, heavy-mineral enrichment develops in the foreshore and the uppermost part of the shoreface environment where sediment is repeatedly reworked by wind, waves, and wave-induced currents. Strong onshore winds winnow shoreface deposits at low tide and ultimately transport sediment inland from the beach environment (Roy, 1999). Shore-parallel transport currents (or littoral drift) move sand along the coast in the direction of prevailing winds, and headlands that protrude from drift-aligned coasts trap heavy minerals on the up-drift side of embayments. Most large coastal placer deposits formed at lower latitudes along passive tectonic margins that have long erosional histories and repeated cycles of sea-level change worldwide (Force, 1991). Although Alaska's western and northern coasts, examples of high-latitude passive margins, are known to host major placer deposits, such as those offshore of Nome (fig. 1; see also Kaufman and Hopkins, 1989; Dashevsky, 2002), the more extreme ocean and climate conditions at higher latitudes usually result in strongly erosional coastlines (Harper, 1990), which are generally less favorable for placer development than are passive-margin settings at lower latitudes. Alaska's southern and southeastern coasts are located along convergent and transform tectonic margins; coastal placer deposits formed along these types of margins are generally much smaller than passive-margin deposits and are dominated by sediment derived from relatively local sources.

PGE(-Co-Cr-Ni-Ti-V) Deposits Associated with Mafic to Ultramafic Intrusive Rocks

Platinum group elements (PGE) are found as primary, coproduct, and byproduct commodities in a wide variety of ore-deposit types. These deposits often are associated with mafic to ultramafic (MUM) intrusive and extrusive igneous rocks, but they also occur in volcanic and plutonic rocks that have other compositions, as well as in sedimentary rocks and concentrated in residual and placer deposits. Deposits may form in magmatic, hydrothermal, or sedimentary environments, or they can reflect secondary weathering or mechanical-transport processes. Because magmatic deposits associated with MUM intrusive igneous rocks contain nearly all of the world's currently economic PGE deposits, we focused on these deposit types (table 1; see also Naldrett, 2004).

The petrogenesis of MUM intrusive igneous rocks reflects a variety of physical and chemical processes, as well as specific combinations of events that occurred as the associated magmas were generated, rose, and crystallized under conditions favorable for PGE-deposit formation. Mafic to ultramafic magmas originate at various depths in the upper mantle, which contains minor quantities of sulfur, PGE, copper, nickel, and other metals (Eckstrand and Hulbert, 2007). High degrees of mantle partial melting favor more complete melting of sulfide minerals and incorporation of the contained metals as dissolved melt components. As mantle-derived silicate magmas, which are initially sulfur undersaturated, are transported to upper crustal levels along translithospheric faults, they may reside in multiple magma chambers and evolve at various levels in the crust before reaching and crystallizing at upper crustal levels. Concentrating the sulfur content of residual MUM magma and attaining sulfur saturation under optimal conditions are critical to PGE-ore-forming processes. Sulfur solubility in mafic magmas is affected by changes in magma bulk composition, sulfur and oxygen fugacities, temperature, and pressure (Zientek, 2012). Sulfur solubility increases during adiabatic ascent and depressurization during magma ascent through the crust (Mavrogenes and O'Neill, 1999); sulfur concentrations also generally increase as magmas change composition during crystallization. Once magmas become sulfur saturated, they can exsolve an immiscible sulfide liquid. Processes that affect the solubility of sulfur and that may trigger exsolution include fractional crystallization, magma mixing, assimilation of sulfur from sources external to the magma, and modification of magma composition by bulk assimilation (Zientek,

2012). Formation of economic PGE deposits is favored by MUM silicate melt reaching sulfide saturation after contained metal concentration; subsequently immiscible sulfide melt exsolves and segregates as sulfide-liquid droplets contained in the MUM silicate magma. Once droplets of immiscible sulfide liquid form, dissolved copper, nickel, and PGE are strongly partitioned into the sulfide liquid (Naldrett and Barnes, 1986; Zientek, 2012). Magmatic PGE deposits represent accumulations of metallic oxide crystals or immiscible sulfide or oxide liquids that formed during cooling and crystallization of silicate magma (Zientek, 2012). Economic-deposit formation requires initially high PGE contents in mantle melts (owing to high degrees of mantle partial melting) or processes that increase the concentrations of metal-bearing sulfide-melt droplets. PGE concentrations can be further enhanced when sulfide droplets coalesce during segregation processes (such as gravitational settling), by continued magma flow and recharge that introduces additional metals and sulfide melt, and (or) by flow restriction (velocity decreases) in lateral or vertical conduits (feeder zones) or where feeder zones intersect magma chambers.

PGE, sulfides, and oxides (usually chromite) form thin but laterally extensive, concordant horizons in layered MUM intrusions where they have crystallized as part of the cumulate mineral assemblage. These mineral segregations also form discordant bodies, which may reflect a coeval crystallizing magma chamber, a separate magma pulse that crosscuts earlier MUM intrusions, or discordant intrusions that served as conduits or feeder zones that supplied magma to a large MUM magma reservoir. PGE and sulfides can also form disseminated to massive ore concentrations near intrusion margins or adjacent country rocks, and some are preferentially localized along contacts with country rocks enriched in sulfur-, iron-, or CO_2-bearing rocks (Zientek, 2012). Disseminated textures originate from the capture of sulfide droplets suspended in silicate magma as it crystallized. Net-textured and massive sulfide accumulations form where sulfides segregated and coalesced more completely. Brecciated textures reflect structurally disrupted zones or conduits that intersected magma reservoirs. Worldwide, MUM rocks associated with PGE deposits form in a variety of tectonic settings. Begg and others (2010) related Ni-Cu-PGE deposits and their associated MUM rocks to areas of thin lithosphere along craton margins during periods of active regional tectonism where translithospheric faults focused melt transport through the crust. Other tectonic settings conducive to PGE deposit formation include intracratonic rifting with attendant mantle upwelling (Miller and others, 2002), island arcs (Tolstykh and others, 2004), and ophiolites (Economou and Naldrett, 1984). Alaska contains several tectonic settings favorable for hosting PGE(-Co-Cr-Cu-Ni-Ti-V) deposits; these include continental-margin and accreted island-arc and ophiolite terranes adjacent to the North American craton (Jones and others, 1987; Monger and Berg, 1987).

Carbonate-Hosted Cu(-Co-Ag-Ge-Ga) Deposits

Carbonate-hosted Cu deposits in Alaska consist of Kennecott- and Kipushi-subtypes (Cox and Singer, 1986, p. 130 and 227, respectively). These deposits typically contain some silver (Ag); in particular, the Kipushi-type deposits may contain three critical elements, Co, Ge, and Ga.

Kennecott-type carbonate-hosted Cu deposits, in the Wrangell Mountains (fig. 1), were mined from 1907 to 1938. The deposits and many related occurrences are currently within Wrangell-St. Elias National Park and Preserve. These deposits are northeast-striking, very high grade (production ore grade averaged 13 percent Cu) replacement veins along faults that cut the Triassic Chitistone Limestone. Wallrock replacement by copper sulfide minerals and broad dolomitic alteration envelopes characterize these deposits. The footwall(?) veins have distinctive triangular cross sections; their bases are bedding-parallel and also along probable bedding-plane faults about 25 m above the contact between the Chitistone Limestone and the underlying Nikolai Greenstone. Silver (production ore grade averaged 65 g/t) was recovered, as well as Cu (MacKevett and others, 1997; Price and others, 2014).

The Ruby Creek deposit, south of the western Brooks Range (fig. 1), is an Alaskan example of Kipushi-type copper deposits in carbonate rocks. Kipushi-type deposits are massive base-metal-sulfide replacement bodies or breccia fillings in carbonate rocks, now dolomitized. They range from nearly concordant with carbonate layering to highly discordant. Deposits classified as Kipushi-type (Cox and Singer, 1986) include Ge-bearing minerals, which distinguishes them from other base-metal-sulfide ores in carbonate rocks such as the Central Colorado carbonate-hosted sulfide deposits (Beaty and others, 1990). The Ruby Creek deposit is hosted by Silurian to Devonian carbonate rocks of the Cosmos Hills sequence (Till and others, 2008). Chalcopyrite, bornite, and chalcocite either fill former open space in breccias or replace both breccia matrix and wallrock within a much larger halo of hydrothermal dolomite that contains minor sphalerite (Runnells, 1969; Bernstein and Cox, 1986; Hitzman, 1986). Carrollite [isometric $Cu)(Co,Ni)_2S_4$], cobaltiferous pyrite, and the germanium sulfides renierite [tetragonal $(Cu,Zn)_{11}Fe_4(Ge,As)_2S_{16}$] and germanite (isometric $Cu_{26}Fe_4Ge_4S_{32}$) are also present; grades of Co, Ge, and Ga in the Ruby Creek deposit have not been published. Elsewhere, Kipushi-type ores contain approximately 1,000 ppm Ge, but production figures from Kipushi itself suggest that the effectiveness of Ge recovery varied dramatically (23 to 600 ppm) over time (Höll and others, 2007).

Sandstone-Hosted U(-V-Cu) Deposits

Sandstone-hosted uranium (ssU) deposits are epigenetic deposits that have worldwide distribution; large deposits are known in the United States, Kazakhstan, Niger, Uzbekistan, Gabon, and South Africa (Cuney and Kyser, 2009). Major domestic ssU provinces include the Powder River Basin in Wyoming, the Colorado Plateau, and the Gulf Coast Plain in south Texas (Cuney and Kyser, 2009). Sandstone-hosted U deposits, which are found in sandstones that range in age from Carboniferous to Tertiary, are commonly divided into four types: basal, tabular, roll-front, and tectonolithologic (table 1; see also Boyle, 1985; Cuney and Kyser, 2009). Regardless of type, ssU deposits seemingly form by processes that can be generalized as (1) oxidative mobilization of the uranium from the source rock, commonly granite or tuff, (2) transport of soluble uranyl (U^{6+}) complexes through an oxidized nonmarine-sandstone aquifer, and (3) reduction and precipitation as uranium (U^{4+}) minerals by encounter with reduced host rocks, which typically contain carbonized plant matter, that are laterally continuous with, or are below, the aquifer in which uranium was transported (Guilbert and Park, 1986; Cuney and Kyser, 2009). Several trace elements, most notably Cu, Mo, Se, and V, may be present in ssU deposits (Boyle and Ballantyne, 1980; Hayes, 1982). In some deposits, V or Cu contents exceed U contents (Turner-Peterson and Hodges, 1986).

In this analysis, all types of ssU deposits were targeted, but basal-type deposits appear to be the most likely to occur in Alaska. The Death Valley deposit, the only known ssU deposit in Alaska, is most consistent with a basal-type deposit. Principal ore minerals in the reduced zones in basal-type deposits include pitchblende, coffinite, and, locally, vanadium minerals (montroseite, corvusite) and hexavalent U minerals. In some basal-type deposits, uranyl vanadates occur in the oxidized zones. Trace elements associated with the basal-type ssU deposits include V, Cu, Fe, Mo, Pb, Zn, Ag, Cd, Cr, Co, Ni, Se, and Sr (Dahlkamp, 1993).

The Death Valley deposit is located near the east end of the Seward Peninsula (fig. 1). Discovered in 1977 by an airborne radiometric survey, it has an average grade of 0.27 percent U_3O_8 in beds averaging three meters thick, and it has calculated reserves of about 1,000,000 lbs U_3O_8 (Dickinson and others, 1987). Host rocks are early Eocene carbonaceous, arkosic sandstones of fluvial or colluvial origin deposited in a graben formed on granitic bedrock (Dickinson and others, 1987). An underlying Late Cretaceous granitic pluton forms the west side of the graben. Basalt and coal are interbedded with the sandstone, as are lacustrine, laminated sideritic mudstone and turbidites. An early Eocene basalt flow dammed the ancestral river valley, forming the lake in which the lacustrine sediments were deposited (Dickinson and others, 1987).

Primary epigenetic ore formed in the early Eocene, and supergene-enriched ore developed in the Holocene. The high-standing adjacent pluton is considered the likely source for the uranium; the interlayered basalt may have contributed V, as basalt is leachable (and has been noted as a common source of V by Skirrow and others, 2009). Primary mineralization seemingly developed when uranium was dissolved by oxidizing surface water, was carried east from the pluton and recharged into the alluvial aquifer, and was deposited in the reducing Tertiary carbonaceous-sedimentary-rock environment (Dickinson and others, 1987). Mineralized rocks are fairly widespread in the subsurface where they are both above and below Eocene basalt and lacustrine rocks and where they extend to a depth of about 91 m. Uranium minerals in the primary ore include coffinite ($U(SiO_4)\cdot nH_2O$) in the reduced zones and autunite ($Ca(UO_2)_2(PO_4)_2\cdot 10\text{-}12H_2O$) where primary ore has been oxidized. Secondary supergene enrichment is related to present-day surface exposures and, thus, may be ongoing, as involvement of recent surficial mudflows and soil-formation processes indicate a recent age (Dickinson and others, 1987). Uranium minerals in secondarily enriched soils include meta-autunite ($Ca(UO_2)_2(PO_4)_2\cdot 6H_2O$). Uranium-rich rocks of the Death Valley deposit are strongly carbonaceous and may have an anomalously low manganese (Mn) concentrations (see chapter 5, this report). Features of the Death Valley deposit are most similar to those of the basal-type ssU deposit (Dickinson and others, 1987) concentrations.

Sn-W-Mo(-Ta-In-Fluorspar) Deposits Associated with Specialized Granites

Ore minerals containing Sn, W, Mo, Ta, In, and fluorspar (industry term for fluorite, cubic CaF_2) are commonly found in various combinations that are closely associated with highly evolved, acidic intrusive rocks, collectively known as specialized granites (for example, Reed, 1986). Specialized granites include granite porphyries, peraluminous granites, and high-silica (>73 percent SiO_2; Rogers and Greenberg, 1990; Blatt and others, 2006) granites that form shallow to hypabyssal intrusions where associated with mineralization. Most of these granites are in tectonic environments that involve thickening, contraction, or extension of continental crust; they are nearly unknown in transitional or thin-crustal environments. With few exceptions, petrogenetic characteristics common to specialized granites and their associated dikes and sills include (1) crystallization from late-stage magmas that contain elevated concentrations of incompatible elements, owing to protracted fractional crystallization (Blevin and Chappell, 1992), and (2) at least some contamination of the associated magmas by assimilated continental crust (Clemens and Wall, 1981). Available strontium-isotopic ratios for Sn-, W-, and Mo-bearing granites in northern Alaska are consistent with local structural data, which indicates that they are hosted in tectonically thickened continental crust involved in magma generation (Hudson and Arth, 1983; Arth and others, 1989b; Roeske and others, 1995). Granitic rocks from low-F, arc-related porphyry Mo deposits are typically located in collisional settings at continental margins such as Quartz Hill in southeastern Alaska, which has initial $^{87}Sr/^{86}Sr$ ratios of ~0.7051, suggesting a primitive source that has low Rb/Sr contents and minimal involvement of older sialic crust in magma generation (Ashleman and others, 1997). Alternatively, porphyry Mo granitic hosts may have formed by remelting of subduction-modified lithosphere (Taylor and others, 2012).

Mineral deposits associated with specialized granites are found in dikes, veins, stockworks, greisens, and in hydrothermally altered zones near the tops of granitic intrusions (Černý, 1991; Černý and others, 2005; Johan and others, 2012). Associated wallrock deposits include stockworks, exogreisens, and skarns developed in carbonate host rocks; these deposits may contain Sn, W, Mo, Ta, In, and (or) F. The tin ore mineral typically associated with specialized granites is cassiterite; less commonly, stannite is present (tetragonal Cu_2FeSnS_4). Tungsten is mainly in scheelite or wolframite, and Mo is mainly in molybdenite. Tantalum is mostly in tantalite [orthorhombic $(Fe,Mn)Ta_2O_6$] and less commonly in wodginite [monoclinic $Mn(Sn,Ta)Ta_2O_8$) or microlite [isometric $(Na,Ca)_2Ta_2O_6(O,OH,F)$]. Indium typically substitutes for primary ore metals in sphalerite, cassiterite,

or stannite, and it rarely forms roquesite (tetragonal $CuInS_2$) (Ishihara and others, 2006; Sinclair and others, 2006). Fluorine is found in fluorspar (CaF_2).

In Alaska, the best known tin mines are associated with the Cassiterite Dike, in the Lost River district on the Seward Peninsula (Hudson and Reed, 1997). Tungsten was mined from greisens, veins, and skarns such as Stepovich in the Fairbanks district (Newberry and others, 1990). Quartz Hill in southeastern Alaska is the largest known porphyry Mo deposit of its type known in the world (Taylor and others, 2012).

Data Sources and Treatments

To evaluate mineral resource potential in Alaska for the deposit groups described above, the following datasets were assembled and analyzed using ArcGIS. Most of the data are publicly available; direct links to the internet resources are included in the dataset descriptions and in this report.

National Hydrography Dataset and Watershed Boundary Dataset

The National Hydrography Dataset and Watershed Boundary Dataset (NHD and WBD, respectively; http://nhd.usgs.gov/) delineate surface-water networks and drainage basins throughout the United States, using standardized criteria that is based on topography and hydrology. Relative drainage basin size, geographic location, and nested hierarchy are encoded within a string of digits known as a hydrologic unit code, or HUC. A classical hydrologic unit is a division of a watershed that has but a single discharging stream; accordingly, it corresponds to a physical watershed that is defined by topography. Herein, HUC (pronounced 'huk') will be used as an abbreviation for hydrologic unit. HUCs are identified by either two or twelve digits that correspond to the largest drainage systems, which are known as regions and subwatersheds, respectively. Numeric codes, names, and boundaries associated with each HUC provide unique identifiers that are useful for associating other geospatial data from multiple sources in a GIS. The term HUC will be commonly used herein to refer to a physical drainage subbasin and not solely to the string of digits used to identify the subbasin. Twelve-digit HUC boundaries were chosen for this study as a geographic reference frame and also the sampling unit for evaluating mineral resource potential across Alaska. Datasets described below were scored for each twelve-digit HUC across the state as they pertained to the mineral deposit groups of interest, and scores were analyzed and classified for mineral resource favorability following the methods described below. Other data from the NHD, primarily rivers and streams, were used only in the placer-model evaluation to map drainage networks downstream from areas that have high and medium placer potential (see below).

Geochemical Data Sources

The geochemical dataset is a compilation derived from three geochemical databases that represent samples of geologic materials collected across Alaska. The file structure and data format of each database is markedly different, which necessitated reformatting for consistency and optimization for geochemical mapping and statistical evaluation.

The USGS Alaska Geochemical Database, Version 2.0 (AGDB2), is the most recent compilation of new and historical geochemical analyses of rock, stream-sediment (henceforth, "sediment samples"), soil, and heavy-mineral-concentrate samples from Alaska (Granitto and others, 2013). The AGDB2 includes analyses of 108,966 rock samples, 92,694 sediment samples, 6,869 soil samples, 7,470 mineral samples, and 48,096 heavy-mineral-concentrate samples. The samples were collected between 1962 and 2009 and were prepared according to various USGS standard methods (Miesch, 1976; Arbogast, 1990, 1996; Taggart, 2002). Data for all sediment and heavy-mineral-concentrate samples, as well as for 48,731 igneous-rock samples and 18,281 sedimentary-rock samples, were synthesized and interpreted.

The National Uranium Resource Evaluation (NURE) database contains data derived from the NURE Hydrogeochemical and Stream Sediment Reconnaissance (NURE-HSSR) program, which was overseen by the U.S. Atomic Energy Commission. NURE sediment samples were collected in Alaska between 1976 and 1979 and were prepared according to various standard methods; data for 65,993 of these Alaska sediment samples were mostly obtained for application in the Alaska Mineral Resource Assessment Program (AMRAP).

The Alaska Division of Geological & Geophysical Surveys (ADGGS) geochemical database includes analyses of 12,437 rock samples, 10,919 sediment samples, 100 soil samples, and 1,061 heavy-mineral-concentrate samples collected between 1960 and 2014. These data, which were provided by the ADGGS, are also available for download (http://www.dggs.alaska.gov/webgeochem/). Data for all the ADGGS sediment and heavy-mineral-concentrate samples, as well as for 5,653 igneous-rock samples, were synthesized and interpreted.

Analyses of many samples in the AGDB2 and ADGGS databases were completed by more than one analytical method; consequently, some samples have determinations for some elements by more than one method. To minimize the complexity inherent in multiple determinations for individual elements, a single "best value" concentration was identified for each element in each sample. Granitto and others (2013) provided a detailed description of the ranking criteria that accompany analytical methods, as well as how they were used to determine "best values."

Many samples included in the synthesized geochemical datasets have also been analyzed more than once. Relative to these samples, both the original and the subsequent data might coexist in the source dataset because samples were issued a second laboratory-identification number upon submission for reanalysis, which effectively created a second data record for these samples. In situations for which more than one analysis for any given element was associated with a specific sample location, the highest "best value" was selected for use in the calculation of statistics, to display on point plots, and to use for gridded map layers during the geochemical synthesis conducted in this study.

Stream-Sediment Geochemistry

The available set of sediment samples represents the most comprehensive, most evenly distributed, and highest density samples and associated geochemical data applicable to the analysis of mineral resource potential across Alaska. Bedrock is concealed in many areas by unconsolidated sediment and vegetation. However, sediment geochemical data portray elemental abundance patterns that reflect rock compositions in their respective drainage basins and, thus, provide clues about rock types in areas of poor exposure or where geologic mapping is lacking. This dataset is herein referred to as sediment geochemistry because, although some samples were collected from a variety of surface-water bodies, more than 80 percent of the sediment samples in the AGDB2 were collected from streams.

Sediment geochemical data from the AGDB2, NURE, and ADGGS datasets were combined into a single dataset for which the median, 75th, 91st, and 98th percentiles for each element were calculated. These percentile cutoff values were used in the mineral-potential-scoring methods described below. Appendix A presents summary statistics for each element, identifies which database(s) contained data for various elements, and identifies the statistical method by which percentile values were determined. Although the combined dataset yields the most synoptic statewide coverage of geochemical data, data comparability between the three data sources was compromised by a lack of consistency among analytical methods used to determine elemental abundances among samples. Furthermore, the data sources employ multiple detection limits for a single element, thus resulting in diverse data-censoring limits. Censored data are those that fall outside the detection limit for a specific element analyzed by a particular method. The data for some elements are highly censored. For these elements, summary statistics were strongly skewed when censored data were omitted or when substitute values were used to replace censored values. For example, if the geochemical data for an element are 90 percent censored,

then substitution of a value such as one-half of the lowest determination limit for the censored data would yield artificially low mean, median, and percentile values. Similarly, if the data are 90 percent censored, then omission of the censored values would yield a dataset composed of elemental abundances for only those samples that have anomalously enriched concentrations, and statistics calculated using that subset would result in artificially high mean, median, and percentile values. Therefore, two methods—the substitution method and the Kaplan-Meier method—were used to calculate statistical values for each element, depending on the amount of censored data.

Both methods were applied to data for several elements that have different relative amounts of censored data. For elements that have relatively low degrees of censoring, results were nearly identical when summary statistical values were calculated by both methods. Critical assessment of these statistics indicates that for elements that have less than about 40 percent censored values, the differences for the median and upper percentiles were negligible to insignificant. Consequently, for elements that have 40 percent or less censored data, substitution was used: all censored values were replaced with a value equal to either one half that of the minimum noncensored value or one half that of the minimum lower limit of detection, whichever value was smaller. The digits 1,1 were added at the end of substituted values to render the replaced values identifiable. Summary statistics were then calculated by standard procedures, using the combined analyzed and substituted values. For elements that have more than 40 percent censored data, the Kaplan-Meier method was used to estimate summary statistics; this nonparametric statistical approach calculates cumulative probability distributions from which summary statistics for censored data were calculated (Helsel, 2012). The procedure was run using the Minitab program (Helsel, 2012). Appendix A shows the level of censoring for each element and identifies the elements for which the Kaplan-Meier method was used.

Igneous-Rock Geochemistry

Igneous-rock geochemical indices, which were calculated for nearly 49,000 igneous-rock samples statewide, were used to identify permissive rock types for associated REE and Sn-W-Mo deposits. The REE deposits considered herein are associated with igneous rocks that have peralkaline, alkaline, or carbonatitic compositions, whereas the Sn-W-Mo deposits of greatest interest are associated with high-silica, peraluminous, intrusive igneous rocks. In many cases, igneous map units might cover broad areas that include four or more different lithologies, whose distributions would not be clearly indicated within the mapped unit and certainly not at the level of detail of a HUC. In addition, we have tested the igneous-rock geochemical indices, defined by element ratios, against map-unit lithology assignments and found that map units in, for example, the Ruby batholith contain both alkaline and peraluminous rock samples, leading to uncertainty regarding the relative abundance of lithologies listed in the igneous-rock map units. Distinctive igneous-rock compositions (such as alkaline and peraluminous) associated with these two deposit groups are relatively easy to identify using geochemical data from individual rock samples or suites of rock samples. The distribution of igneous-rock samples across the state is sufficient to provide more geographically continuous detail than what is portrayed in available geological mapping, especially considering the compositional complexity of many igneous systems and the sparsity of detailed geologic mapping statewide. Thus, the geochemical characteristics of individual rock samples provide a means to identify favorable rock types within broader igneous-rock belts, as well as in areas where exposed igneous rocks show more complexity than is represented on available geologic maps or in cases where favorable geochemical trends are not obvious or apparent in outcrop.

Major- and trace-element geochemical data for igneous-rock samples were compiled from four primary sources: (1) the AGDB2, (2) the ADGGS database, (3) peer-reviewed literature (see appendix B for a list of literature sources), and (4) unpublished USGS data. For this exercise we didn't include samples that were submitted as altered or mineralized. Unfortunately, information in the database or

published literature that would allow the screening of possible altered igneous-rock samples is inconsistent; therefore, we acknowledge the potential for inclusion of altered rocks in our analyses, but we also infer that the size of the igneous-rock geochemical database provides relatively robust statistics. All geochemical ratios discussed below were computed using only high-resolution data. Specifically, all igneous-rock geochemical data that were used to compute ratios or geochemical indices (see below) have similar high precision. Most of the major-element-composition data used to evaluate resource potential were determined by x-ray fluorescence (XRF) methods. Similarly, most trace-element abundances used to evaluate resource potential were determined both by XRF and by inductively coupled plasma mass spectrometry (ICP-MS). All major-element-oxide concentrations were recalculated on a volatile-free basis.

Single-element geochemical data can identify some geochemically anomalous igneous rocks, but most geochemistry-based igneous-rock classification schemes require data for two or more elements or major oxides. Geochemical criteria used to classify igneous rocks, including relative alkali and silica saturation (for example, Irvine and Baragar, 1971; Frost and others, 2001; Frost and Frost, 2008; Frost and Frost, 2011), are well established. Similarly, aluminum saturation index [ASI] (molar Al/[(Ca-1.67P)+Na+K]) (Shand, 1943; Frost and others, 2001) and ANK (molar Al/[Na+K]) were calculated from major-element-oxide data (Maniar and Piccoli, 1989); these parameters were used to identify peraluminous (ASI >1), metaluminous (ANK >1), and peralkaline (ANK <1) samples.

Some trace-element-concentration ratios (for example, Nb/Y >1; 10,000Ga/Al >2.6) yield values that allow drawing distinctions between alkaline and subalkaline igneous rock types (Winchester and Floyd, 1977; Pearce and others, 1984; Whalen and others, 1987; Pearce, 1996). However, many useful geochemical-discrimination diagrams include composition fields defined by one or more elements. For example, sample characteristics, including relative abundances of Fe and Mg (Fe# = (FeO/[FeO+MgO]) and the alkalis (modified alkali-lime index [MALI] = Na_2O+K_2O-CaO) can be evaluated using major-element-oxide data (Frost and others, 2001).

Igneous-rock classifications that are based on comparisons relative to boundaries or fields are traditionally conducted by visual inspection of plots. However, such an approach is inefficient relative to datasets that contain thousands of samples such as those pertinent to Alaska (ADGGS and AGDB2; Granitto and others, 2013). Consequently, we devised a method to quantify a sample composition displacement from established field boundaries. Specifically, the displacement in the Y-axis direction above or below accepted boundaries were calculated for each igneous-rock sample. For example, relative to the MALI array (that is, the alkali-calcic/calcic-alkalic boundary of Frost and others, 2001), the displacement equation for a sample is:

$$MALI_{displacement} = MALI_{calculated} - MALI_{expected}$$

where $MALI_{expected}$ is the MALI predicted by the boundary equation and SiO_2 values for individual samples, as chosen for specific rock types. Accordingly, the $MALI_{displacement}$ and $Fe\#_{displacement}$ index values were calculated for each sample, assuming availability of the required data. $Fe\#_{displacement}$ was calculated relative to the boundary proposed by Frost and Frost (2008), which is based on total iron content, expressed as ferrous iron. Fe# and MALI displacements are positive for samples that have ferroan and alkalic compositions and negative for magnesian and subalkaline compositions, respectively.

Displacement-type ($MALI_{displacement}$, and $Fe\#_{displacement}$) and simpler critical-value ratio (Nb/Y, Ga/Al) geochemical-discriminant indices foster rapid recognition of geochemical anomalies and potentially associated mineral deposits. The Ga/Al ratio (calculated as 10,000Ga/Al >2.6), which distinguishes alkaline and subalkaline igneous rock types, can provide a proxy monitor of fluorine contents because of the higher solubility of GaF_6 relative to AlF_6 (Whalen and others, 1987), which is useful because of the role fluorine has as a transport agent for many of the incompatible elements of

interest in our analyses. Niobium is a targeted commodity with REE in the alkaline igneous-rock deposit group, and high Nb/Y is a reliable predictor of tectonic settings that are favorable for generation of alkaline igneous rocks (Pearce and others, 1984; Eby, 1990; Pearce, 1996). Combinations of these indices constrain the composition, sources, and mineral resource potential of igneous rocks in Alaska.

Heavy-Mineral-Concentrate Mineralogy and Geochemistry

Mineralogical data that are based on visual identifications are available for more than 18,137 nonmagnetic bulk-panned-concentrate or heavy-mineral-concentrate (HMC) samples in the AGDB2 (Granitto and others, 2013). The HMC samples were derived from sediments, soils, or rocks, and data were derived from data-entry sheets, USGS Open-File Reports, and archival digital spreadsheets. The entries include several different quantifications of heavy-mineral abundances, including gold, cassiterite, monazite, and scheelite (Granitto and others, 2011, 2013). Grain-count data are available for some samples. Abundances in other samples are described by a variety of qualitative values (for example, "present," "abundant," "trace"), estimated percentages, or percentage ranges. Null values indicate that the mineral was not observed in particular samples. Mineralogy data in the AGDB2 are presented as they were originally recorded and interpreted; data sources are listed in Granitto and others (2011). The AGDB2 also contains best-value geochemical data for 49,783 HMC samples across the state. The specific methods used to incorporate HMC mineralogy and (or) geochemistry into our analysis of mineral resource potential are more fully described in relevant sections below.

Alaska Resource Data File

The Alaska Resource Data File (ARDF; http://ardf.wr.usgs.gov/) contains more than 7,000 reports of mines, prospects, and mineral occurrences in Alaska. ARDF records, which are published for individual USGS 1:250,000-scale quadrangles, can be downloaded either as USGS Open-File Reports for each quadrangle or as part of the statewide ARDF database (http://ardf.wr.usgs.gov/). ARDF records include a broad spectrum of mineral deposit types. Particular search criteria were developed to identify records that most likely represent the six deposit model groups included in this resource assessment. For each deposit group, a list of searchable keywords was developed relative to pertinent ARDF record fields. Keywords were weighted for their relevance to the mineral deposit types of interest and were also assigned to a "definite" or "maybe" column depending on the strength of their association with, or relevance to, models of interest (appendix C). In some cases, keywords were assigned negative scores when indicative of geological systems known to be unassociated with the mineral deposit type of interest. Complete lists of keywords and associated weights for each deposit group are listed in appendix C.

Using a custom Python script in ArcGIS, all ARDF records were searched, and each record was assigned a total score for each of the six deposit groups on the basis of the total keyword hits and the sum of the associated scores. High-scoring ARDF records for each deposit group were initially reviewed relative to areas having known mineral potential and (or) mining activity to ensure that known occurrences were appropriately identified using this approach. When ARDF-record scoring results did not adequately reflect known deposits, scoring parameters were modified to better calibrate the method. In areas that have multiple relevant ARDF records, only the highest scoring record was used as the representative ARDF-record score for any single HUC. Scores for all ARDF records within a HUC were not aggregated.

In some cases, scrutiny of individual ARDF records revealed misspellings and imprecise location information that hindered appropriate scoring. Records that contained errors were corrected in the database prior to final analysis, as described below. Future ARDF users are cautioned because the database may still contain unrecognized errors; however, the preponderance of accurate ARDF records and other data utilized will likely outweigh or counteract spurious ARDF records. Specific deposit-

group analyses included below provide more information on details of how ARDF-record scores were used to assess mineral potential.

Geologic Map of Alaska

The digital "Geologic Map of Alaska" (Wilson and others, 2015) portrays the distribution of diverse rock types across the state. The catalog of lithologic descriptions associated with the geologic map database was searched to identify rock types most prospective as sources and (or) best suited for hosting particular deposit types. Lithology query results were used to develop derivative, generalized lithology map layers that show the distribution of rock types favorable for the occurrence of each deposit group across Alaska. Specific lithologies considered favorable for the occurrence of each deposit group, which are described in detail below, are summarized in appendix D.

Aerial Gamma-Ray Surveys

Aerial gamma-ray surveys that reflect the radioactive signatures of bedrock and surficial materials for the state of Alaska were calibrated and compiled by Saltus and others (1999) and Duval (2001). These surveys, flown as part of the National Uranium Resource Evaluation (NURE) Program by the U.S. Department of Energy in 1976–80, cover most of Alaska except for parts of the Brooks Range and southwestern Alaska and also the Livengood 1° × 3° quadrangle. These surveys document gamma-ray flux associated with decay of the naturally occurring radioactive isotopes. Radioactivity from ^{40}K, ^{238}U, and ^{232}Th were used to identify areas that have potential for REE, Sn-W-Mo, Th, and U deposits, as described below.

GIS-Based Methods

The goal of this project was to identify and rate mineral resource potential across Alaska with respect to the selected deposit groups described above. Only six deposit groups were prioritized for specific elements and minerals, for reasons given above, and we acknowledge that considerable mineral resource potential for many other important deposit groups exists across Alaska. Subwatersheds defined by 12-digit HUCs were used as the primary spatial framework and sampling unit to delineate, evaluate, and portray mineral resource potential. Using HUCs as analysis cells provided a few key advantages relative to other types of survey units (for example, Public Land Survey System, latitude-longitude quadrangle). First, each HUC in Alaska has unique, numeric identifiers and names that can be used in a GIS to geographically associate digital data derived from multiple sources. Such an approach is useful to land-management agencies when required to address multiple competing issues involving land-use decisions. Second, the HUC dataset is standardized, and it is available for, and is continuous across, most of the state and surrounding region. The average area of the 17,177 twelve-digit HUCs in Alaska is approximately 100 km^2, or 27,500 acres. Units of this size are generally larger than single mineral deposits and some mining districts, but, with 17,177 HUCs in Alaska, the geospatial resolution is sufficient for most interpretive requirements. The HUCs represent a balance commensurate with the need to display data patterns at a range of scales while optimizing computing efficiency when using data from large relational databases. Perhaps most importantly, subwatershed boundaries (most commonly defined by drainage divides) typically are easily identifiable on the ground, and they form physiographic features that are directly linked to processes (for example, erosion and weathering), as well as features (for example, streams and rivers) that expose, transport, and potentially enrich sought-after ore minerals. Using subwatersheds as an organizational construct also provides a direct link to sampling focused along streams and other surface-water bodies. In addition, drainage basins provide a logical approach for tracing sources of elements and minerals in stream sediments.

Using a customized Python script in ArcGIS, each HUC was assigned a mineral-prospectivity score, using the criteria and treatments described below and tailored to each deposit group. Total scores were used to classify resource *potential* of each HUC as High, Medium, Low, or Unknown, relative to each deposit group. The relative *certainty* of estimated resource potential associated with each HUC was also assigned High, Medium, or Low values, using procedures described for each deposit group below. Scoring templates and *potential* versus *certainty* classification templates (tables 2, 4, 7, 9, 11, 14), which are unique to each mineral deposit group, correspond to the resource-potential descriptions provided below. Maps on plates 1, 3, 5, 7, 9, and 11 show relative resource potential for each deposit group. The accompanying geospatial-attribute tables (appendix E), which present results by deposit group, include the scores for each HUC by individual component, the percent contribution of each scoring element to the total score, and the resulting classification. Annotated maps on plates 2, 4, 6, 8, 10, and 12 highlight specific deposits and (or) selected areas that have high to medium resource potential for each deposit group.

Chapter 1. REE-Th-Y-Nb(-U-Zr) Deposits Associated with Peralkaline to Carbonatitic Intrusive Rocks

By Susan M. Karl, Erin Todd, Matthew Granitto, Keith A. Labay, and Nora B. Shew

Deposit-Group Characteristics

Economic REE-Th-Y-Nb(-U-Zr) deposits are typically associated with alkaline to carbonatitic intrusive rocks (Wall, 2013; Verplanck and others, 2014). Minerals enriched in REE in alkaline intrusive rocks are found as primary igneous minerals, products of postmagmatic orthomagmatic mineralizing fluids, or as secondary assemblages in late-stage hydrothermal deposits (Verplanck and others, 2014). Orthomagmatic fluids precipitate REE-Th-Y-Nb(-U-Zr) minerals in cupolas, pegmatites, breccia pipes, veins, and dikes. Lower temperature fluids derived from alteration of wallrock that hosts some REE-enriched intrusions may also contribute to the genesis of hydrothermal deposits associated with these rock types (Wall, 2013). In addition, weathering products of alkaline igneous complexes may contain REE- and HFSE-bearing minerals in clays and placer deposits associated with the igneous complexes.

By definition, alkaline igneous rocks are enriched in Na_2O, K_2O, and CaO relative to SiO_2 and Al_2O_3, in excess of amounts needed to form feldspars. Peralkaline igneous rocks have molar (Na+K)/Al values greater than 1 and aluminum saturation index (ASI) molar [Al/(Ca-1.67P+Na+K)] values less than 1 (Frost and others, 2001). “Alkaline” igneous rocks, as defined herein, include peralkaline and alkaline granites and their volcanic equivalents [rocks that have alkali contents within or above the basalt undersaturation field on the total alkali versus silica diagram of Le Bas and others (1986)]. Carbonatites are alkaline rocks that contain more than 50 modal percent primary carbonate minerals and less than 20 percent silica (Le Maitre, 2002). They may also contain albite and (or) potassium feldspar. Alkaline igneous rocks are common in Alaska, but only a single occurrence of carbonatite is documented in the state (see below).

Alkaline igneous rocks include a range of compositions, and their petrogenesis is debated. Their petrogenesis can involve a variety of processes, but all of these rocks require a mantle source enriched in lithophile elements, H_2O and CO_2 (Bailey, 1987, 1989). Mantle sources for alkaline and carbonatitic igneous rocks are supported by radiogenic and stable isotopic studies (Bailey, 1987; Winter, 2001). Primary magmas enriched in REE and HFSE are derived from enriched mantle and by partial melting of continental mantle and continental crust (Arth and others, 1989a; Bea, 1996), and most enriched mantle-derived magmas are in tectonic environments that involve thickening, contraction, or extension of continental crust. Although alkaline and carbonatitic intrusions are commonly associated with continental-rift settings (Verplanck and others, 2014, and references therein), the Bokan Mountain peralkaline granite in southeastern Alaska formed in an oceanic-arc complex (Dostal and others, 2013), indicating that continental crust is not required. Neodymium-isotopic data for peralkaline granite at Bokan Mountain are consistent with incompatible element derivation from a parental mantle magma (Philpotts and others, 1998; Dostal and others, 2014), suggesting that protracted fractional crystallization of enriched mantle magmas in additional tectonic settings associated with crustal thickening can yield derived magmas with elevated abundances of the REE and other incompatible elements, including Y, Nb, Zr, U, and Th. Mineralization at Bokan Mountain may reflect such a process of protracted fractional crystallization (fig. 1; see also Thompson, 1988; Philpotts and others, 1998; Dostal and others, 2013, 2014).

Abundances of incompatible elements such as HFSE, REE, U, and Th can be enriched by fractional crystallization of alkaline magmas (Salvi and Williams-Jones, 2005). Fluorine, which is also concentrated in highly fractionated magmas, is critical for the transport of REE and Th in late-stage

melts and aqueous fluids because it suppresses melt polymerization, lowers final crystallization temperatures and viscosity, and increases solubility of trace-mineral phases (Keppler, 2003). As a result, fractional crystallization of primary mineral phases that don't accommodate REE and HFSE yields greater concentrations of incompatible elements in minerals formed at lower temperatures (Whalen and others, 1987; Blundy and Wood, 2003; Černý and others, 2005).

The REE and HFSE are concentrated in late-stage magmatic phases because they are incompatible in phases crystallized relatively early from the magma. They do not easily substitute into crystal lattices of the common rock-forming minerals and, therefore, behave as incompatible elements in most igneous systems. The REE consist of 15 elements in the lanthanide series (La to Lu); the atomic radii of REE increase systematically from light (LREE) to heavy (HREE), and so LREE are more incompatible than HREE (for example, see Blundy and Wood, 2003). The HFSE, which include Nb, Zr, Hf, Ti, and Ta, have low atomic radii and high valences, and so they behave similarly to REE. Electron configurations in REE are also similar to other Group 3[3] elements in the periodic table that include transition metals Sc and Y, which are sometimes called "rare earth metals." The actinide series elements, of which only Th and U are naturally occurring, have similar ionic radii and valences to Zr, Hf, and Ce and, thus, substitute for LREE and HFSE in accessory-mineral phases. As a result of their incompatibility, all of these elements are often concentrated in the last minerals to crystallize from magma or aqueous fluid (Černý and others, 2005), and REE-enriched accessory minerals can also crystallize in hydrothermal alteration zones associated with magmatic volatile exsolution. These incompatible elements are commonly incorporated in monazite, allanite, and zircon; trace amounts are present in apatite, fluorite, hematite, feldspars, and micas (Sheard and others, 2012).

In summary, protracted fractional crystallization of enriched magmas yields alkaline intrusive rocks that tend to contain significantly elevated abundances of incompatible elements; consequently, the presence of alkaline intrusive rocks is an important exploration guide for deposits containing these elements. Because of the similar behavior of the incompatible elements, deposits that contain REE, Th, Y, Nb, U, and (or) Zr were focused into a single deposit group for this analysis.

Mineral-Resource-Potential Estimation Method

In conducting REE-Th-Y-Nb(-U-Zr) resource-potential estimates, HUCs were assigned favorability, or prospectivity scores for *potential* to contain concentrations of the target elements, on the basis of the following criteria: (1) the presence of alkaline igneous rocks, (2) references to target elements and minerals in Alaska Resource Data File (ARDF) records, (3) favorable igneous-rock geochemistry, (4) favorable stream-sediment chemistry, (5) favorable pan-concentrate mineralogy and geochemistry, and (6) radioactivity measured by aerial gamma-ray surveys (tables 2, 3). Based on either the availability of data or the number of datasets that contributed to the scores for mineral potential, each HUC was assigned a score for favorability *certainty* in order to display the level of confidence the analysis provides for the *potential* score. Criteria applied to scoring these parameters are explained below.

Lithology

Igneous rock names from the digital database of the "Geologic Map of Alaska" (Wilson and others, 2015) were used to identify the spatial distribution of carbonatites and alkaline igneous rock that are permissive for associated REE-Th-Y-Nb(-U-Zr) deposits. Map-unit descriptions from the digital

[3] "Group 3" is a division of the periodic table.

geologic-map database that identified map units composed of more than 33 percent alkaline rocks or carbonatites were considered favorable for a concentration of REE-Th-Y-Nb(-U-Zr). However, map-unit descriptions are generalized, and they pertain to units that cover large areas; thus, they are considered unreliable at the drainage-basin scale. Consequently, a maximum of one point could be included in the resource-potential score (table 2), and the digital map database did not contribute points for the certainty score for a HUC.

Igneous-Rock Geochemistry

Igneous-rock geochemical data are diagnostic of peralkaline, alkaline, or carbonatitic rocks permissive for associated REE-Th-Y-Nb(-U-Zr) deposits, as discussed above. Distinctive compositions of these igneous rocks are readily identifiable using geochemical data. Identification of alkaline igneous rocks using geochemical data for precisely located samples is advantageous because they provide (1) objective information that is useful for identification of alkaline igneous rocks, (2) high geospatial resolution of igneous rocks having appropriate compositions, and (3) locations of dikes and small intrusive bodies that often are not portrayed on geologic maps and that may contain REE-HFSE mineralization. Consequently igneous-rock geochemistry was positively weighted in scoring the potential and certainty for REE-HFSE prospectivity.

The geochemical criteria used to identify igneous rocks that are favorable for associated REE-Th-Y-Nb(-U-Zr) deposits are (1) $MALI_{displacement}$, (2) $Fe\#_{displacement}$ (described above), (3) Ga/Al, and (4) Nb/Y (table 2). As discussed above, positive values for $Fe\#_{displacement}$ and (or) $MALI_{displacement}$ are typical of A-type, intraplate, peralkaline to alkaline rocks (with potential for associated REE-Th-Y-Nb(-U-Zr) deposits). However, few, if any, exploitable REE deposits are associated with mafic rocks (for example, see Linnen and others, 2014). Therefore, assigning positive scores to samples that have appropriate $MALI_{displacement}$ values was restricted to samples having intermediate to felsic compositions because mafic rocks, especially cumulates that have elevated concentrations of olivine, cause MALI to increase with decreasing SiO_2 content. Consequently, positive favorability, based on the $MALI_{displacement}$ values, was assigned to samples with SiO_2 contents greater than 56 weight percent.

Similarly, application of Ga/Al to identify A-type granites (Whalen and others, 1987) was limited to intermediate- to felsic-composition samples. Because of the higher solubility of GaF_6 relative to AlF_6, the Ga/Al ratio is useful because of the role of fluorine as a transport agent for REE and HFSE. However, for fluorine content to be an effective index of a potential for REE deposits, incompatible element concentrations must be high enough to combine with fluorine to form accessory mineral phases containing REE and HFSE, which is more likely in late-stage, differentiated magmas. For this reason, use of the Ga/Al ratio in scoring was limited to samples with SiO_2 contents greater than 60 weight percent.

In contrast, $Fe\#_{displacement}$ and Nb/Y are pertinent and applicable to igneous rocks across a broad compositional range. For example, Frost and others (2001) and Frost and Frost (2008) demonstrated that alkaline igneous rocks that have SiO_2 contents greater than 48 weight percent are generally ferroan ($Fe\#_{displacement} > 0$). Many petrogenetic studies have used Nb/Y to deduce the tectonic setting in which various igneous systems evolved (Winchester and Floyd, 1977; Pearce and others, 1984; Eby, 1990; Pearce, 1996). Whereas $Fe\#_{displacement}$ and Nb/Y do not directly correlate with REE-enriched rocks, they do identify tectonic environments, such as within-plate settings, that have the highest potential for REE-enriched igneous rocks.

The spatial distribution of igneous rocks in Alaska having available geochemical analyses is inconsistent, as many HUCs lack analyses, and some HUCs contain multiple analyses. To minimize effects of inconsistent sample density on HUC scores, a maximum of one point was assigned for each of the four possible geochemical indices (table 2) for *potential* for each HUC. If a HUC contains a sample

that has igneous geochemical data, the HUC was assigned one *certainty* point for the contribution from this dataset, regardless of whether the *potential* score for the HUC was zero or more (table 3).

Alaska Resource Data File

Records in the Alaska Resource Data File (ARDF) were scored with respect to REE-Th-Y-Nb(-U-Zr) potential on the basis of specific keywords in various categories of the ARDF record (see appendix C). Descriptive keywords associated with the REE-Th-Y-Nb(-U-Zr) deposit group include component terms such as carbonatite and riebeckite, as well as alkaline-rock-associated and mineralization-related terms such as hydrothermal, radioactive, uraniferous, carbonatization, dolomitization, albitization, metasomatism, Fe-carbonate, pyroxene-fluorite, and potassic. Keywords for commodities include individual elements such as La, Ce, Nd, U, Th, Y, Zr, Nb, as well as the terms REE and HFSE. Important keywords were weighted such that mention of REE ore or gangue minerals, including monazite, bastnäesite, and synchysite, received three points, whereas less economic minerals such as uranothorite received two points. Mention of relevant indicator minerals, such as zircon and fluorite, received one point. The cumulative keyword hits contributed to a total ARDF-record keyword score. The total scores were statistically grouped by the Jenks (1967) method (using natural breaks). ARDF-records that have keyword scores higher than 3 appear to contain all the known REE-Th-Y-Nb(-U-Zr) deposit occurrences statewide, and they also include other occurrences that have potential for REE-Th-Y-Nb(-U-Zr) deposits. Many ARDF-record localities that have scores greater than 3 are coincident with placer occurrences that contain REE-, HFSE-, or U-Th-bearing minerals. Placer occurrences (in unglaciated areas) suggest a nearby bedrock source and are, therefore, considered significant. Occurrences having total keyword scores higher than 9 represent keyword hits derived from multiple categories in the ARDF record. These occurrences are considered to have higher REE-Th-Y-Nb(-U-Zr) deposit potential than records having lower scores. A keyword score higher than 21 identified prospects and occurrences that have a considerable amount of data that are consistent with the presence of REE-Th-Y-Nb(-U-Zr) mineralization. Accordingly, HUCs that contain ARDF-record localities that have scores of 3 to 9 were assigned 1 point; those having scores of 10 to 21 were assigned 2 points; and those having scores higher than 21 were assigned 3 points (table 2). As discussed above, only the highest scoring ARDF record in a HUC was applied to the total score of the HUC, and so the maximum possible ARDF-record score for any HUC was 3. This scoring cap was also applied to limit the potential bias associated with ARDF records having long, detailed descriptions, within which an individual keyword might be repeated. Detailed and lengthy descriptions do not necessarily indicate higher potential for a REE-Th-Y-Nb(-U-Zr) deposit. The presence of an ARDF record in a HUC (regardless of whether the score for *potential* was zero, negative, or positive) contributed a maximum of one point to the *certainty* score (table 3). The lack of an ARDF record in a HUC yielded a null score, which contributed zero points to the *certainty* score.

Stream-Sediment Geochemistry

In Alaska, stream-sediment samples and associated geochemical data are more abundant and evenly distributed than any other type of geologic data and, therefore, provide the most uniform measure of potential for REE concentration in a HUC. High values for REE and other HFSE in stream sediments commonly are spatially coincident with exposed alkaline igneous rocks and also coincide with known occurrences and prospects that contain these elements. These relations confirm that elevated abundances of the elements of interest in stream sediments suitably indicate the presence of permissive rock types. Elevated values for multiple elements of interest further support the potential for undiscovered concentrations of these elements in particular HUCs.

Not all REE were analyzed for every sediment sample. The most comprehensive analysis for LREE in stream-sediment samples statewide is best represented by abundances of Ce, whereas

abundance data for Yb is most representative of HREE contents. Thorium is another important trace element that is commonly associated with REE (Portnov, 1987; Bea, 1996); its radioactivity renders Th a useful exploration tool because its relative abundance can also be measured by airborne radiometric surveys. Niobium is a less common representative of HFSE than Y or Zr in rocks and, therefore, is considered a stronger indicator for REE-Th-Y-Nb(-U-Zr) concentrations. Consequently, geochemical data for Ce, Yb, Nb, and Th in stream-sediment samples were used to score HUCs for their REE-Th-Y-Nb(-U-Zr) potential. HUCs containing samples that have concentrations of Ce, Yb, Nb, and (or) Th between the 91st and 98th percentile values (appendix A) received one point for each element having an abundance in that range (table 2); those that have concentrations of Ce or Yb above the 98th percentile values received two points for each element having an abundance in that range. Each of the four elements contributed just once to a HUC's score. Thus, the maximum score for REE *potential* for any HUC on the basis of stream-sediment chemistry was six. HUCs for which stream-sediment data are available received a maximum of one point toward the HUC total *certainty* score (table 3).

Heavy-Mineral-Concentrate Data

The heavy-mineral-concentrate (HMC) dataset for Alaska contains 49,783 sample records that have chemistry and 18,137 samples that have mineralogy data. Although this is not a comprehensive dataset, these localities are important because they demonstrate REE-mineral-bearing rocks in a HUC. The HMC data are divided into two components, mineralogy and chemistry, in the AGDB2. The database also includes estimates of relative amounts of identified minerals (from "trace" to "abundant") for some samples, but relative abundance was not factored into the scoring process because of incomplete coverage in the dataset. HUCs that contain HMC having REE-bearing minerals such as columbite or xenotime were assigned a score of three points. HUCs that contain indicator minerals, such as fluorite or uranothorite, that are commonly associated with REE received two points, whereas identification of HFSE-bearing minerals, such as allanite or zircon, resulted in a score of one point. The maximum *potential* score derived from identified heavy minerals was capped at three points per HUC (table 2). HMC chemistry also contributed to HUC *potential* scores for REE-HFSE. The abundances of Nb, Th, Ce, and Yb used for scoring in table 2 reflect approximately the 80th percentile for the "best value" dataset and for the semiquantitative emission-spectroscopy (ES_SQ) dataset, which are different quantities because of the stepwise method of reporting results for that method; these resulted in one additional point per HUC, whereas values for Ce and Yb above the 95th percentile resulted in two points per HUC. HMC chemistry contributed a maximum of three points to overall HUC scores for REE-HFSE *potential* (table 2). Availability of HMC data, regardless of whether the score was zero (that is, no minerals of interest present) or more (that is, minerals of interest identified), contributed one point to HUC *certainty* scores (table 3); a lack of HMC data for a HUC—a null value—contributed no points to the *certainty* score for a HUC.

Aerial Gamma-Ray Survey Data

Aerial gamma-ray survey data cover most of Alaska (Duval, 2001). The aerial radiometric-survey data are gridded in 5-km cells, which permitted calculation of average scores for individual HUCs, and are reported in four channels, including (1) total count, (2) equivalent uranium (eU), (3) equivalent thorium (eTh), and (4) equivalent potassium (eK) (Saltus and others, 1999; Duval, 2001). Handheld radioactivity measurements locally confirm that alkaline igneous rocks are the source of radioactivity in Alaska.

Radiometric surveys, therefore, provide a remote-sensing proxy to identify areas possibly underlain by Th- and REE-bearing rocks. High Th/K ratios are characteristic of igneous rocks associated with Sn, W, and rare-metal deposits (Portnov, 1987); an eTh/eK ratio greater than 5 indicates Th and HFSE concentrations in igneous rock or sediment that substantially exceed background levels in Alaska

(Saltus and others, 1999). Consequently, an eTh/eK ratio greater than 12 represents the top 1 percent of rocks in Alaska; these may contain concentrations of REE. Accordingly, the resource potential of HUCs that have eTh/eK ratios greater than 5 were assigned a score of one; those that have eTh/eK ratios greater than 12 were assigned a score of 2 for REE-HFSE *potential* (table 2). HUCs for which airborne radiometric-survey data are available were assigned one point for *certainty* (table 3).

Results and Discussion

Resource *potential* and *certainty* scores were summed and classified for each HUC in Alaska (tables 2, 3). Data are lacking for 3,337 HUCs (19 percent of the 17,177 HUCs statewide), and these HUCs were assigned Unknown *potential* (colored gray on plate 1). Total HUC scores that are based on parameters in table 2 were classified by the Jenks method into three categories, which correspond to High, Medium, and Low *potential* for REE-bearing mineral deposits. Score ranges for High, Medium, and Low *potential* are 22–7, 6–3, and 2–0, respectively (colored red, yellow, and green, respectively, on plate 1). A measure of *certainty* was also assigned to each HUC on the basis of the number of datasets that contributed to the resource *potential* score (table 3). HUCs that were assigned High *certainty* received scores from at least five contributing datasets; those assigned Medium *certainty* received scores from 3 or 4 datasets; and those assigned Low *certainty* reflect contributions from only one dataset (table 3) (these are shown in bold, medium, or light shades of color, respectively, on plate 1). Approximately 5 percent (696) of the 13,840 scored HUCs were ranked as having High *potential* to contain REE-Th-Y-Nb(-U-Zr) deposits associated with alkaline igneous rocks. High *certainty* was assigned to 222 of the high-*potential* HUCs; 456 were assigned Medium *certainty*; and 18 were assigned Low *certainty*. About 20 percent (2,784) of the scored HUCs were assigned Medium *potential* for REE-Th-Y-Nb(-U-Zr) deposits. Of these, 414 were assigned High *certainty*; 1,639 were assigned Medium *certainty*, and 731 were assigned Low *certainty* (table 3; plate 1). The remaining 75 percent of the scored HUCs (10,360) were assigned Low *potential* for REE-Th-Y-Nb(-U-Zr) mineralization, but HUCs that have Low *potential* and Low *certainty* reflect a lack of data, and they could have higher resource potential if additional data were available (table 3; plate 1). The HUCs that have Low *certainty* should be considered important areas for additional data collection, regardless of their *potential*.

Known REE-Th-Y-Nb(-U-Zr) Mineralization in Peralkaline to Carbonatitic Intrusive Rocks in Alaska

Few REE-Th-Y-Nb(-U-Zr) deposits in alkaline igneous rocks are presently known in Alaska (table 1). The sole carbonatite consists of a set of 30-m-thick dikes that extend for about 20 km at Tofty (plate 2). The best known example of mineralization associated with peralkaline granite is Bokan Mountain, the location of the Ross Adams mine, which produced 77,000 metric tons of high-grade uranium ore (Long and others, 2010). At Bokan Mountain, unusually HREE-rich mineral concentrations are found in a swarm of veins and dikes that extend southeastward from the pluton. Most known REE-Th-Y-Nb(-U-Zr) prospects and occurrences in Alaska are either small features, such as veins or greisens associated with larger igneous bodies (for example, see Barker and Foley, 1986), or placer deposits that contain REE-bearing minerals (for example, see Barker and others, 2009). Areas of known REE mineralization associated with alkaline igneous rocks include, from north to south, (1) the Porcupine area, (2) the Darby-Hogatza belt, (3) the Kokrines-Hodzana belt, (4) the Kuskokwim–White Mountains belt, which includes Tofty, (5) the Yukon-Tanana uplands, (6) the western Alaska Range, and (7) the Alexander belt, which contains Bokan Mountain (plate 2).

The Porcupine area (plate 2) is partly underlain by the Old Crow batholith, which consists of Carboniferous granite and quartz monzonite with associated quartz veins and derivative placer deposits that contain xenotime, uranophane, arsenuranylite, and metatorbernite (Barker, 1981b).

The Darby-Hogatza igneous belt contains middle to Late Cretaceous alkaline intrusive and extrusive rocks that extend from the Darby Mountains northward to the Selawik Hills and eastward to

the Hogatza River (plate 2). The igneous rocks in this belt, which include syenite, nepheline syenite, lamprophyre, monzonite, and granite, variably contain disseminated fluorite, goethite, xenotime, zircon with radioactive haloes, and radioactive minerals. The igneous rocks are cut by numerous contemporaneous shear zones that contain quartz, xenotime, and radioactive minerals (Barker, 1985). In the Zane Hills, monzonite, syenite, bostonite stocks, various dikes, and associated polymetallic quartz veins contain allanite, betafite, fluorite, and tourmaline (plate 2; see also Miller and Ferrians, 1968; Miller and Elliott, 1977). These rocks, which also contain known U-Th-Nb-Y mineralization, are overlain by sedimentary rocks that also contain U-bearing minerals, presumably sourced from these alkaline intrusive rocks (Miller and Ferrians, 1968). In the Hogatza placer deposit, Staatz (1981) identified thorianite [isometric $(Th,U)O_2$] as sand-sized cubes that matched the thorianite identified in the gneissic monzonite border phase of the Zane Hills pluton.

The Kokrines-Hodzana belt is underlain by the Ruby batholith, which intruded a displaced Paleozoic continental margin terrane, and it extends from the southeastern Brooks Range southwestward to the Kaiyuh Mountains (Patton and Moll-Stalcup, 2000; Patton and others, 2009, their plate 2). The Ruby batholith contains late Early Cretaceous calc-alkaline, alkaline, and peraluminous intrusive rocks that have localized REE, HFSE, and Sn mineralization. Multiple placer occurrences throughout and around the Ruby batholith contain REE- and (or) HFSE-bearing minerals, such as monazite and uranothorite. Placer proximity to exposures of the Ruby batholith and a lack of glacial history indicate the likelihood of local sources. Individual plutons within the Ruby batholith host Sn-bearing veins that also have high HFSE concentrations. The Sithylemenkat pluton (plate 2) hosts one or more tin greisen deposits that have high concentrations of Sn, Nb, Ta, W, and Cs, as well as variable amounts of REE, Th, and U (Barker and Foley, 1986). The Ray Mountains pluton is cut by polymetallic veins that contain hematite, Ag, Pb, Zn, Bi, La, Mo, Sn, U, and W; adjacent gravel deposits contain monazite and xenotime likely derived from the pluton. Porphyritic granite of the Melozitna pluton contains fluorite, monazite, tourmaline, pyrite, molybdenite, and Th- and U-bearing veins (Solie and others, 1993).

A parallel igneous belt southeast of the Ruby batholith, which extends from the White Mountains to the Kuskokwim Mountains (plate 2), contains alkaline intrusive rocks of Late Cretaceous to Paleocene age that include (1) carbonatite sills that contain aeschynite, apatite, monazite, hematite, and magnetite, just northwest of the Tofty district placer workings (Warner and others, 1986; Reifenstuhl and others, 1998), (2) syenite at Roy Creek that contains Th-REE(-U) mineralization (Burton, 1981; Armbrustmacher, 1989), (3) volcanic rocks at Sischu Mountain that contain high concentrations of U, Th, and REE (Miller and others, 1980), and (4) quartz veins and placer deposits in the Iditarod mining district that (in addition to gold) contain zircon, monazite, uranothorite, and fluorapatite and also have high concentrations of U, Th, and REE.

The Yukon-Tanana uplands area (plate 2) contains mineralized veins that include allanite, monazite, and thorite, as well as placer deposits that also contain these minerals. The veins are associated with middle Cretaceous plutons (for example, the Ruby Creek granite) and Late Cretaceous to early Tertiary plutonic complexes (for example, the Charley River batholith, which intrudes ubiquitously mineralized Precambrian and Paleozoic rocks).

In the western Alaska Range, pulses of arc and post-arc magmatic activity resulted in overlapping intrusive complexes that range in age from Early Jurassic to Oligocene. Early Tertiary plutons such as the Tired Pup granite locally contain disseminated allanite, monazite, xenotime, and fluorite (Reed and Anderson, 1969). The early Tertiary Styx River granite porphyry contains abundant accessory fluorite, elevated U and Th contents, and associated U-bearing veins (Reed and Miller, 1980). The Oligocene Windy Fork peralkaline granite, which contains zircon, fluorite, monazite, and apatite, also has associated thorite- and eudialyte-bearing dikes and adjacent placer deposits that contain chevkinite, monazite, eudialyte, thorite, and allanite (Solie, 1983).

Bokan Mountain, in southeasternmost Alaska (plate 2), is the richest REE-bearing deposit currently known in the state (MacKevett, 1963; Dostal and others, 2013, 2014; Verplanck and others, 2014). Bokan Mountain is underlain by a structurally controlled Early Jurassic peralkaline granite pluton cut by late-stage pegmatites, dikes, veins, and hydrothermal alteration zones that are sequentially enriched in U, Th, REE, and (especially) HREE (Dostal and others, 2014). Other alkaline intrusions that trend northward from Bokan Mountain (including one in Dora Bay) also contain concentrations of REE, U, Th, and HFSE (Philpotts and others, 1998). Uranium- and REE-rich dikes at multiple localities east of Salmon Bay (plate 2) are undated but may be related to Tertiary alkaline volcanic rocks that extend to the north as far as Port Camden, where sandstone that is slightly anomalous in uranium is interlayered with the Tertiary volcanic rocks (Dickinson, 1979).

Areas Recognized from this Study that have Potential for REE-Th-Y-Nb(-U-Zr) Deposits

Noteworthy areas in Alaska that have High to Medium *potential* for REE-Th-Y-Nb(-U-Zr) mineralization include the Porcupine area, the Darby-Hogatza belt, the Kokrines-Hodzana belt, the Kuskokwim–White Mountains belt, the Yukon-Tanana uplands area, the western and northern Alaska Range, and southeastern Alaska (plate 2). Many of these areas contain known or suspected REE-Th-Y-Nb(-U-Zr) mineral prospects and (or) occurrences. The distribution of HUCs that have high *potential* scores in these belts delineates geologic trends, whereas individual HUCs highlight specific areas of interest.

Although the maximum possible score for REE-Th-Y-Nb(-U-Zr) resource potential is 22 points, the two highest scoring HUCs (one near the Roy Creek deposit in the White Mountains, and one in the Tired Pup pluton in the western Alaska Range) garnered only 16 points. Both HUCs have ARDF-record scores of only one point, and their high scores result primarily from geochemical and heavy-mineral indicators. Several HUCs, including those in the Kokrines-Hodzana belt, plus a few each in the Darby-Hogatza belt, the White Mountains, and the western and northern Alaska Range, have scores of 15 points; most of these HUCs have null ARDF-record scores (that is, no known mineral occurrences are in the HUC), zero points (the HUC contains an ARDF record, but the record has no REE keywords), or one point (that is, the HUC contains an ARDF record that has a very low REE keyword score). The HUCs that have scores of 12 to14 points are mainly clustered in the Kokrines-Hodzana belt and in the western Alaska Range; additional 12- to 14-point HUCs are scattered in the Darby-Hogatza belt, the White Mountains, the Yukon-Tanana belt, and southeastern Alaska. Most of these HUCs also have low ARDF-record scores, and many have Medium *certainty* classification, which indicates that, despite relatively high scores, some datasets contributed nothing to the final score; these areas warrant further investigation.

Additional HUCs having High *potential* for REE deposits are located outside of previously identified areas in Alaska that have potential for REE mineralization (Szumigala and Werdon, 2011; Barker and Van Gosen, 2012). These areas, described below, highlight the utility of data-driven analysis.

In the central Seward Peninsula, High-*potential* HUCs are coincident with the Kigluaik and Bendeleben Mountains batholiths (plate 2). Their host rocks, metamorphosed Proterozoic and Paleozoic continental-margin rocks, contain abundant dikes and pegmatites associated with the intrusive bodies. The High-*potential* HUCs are coincident with areas underlain by clusters of dikes (Till and others, 2011) that are not shown on the “Geologic Map of Alaska” (Wilson and others, 2015) or included in its accompanying database, but are represented in the rock geochemical database. The HUCs that are coincident with the Kigluaik pluton have low ARDF-record scores of null, zero, or one, and High-*potential* HUCs in the Bendeleben Mountains have ARDF-record scores of null or zero, which indicates that the high scores for these HUCs are derived from datasets other than map lithology and ARDF records.

An area in the central Brooks Range includes eight contiguous HUCs that have High *potential* scores, in spite of having ARDF-record scores of zero (plate 2). These HUCs are underlain by intrusive-rock-associated, Sn-bearing skarns and greisens (Newberry and others, 1986) that, as mentioned above, are products of late magmatic fluids that may locally have been enriched in incompatible elements, including REE and HFSE.

The northern Alaska Range contains four clusters of HUCs that have High *potential* and Medium to High *certainty* for REE potential (plates 1, 2). These HUCs are underlain by tectonically thickened fragments of continental crust intruded by Cretaceous and Tertiary plutons north of the Denali Fault; their bedrock geology is similar to that of the Yukon-Tanana uplands. Some of these HUCs have scores of 12 to 15 points and ARDF-record scores of null or zero, which indicates that they contain no known REE-bearing mineral occurrences; therefore, the high scores must be derived from other datasets. Although the density of High-*potential* HUCs is not as great as in the western Alaska Range, this area similarly merits further evaluation for REE potential.

The largest cluster of High-*potential* HUCs in Alaska is in the western Alaska Range (plate 2). The area contains several small occurrences of REE and U-Th mineralization, but the High-*potential*, Medium- and High-*certainty* HUCs in this area have ARDF-record scores of null, zero, or one, which indicates that their high scores are derived from other datasets; this area appears to be underexplored relative to REE deposits.

In southeastern Alaska, the Coast batholith contains about 20 HUCs that have High *potential* for REE deposits (plate 2). Rocks that host the Coast batholith are of thickened continental crust that is similar in age and composition to basement rocks of the Yukon-Tanana uplands area. Magma-genesis models that are applicable to the Tertiary intrusive rocks underlying the High-*potential* HUCs in the Coast Mountains are similar to those of alkaline intrusive rocks in the other belts on plate 2. In addition, pegmatites are common in the Coast batholith and may contain local concentrations of REE-bearing minerals.

Importantly, many HUCs distributed throughout Alaska that have Medium and High *potential* have Medium and Low *certainty*. Many of these are in areas not known to be associated with REE-Th-Y-Nb(-U-Zr) mineralization. The Medium and Low *certainty* scores indicate that these areas warrant further study in order to clarify their mineral resource potential.

Chapter 2. Placer and Paleoplacer Gold (Au) Deposits

By James V. Jones, III, Jeffrey L. Mauk, Keith A. Labay, Nora B. Shew, and Matthew Granitto

Deposit-Group Characteristics

Placer deposits are concentrations of high-density minerals formed by gravity separation during sedimentary processes. Heavy minerals are separated from their primary host rocks by weathering and erosion and then transported and concentrated in surficial deposits. Placer deposits exhibit a wide range of textures, and they form in many different environments. In addition, they host a variety of minerals, and so they are locally valuable resources for gold, platinum group elements, tin, tungsten, silver, REE, titanium, and iron (Slingerland and Smith, 1986; Garnett and Bassett, 2005; Van Gosen and others, 2014). Gold (Au) in placer deposits was initially derived from bedrock that contains gold-quartz veins, disseminated gold, or other types of gold-bearing mineral deposits such as porphyry Cu, Cu-skarn, and polymetallic-replacement deposits (Yeend, 1986). Primary gold-bearing deposits are typically associated with igneous (Baker, 2002; Seedorff and others, 2005; Hart, 2007; Sinclair, 2007; Taylor, 2007) or metamorphic (Berger and Henley, 1989; Groves and others, 1998; Goldfarb and others, 2005) rocks, although sedimentary rocks can also host veins, replacement deposits, skarns, paleoplacers, and modified paleoplacers (Pretorius, 1981; Minter, 2006).

Within drainage networks, alluvial placer deposits form in fluvial environments, and they represent the initial concentration of heavy minerals relative to source deposits. Heavy-mineral concentration and deposition occurs where gradients flatten and (or) transport velocities decrease, such as at the inside of meanders, below rapids and falls, beneath boulders, and in vegetation mats (Yeend, 1986). Placer gold deposits are typically in alluvial gravel and conglomerate. Gold grains and, more rarely, nuggets are most concentrated at the base of gravel deposits where natural traps such as riffles, fractures, bedding planes, or other features are oriented transverse to water flow. Additional concentration occurs where sediment moves downstream and older alluvial deposits are reworked by younger systems. These processes occur in geomorphologically stable areas that have extended erosional histories and where many generations of sediment and (or) sedimentary rock have been recycled into potentially multiple stages of terrace and streambed gravels (Yeend, 1986).

Coastal placer and paleoplacer deposits, or beach placers, form in a variety of coastal sedimentary environments that are dominated by eolian, wave, and tidal processes (Hamilton, 1995; Van Gosen and others, 2014). Heavy minerals in the coastal environment are derived from sources that include deeply weathered local bedrock exposures, sediment deposited at river mouths, or offshore sand deposits scoured from the seafloor during storm events. Along wave-dominated coastlines, heavy-mineral enrichment prevails in the foreshore and uppermost shoreface environments where sediment is repeatedly reworked by wind, waves, and wave-induced currents. Strong onshore winds winnow shoreface deposits at low tide and ultimately transport sediment inland from the beach environment (Roy, 1999). Longshore transport currents, or littoral drift, move sand along the coast in the direction of prevailing winds, and headlands that protrude from drift-aligned coasts trap heavy minerals on the updrift side of embayments. Most large coastal placer deposits form along passive tectonic margins that have long erosional histories and repeated cycles of sea-level change (Force, 1991). Worldwide, coastal placer deposits that form along convergent and transform tectonic margins, which are generally much smaller than those formed on passive margins, are dominated by sediment derived from relatively local sources.

Alaska has more than 9,600 km (6,000 mi) of coastline and as many as 584,000 km (365,000 linear miles) of fluvial environments. Known placer districts are present throughout the state in both

coastal and interior regions (plate 4). Several regions, such as those surrounding Nome and Fairbanks (plate 4), have been the locus of significant placer-gold production. In addition to Au, Alaskan placer deposits contain combinations of PGE, Sn, W, Ag, Hg, Ti, and REE (Nokleberg and others, 1987). Alaska was well known worldwide for production of PGEs between 1934 and 1963 from placer workings along the Salmon River and its tributaries and terraces, south of Goodnews Bay (Mertie, 1976). Placer gold is the only commodity evaluated herein because it remains the primary commodity presently produced from placer mines in Alaska (Athey and others, 2013).

Mineral-Resource-Potential Estimation Method

Placer and paleoplacer Au *potential* was scored on the basis of the following criteria: (1) ARDF records, (2) heavy-mineral-concentrate (HMC) mineralogy, (3) stream-sediment geochemistry, (4) lithology, and (5) identification of river or stream reaches downgradient from HUCs that have high or medium favorability (table 3).

Lithology

Generalized igneous-rock- and sedimentary-rock-distribution maps, which were derived from the digital "Geologic Map of Alaska" (Wilson and others, 2015), were used to identify areas of igneous- or sedimentary-host lithologies that are permissive for the occurrence of associated placer deposits. Lithologic map units had different point values as outlined in table 4. The HUCs that contain multiple types of igneous rocks received points according to the rock unit that has the highest point score. Thus, the maximum possible score derived from igneous lithology for a HUC is 3 (table 4). Three classes of coarse-grained sedimentary rocks that have potential for derivative placer deposits were identified from the geologic map. HUCs that contain "high-level gravel" or "placer and anthropogenic deposits" received 5 points, whereas those that contain undivided older surficial deposits received 3 points (table 4). However, the general lack of detailed surficial-map-unit data made it difficult to confidently identify surficial and sedimentary units that may be most suitable for associated placer and paleoplacer deposits. Therefore, points were not assigned to areas underlain by other sedimentary rocks and surficial deposits. For each HUC, maximum points derived from igneous- and sedimentary-rock or deposit data were summed, resulting in a maximum possible lithology score of 8.

Alaska Resource Data File

Alaska Resource Data File (ARDF) records were scored in a two-step process. First, ARDF records for placer mines, prospects, and occurrences were identified by searching for appropriate keywords in the deposit model number and deposit-model definition fields. These initial results, which are described as tier 1 totals (appendix C), were labeled "TOTAL" in the associated ARDF data file (appendix E). Only ARDF records that received a nonzero tier 1 total were considered to be a placer or paleoplacer record. Records having a total of zero were not considered further for this deposit group. Tier 2 totals (labeled "PLACER_TOTAL" in appendix E) were assigned according to keywords in the fields for site type (for example, mine, prospect, occurrence), site status (for example, active, inactive, undetermined), and production estimates (for example, yes, no, undetermined). The maximum possible tier 2 total for each ARDF placer or paleoplacer record is 57 (appendix C). For each individual HUC, the ARDF record that had the highest tier 2 total was used to assign a derivative score, following the criteria outlined in table 4. For example, a HUC containing an ARDF record that had a tier 2 total of 38 was assigned a score of 18 (table 4). Even if the HUC contains other ARDF records having nonzero tier 2 totals, only the record that had the highest total was used to assign the score. HUCs that contain ARDF records that did not meet the placer or paleoplacer criteria (that is, had a tier 1 total of zero) received an ARDF-record score of zero. HUCs that contain no ARDF records received an ARDF-record score of

null. A score of 20 points is the maximum possible that can be derived for each HUC from ARDF data (table 4). HUCs that had an ARDF-record score of 12 or higher were automatically assigned high *potential*.

Heavy-Mineral-Concentrate Mineralogy

HUCs that contain one or more HMC samples in which visible gold was present or inferred (that is, value not null) were given 10 points and automatically assigned high *potential*. The term "inferred" for a particular mineral in HMC samples indicates the probability of that mineral's presence in a sample on the basis of chemical analyses and previous USGS map publications (Granitto and others, 2011). HUCs containing one or more samples that had an HMC report indicating cassiterite, powellite, scheelite, cinnabar, monazite, and (or) thorite (that is, value not null) were given 1 point for each of these minerals present. For each HUC, the possible points derived from HMC mineralogy is a maximum of 10, or the total number of other non-Au heavy ore-minerals present (table 4).

Stream-Sediment Geochemistry

HUCs that contain one or more stream sediment samples having Au and (or) Ag values in the 75th percentile or higher (Au, ≥0.007 ppm; Ag, ≥0.16 ppm) received 3 points for each element. HUCs that contain one or more stream sediment samples having Ti and (or) W values in the 75th percentile or higher (Ti, ≥0.57 ppm; W, ≥2 ppm) received 1 point for each element. For each HUC, the maximum possible points derived from stream-sediment chemistry is 8 (table 4).

Results and Discussion

All HUCs were initially scored using the four datasets and corresponding values and criteria described above (table 4); mineral resource *potential* and *certainty* were estimated accordingly (table 5). All HUCs that had ARDF-record scores of 12 or higher or that had mineralogy scores of 10 were automatically assigned High *potential* because the presence of a known placer occurrence, prospect, or mine and the presence of gold (either visually confirmed or inferred from other data) in one or more HMC samples are presumably robust predictors of placer or paleoplacer potential. All other HUCs that had total scores of 16 or higher were assigned High *potential* (table 4). The 16-point cutoff value is consistent with HUCs that have the maximum possible score for at least three of the remaining scoring components. HUCs that had scores of 6–15 and 1–5 were assigned Medium and Low *potential*, respectively. The 6-point cutoff value that corresponds to minimal Medium *potential* was chosen because scores of 6 or higher generally correspond to a maximum possible score from at least one of the component scoring sources. HUCs that had a score of zero and HUCs for which stream-sediment geochemical data are unavailable were assigned Unknown *potential*. Following preliminary scoring and classification using the four scoring components described above, a fifth scoring component was added to the analysis to account for potential placer occurrences downstream from HUCs with high placer or paleoplacer Au potential (table 4). All river and stream segments downstream from each High-*potential* HUC were selected from National Hydrography Dataset and assigned an additional score of 6 points, whereas HUCs adjacent to and downstream from Medium-*potential* HUCs received an additional 3 points. Downstream HUC scores were reclassified if needed using the criteria described above (table 4). Rescoring downstream HUCs excluded those already assigned High *potential*; consequently, only HUCs that have Medium, Low, or Unknown *potential*, as defined in the initial scoring process, could receive augmented ratings. Downstream score augmentation was continued iteratively until all possible scores and reclassifications were propagated downstream.

Estimated resource potential *certainty* was largely defined by the number of datasets that contributed to total HUC scores (table 5). For example, High *certainty* was assigned to HUCs that have

ARDF-record scores of 18 or higher or if all five datasets contributed to the total HUC score (table 5). HUCs that have Unknown *potential* (that is, zero points and no associated stream-sediment geochemical data) could not be assigned any level of *certainty*.

Resource *potential* and *certainty* scores were summed and classified for each HUC in Alaska (tables 4, 5; plate 3; appendix E). Accordingly, 1,472 (8.6 percent) of the 17,177 HUCs in Alaska were estimated to have High *potential* for associated placer or paleoplacer Au deposits, of which less than half (42.3 percent) have High *certainty*. Of the 3,094 HUCs (18.0 percent) that were estimated to have Medium *potential*, most (89.8 percent) have Medium *certainty*. More than half (10,288, or 59.9 percent) of the HUCs were estimated to have Low *potential* for placer or paleoplacer Au deposits, and the majority (61.6 percent) of these have Medium *certainty*. A total score of 0 was assigned to 4,660 HUCs, and nearly half of these (2,323 total) have Unknown *potential* and *certainty* because they contain no stream-sediment data; these 2,323 HUCs that have Unknown *potential* represent more than 80,000 km^2, an area only slightly smaller than that of the state of South Carolina. The total area having Low *certainty* is similarly large, exceeding 88,000 km^2.

Regions that have the greatest concentration of high-scoring HUCs include known placer districts in the central, southern, and eastern Seward Peninsula (Nome and Fairhaven districts); large parts of the Yukon-Tanana uplands area (Eagle and Fortymile districts); the central and eastern Alaska Range (Bonnifield, Valdez Creek, Delta, and Chistochina districts); and parts of the Kenai Peninsula (Hope district) and Chugach Mountains (plate 4). A more diffuse High-*potential* terrane extends across the southern Brooks Range from the Baird Mountains quadrangle east to the Chandalar quadrangle (Wiseman and Chandalar districts). Another High-*potential* terrane extends across parts of southwestern Alaska from the Goodnews Bay quadrangle northeast to the Ruby and Medfra quadrangles (Aniak, Iditarod, Innoko, and Ruby districts) and east-northeast to the Lime Hills and Circle quadrangles (Hot Springs, Fairbanks, and Circle districts). Localized coastal areas that have High *potential* include the southern coast of the Seward Peninsula; the southern Kenai Peninsula; Prince William Sound; near Yakutat; and parts of southeastern Alaska (Porcupine Creek district).

Most areas that include many HUCs that have High to Medium placer *potential* also contain known placer districts (plate 4; see also, Nokleberg and others, 1987). The most prominent examples that were estimated to contain significant areas of High *potential* include the entire Lime Hills quadrangle, the western Alaska Range, and parts of the Taylor Mountains and Bethel quadrangles in southwestern Alaska. The eastern part of the Lime Hills quadrangle contains extensive Late Cretaceous and Paleocene igneous rocks of the western Alaska Range, as well as multiple associated intrusion-related and porphyry prospects and occurrences (Gamble and others, 2013; Graham and others, 2013). Similar-age igneous intrusions crop out in the western part of the Lime Hills quadrangle and also to the south and west in the Lake Clark and Taylor Mountains quadrangles. In these areas, mapped igneous bodies are far less extensive and, in some cases, form dike and sill networks rather than discrete plutons (Bundtzen and Miller, 1997). These areas are characterized by their more subdued topography relative to that of the Alaska Range to the east and the Kuskokwim Mountains to the west, resulting in poor exposures. The terrane that has elevated placer and (or) paleoplacer Au potential in the Lime Hills and Taylor Mountains quadrangles is consistent with a relatively continuous belt of late Mesozoic to early Cenozoic gold mineralization (plate 4), which extends from the Alaska Range westward to the Kuskokwim Mountains (Bundtzen and Miller, 1997; Graham and others, 2013).

Ready identification of placer potential in the Taylor Mountains, Sleetmute, Iditarod, and Lime Hills quadrangles is an outcome of studies of the Alaska Mineral Resource Assessment Program (AMRAP) that involved extensive and systematic sampling of stream sediment, heavy-mineral concentrates, and bedrock (Eppinger, 1993; Miller and others, 2006). However, some uncertainty remains. For example, stream-sediment and heavy-mineral-concentrate sampling was focused in the northwestern part of the Sleetmute quadrangle (Gray and others, 1997), where placer and paleoplacer Au

potential is generally High or Medium (plate 4). In contrast, resource potential is largely unknown in the southeastern part of the Sleetmute quadrangle, where sampling and interpretation are inadequate.

In Alaska, the total area that had either Unknown *potential* or Low *certainty* is more than 169,000 km^2, which is more than 11 percent of the state and which is an area larger than that of the state of Georgia. These large, poorly studied areas having Unknown *potential* or Low *certainty* require considerably more study statewide; discrepancies in the density of stream-sediment sampling and the disparate quality of geochemical datasets further underscore the need for additional investigations.

Chapter 3. PGE(-Co-Cr-Cu-Ni-Ti-V) Deposits Associated with Mafic to Ultramafic Intrusive Rocks

By Melanie B. Werdon, Jeanine M. Schmidt, Keith A. Labay, and Nora B. Shew

Deposit-Group Characteristics

The platinum group elements (PGE), which consist of six metallic elements—Ru, Rh, Pd, Os, Ir, and Pt—that have similar physical and chemical properties, often coexist in single mineral deposits (Harris and Cabri, 1991). The PGE are subdivided into the iridium (Os, Ir, Ru) and palladium (Rh, Pt, Pd) subgroups because the members of each subgroup each behave coherently during magmatic processes (Rollinson, 1993). The PGE, which form more than 100 PGE-bearing minerals, are also constituents of native metals, alloys, and complex solid solutions (Cabri, 2002). PGE also variably associate with Co, Cr, Cu, Ni, Ti, and V in deposits associated with mafic to ultramafic (MUM) rocks.

Diverse MUM-related deposit types contributed to the Alaskan resource analysis (tables 1, 6). The MUM-rock-related PGE-bearing deposit types that are recognized in Alaska include (1) placer (for example, Goodnews Bay in southwestern Alaska); (2) Alaska-Ural-type zoned MUM complexes (for example, Red Mountain and Goodnews Bay in southwestern Alaska; also, numerous occurrences in southeastern Alaska); (3) differentiated MUM intrusions (sills) that are part of the magmatic delivery and storage system associated with overlying mafic volcanic rocks (for example, the Nikolai Greenstone, part of the Wrangellia terrane in south-central Alaska); (4) suprasubduction ophiolites (for example, Misheguk Mountain, part of the Angayucham terrane in the western Brooks Range, northern Alaska); (5) synorogenic layered mafic complexes near major suture zones (for example, Brady Glacier deposit, along the Fairweather trend in southeastern Alaska); and (6) mantle rocks exposed at the base of island arcs (for example, Tonsina-area occurrences, Talkeetna arc, part of the Peninsula terrane in south-central Alaska). Alaska may include other unrecognized MUM-related PGE deposit types (table 6). Additional non-MUM-related ore-deposit types in Alaska may include associated PGE enrichments (table 6). The scoring criteria outlined below were optimized for deposits generally associated with MUM rocks, but some more diagnostic PGE indicators, including geochemical data, might reveal potential for non-MUM-related PGE deposit types or deposit types not presently known in Alaska.

Mineral-Resource-Potential Estimation Method

The datasets described below were evaluated for parameters that identify PGE(-Co-Cr-Cu-Ni-Ti-V) deposit potential (table 7). These datasets were ranked according to their effectiveness relative to predicting potential for deposits of these elements. HUCs were scored on the basis of the following criteria: (1) MUM rocks, (2) PGE mineral occurrences, prospects, or mines, (3) PGE-bearing or PGE-indicator minerals in placers and heavy-mineral-concentrate mineral reports, and (4) abundances of Pt, Pd, Os, Ir, Rh, Ru, Co, Cr, Cu, Ni, Ti, and (or) V in either (a) heavy-mineral-concentrate samples, (b) stream-sediment samples, or (c) rock samples (table 7). Although copper is often associated with various PGE deposits, it is also present in numerous non-PGE-bearing deposit types. Consequently, copper was excluded from the PGE scoring schema to avoid generating false-positive PGE responses.

Lithology

A generalized lithology layer from the digital "Geologic Map of Alaska" (Wilson and others, 2015) that included all mafic to ultramafic igneous rock units statewide was used to identify areas underlain by rock types permissive for PGE deposits, particularly MUM rocks (Wilson and others,

2015). The HUCs that contain mafic or ultramafic igneous rocks as major components of the geologic map units received 2 points, and those that contain mafic or ultramafic igneous rocks as minor or incidental components received 1 point (table 7). The HUCs that contain multiple rock types received the number of points associated with the most highly rated MUM rock type present, whether or not that lithology is distributed throughout the HUC. Thus, the maximum possible score assigned to a HUC on the basis of lithology is 2 (table 7).

Alaska Resource Data File

Alaska Resource Data File (ARDF) records for placer occurrences, prospects, and mines were removed from the ARDF dataset and incorporated with available heavy-mineral-concentrate mineralogy data (see below). The remaining lode-related ARDF records were scored for PGE favorability on the basis of the keyword method described above; targeted keywords include MUM lithologies, associated elements (Pt, Pd, Ir, Os, Rh, Ru, Co, Cr, Ni, Ti, V), and PGE-bearing minerals (for example, sperrylite, native platinum) (for complete list, see appendix C). Each highly ranked ARDF record was reviewed after scoring, and occurrences clearly unrelated to one of the appropriate PGE models enumerated above were excluded. The remaining ARDF records were further classified into those that have either (1) PGEs reported as major or minor commodities, which received 3 points, (2) chromite and favorable geology, which received 2 points, or (3) permissible geology but no direct evidence for PGEs, which received 1 point. The maximum possible HUC score derived from keywords from ARDF records is 3 points (table 7).

Heavy-Mineral-Concentrate Mineralogy

The ARDF placer records and the HMC mineralogy dataset both indicate locations in streams where targeted PGE-indicator minerals and elements are present. The HMC mineralogy dataset has incomplete spatial coverage statewide, and some ARDF placer records spatially coincide with those of the HMC mineral localities. As such, these two datasets were combined in order to not overweight these criteria and also to evaluate lithological, ARDF-record lode, and geochemical factors.

Using the keyword method, ARDF placer records that have reported occurrences of MUM-related minerals were subdivided and assigned points as follows: (1) records that have PGEs reported as major or minor elements received 3 points, (2) records that list chromite or other PGE-related minerals or that have uncertain PGE mentions received 2 points, and (3) records that have mineralogy appropriate for the occurrence of MUM rocks (for example, jade or serpentine-group minerals) but that lack direct evidence for PGEs received 1 point (table 7). The HUCs lacking ARDF placer records that have PGE scores but containing one or more samples from the HMC dataset that have mineral identifications of chromite, Cu-Co sulfides, Ni-Co-sulfides, Ni-sulfides, or Cr-Ni silicates received 2 points. The HUCs that contain HMC mineral identifications of serpentine or Cr-diopside in one or more samples received a score of 1 point. The maximum possible score for a HUC on the basis of combined ARDF placer records and HMC mineralogy was 3 points (table 7).

Approach for Geochemical Datasets

Geochemical data for heavy-mineral concentrates, stream sediment, and rocks were evaluated statistically and assigned points according to relative element abundance. Samples whose PGE abundances are in the 91st or higher percentile initially received 3 points. Similarly, samples whose abundances of Co, Cr, Ni, Ti, and (or) V are in the 98th or higher percentile initially received 2 points, and those with abundances between the 91st and 98th percentiles received 1 point.

The spatial distribution of samples that have elemental abundances assigned to these percentile categories was examined to check for spatial artifacts, which commonly can result from the “qualitative

step levels" associated with semi-quantitative emission spectroscopic analyses. Identified artifacts were manually resolved; abundance scores were reassigned by examining the histogram of values for each element and visually selecting a reasonable cutoff abundance corresponding to anomalous (1 point) and highly anomalous (2 points) values. Highly anomalous values were also checked for possible spatial correlation with known PGE occurrences. Cutoff values (in ppm) were defined to yield geologically reasonable numbers of anomalous samples where PGE occurrences are known or unknown. The process of assigning points for abundances of each element for each dataset is discussed below (table 7). Geochemical data for heavy-mineral concentrates, stream sediment, and rocks contributed a maximum of 3 points each to a HUC.

Heavy-Mineral-Concentrate Geochemistry

The HUCs that contain one or more HMC samples having Pt, Pd, Os, or Ir contents greater than 0 ppm received 3 points (the dataset contains no abundance data for either Rh or Ru). The HUCs that contain one or more HMC samples having TiO_2 contents greater than 5 weight percent received 1 point. The scores for Co, Cr, Ni, and V were manually assigned by examining their abundance histograms; cutoff values were defined to yield reasonable numbers of anomalous (1 point) and highly anomalous (2 points) abundances for each element. The maximum possible score for each HUC derived from HMC geochemical data is 3 points (table 7).

Stream-Sediment Geochemistry

The HUCs containing one or more stream-sediment geochemical samples that have Pt, Pd, or Os contents exceeding the 91st percentile cutoff value received 3 points (the dataset contains no abundance data for Ir, Rh, or Ru). For Co, the natural-breaks method was used to assign scores of 2 points to the 98th percentile values and 1 point to the 91st percentile values. The scores for Cr, Ni, Ti, and V were manually assigned by examining their abundance histograms; cutoff values were defined to yield reasonable numbers of anomalous (1 point) and highly anomalous (2 points) abundances for each element. The maximum possible score for each HUC derived from stream-sediment chemical data is 3 points (table 7).

Rock Geochemistry

Rock geochemical data in the USGS and ADGGS datasets were scored separately. The ADGGS database primarily contains samples collected for mineral resource assessments, whereas the USGS database contains samples collected to define background rock-geochemical abundances, in addition to samples collected for mineral resource assessments. Accordingly, natural breaks in element-abundance distributions for the two datasets are significantly different. Historically, USGS investigators collected hundreds of samples to determine low-level background values for igneous-rock terranes, thus, resulting in relatively low mean and median values for the associated abundance distributions. Relative to the USGS dataset, HUCs that contain one or more rock samples having Pt contents greater than 0.004 ppm or Pd contents greater than 0.005 ppm received 3 points. Relative to the ADGGS dataset, HUCs that contain one or more rock samples with Pt contents greater than 0 ppm or Pd contents greater than 0 ppm received 3 points. Relative to both the USGS and ADGGS datasets, HUCs that contain one or more rock samples having Ir, Rh, or Ru contents greater than 0 ppm received 3 points. Neither dataset contains abundance data for Os. Co, Cr, Ni, Ti, and V, and so these scores were manually assigned by examining their abundance histograms; cutoff values were defined to yield reasonable numbers of anomalous (1 point) and highly anomalous (2 points) abundances for each element. The maximum possible score for each HUC derived from rock chemistry is 3 points (table 7).

Results and Discussion

PGE(-Co-Cr-Ni-Ti-V) resource *potential* and *certainty* were established for each HUC (table 8); total scores range from 0 to 11, based on all available data (appendix E). Accordingly, 2,426 HUCs (14 percent) of the 17,177 HUCs in Alaska were estimated to have High PGE *potential* (plate 5; appendix E). Of these, 593 HUCs (24.4 percent) have High *certainty*. Of the 3,295 HUCs (19 percent) that were estimated to have Medium PGE *potential*, about half have Medium *certainty*. About 45 percent of HUCs have Low PGE *potential*, although most (57.9 percent) Low PGE *potential* HUCs also have Low *certainty*. The 3,780 HUCs that have a total score of 0 were assigned Unknown *potential* and *certainty*.

Future geologic investigations should focus on areas that have relatively High *potential* scores but for which available data are limited. Areas that have High *potential* include (1) the Angayucham terrane (in the northwestern Brooks Range and south of the central Brooks Range); (2) the Goodnews Bay-Kilbuk terrane (in southwestern Alaska); (3) the Wrangellia terrane (in south-central Alaska); (4) the Peninsular terrane (in south-central Alaska); and (5) most of southeastern Alaska (plate 6). In areas that have High and Medium PGE *potential*, future investigations should include (1) using the generic MUM-related-deposit criteria to refine individual MUM-related and non-MUM-related PGE deposit models (table 6); (2) using MUM rock geochemistry to determine the spatial distribution, types, and geologic settings of MUM rocks; (3) completing modern geochemical analyses of archived sediment and rock samples originally analyzed for a limited number of elements by semi-quantitative emission spectroscopic methods; (4) conducting stream-sediment and rock geochemical sampling in High and Medium PGE *potential* HUCs to identify lode source(s) of PGE, Co, Cr, Cu, Ni, Ti, and (or) V anomalies; (5) conducting rock sampling to fill gaps in igneous-rock geochemical and geochronology databases; (6) analyzing available geophysical data to identify areas that may contain PGE-deposit-associated rock types; and (7) conducting geologic mapping in High and Medium PGE *potential* HUCs to delineate MUM rocks and to identify other PGE-deposit-associated rock types. The scoring criteria described above for PGE deposits were optimized for PGE deposits associated with MUM rocks. Consequently, scoring parameters relevant to other types of PGE deposits (for example, those not associated with MUM rocks or not presently known to occur in Alaska) might be modified to best identify additional PGE-deposit potential.

Chapter 4. Carbonate-Hosted Cu(-Co-Ag-Ge-Ga) Deposits

By Timothy S. Hayes, Jeanine M. Schmidt, Jeffrey L. Mauk, Matthew Granitto, Nora B. Shew, and Keith A. Labay

Deposit-Group Characteristics

The Alaskan carbonate-hosted Cu deposits evaluated herein are of two distinct types, Kennecott-type and Kipushi-type. Both types commonly contain Ag; in addition, Kipushi-type deposits are characterized by the critical elements Co, Ge, and Ga. Both are stratabound, but not stratiform, within sequences of shallow-water carbonate rocks. The Kennecott-type deposits are named for Cu mineralization found at the Kennecott mine in east-central Alaska; the Kipushi-type deposits are named for Cu mineralization found at the Kipushi mine in the Democratic Republic of Congo, Africa.

Deposits in the Kennecott district consist of veins in the Chitistone Limestone that are as much as about 150 m above its contact with the underlying Nikolai Greenstone. The Nikolai Greenstone is a flood basalt that has high intrinsic copper content. It commonly contains minor quartz+Cu-sulfide or native Cu±calcite veins or broadly conformable zones of amygdules filled with one or more Cu minerals plus quartz, epidote, calcite and chlorite. Although Cu occurrences are very widespread in the Nikolai Greenstone, very little copper has been produced at any of these locations. Copper in the Kennecott veins was apparently derived from the Nikolai Greenstone during prehnite-pumpellyite-facies metamorphism in Early Cretaceous time when copper-bearing metamorphic fluids moved up and away from zones of higher temperature and higher grade metamorphism (Silberman and others, 1980; MacKevett and others, 1997; Price and others, 2014). Consequently, the veins at Kennecott are simply basaltic Cu deposits, similar to occurrences in the Nikolai Greenstone but, instead, hosted by the overlying limestone. Therefore, epigenetic Cu mineralization in the Nikolai Greenstone indicates a high potential for copper deposits in any carbonate rocks that are stratigraphically or structurally above the Nikolai Greenstone. Copper occurrences in the metabasalt are currently not economic targets but can guide exploration for Kennecott-type deposits in nearby carbonate rocks.

The Ruby Creek deposit is the best example of a Kipushi-type deposit in Alaska. At Ruby Creek (plate 8), underground mining (starting in 1965, and continuing at the Bornite Mine) developed two levels in the "Number 1 orebody," a high-grade body of bornite and chalcocite (Bernstein and Cox, 1986). However, most of the currently defined deposit consists of veinlet-controlled, breccia-hosted, replacement chalcopyrite. The Number 1 orebody is a nearly concordant lens that is 3 to 20 m thick, 60 m wide, and 80 m long (Bernstein and Cox, 1986); it is hosted by dolomite breccia that has pyritic fringes on clasts atop a phyllite (formerly argillite) bed. The Ruby Creek deposit (as currently identified by drilling) extends through a thickness of at least 600 m across an area, still open to the northeast and southeast, that is roughly 1.5 km on each side (Davis and others, 2014). Minor pyrite, sphalerite, and hydrothermal dolomite are distributed much more broadly across a 1-km-thick section (Hitzman, 1986). Newly drilled, approximately concordant copper-rich bodies in the South Reef zone are larger than the Number 1 orebody, having a total length that exceeds 750 m (Davis and others, 2014). Reconnaissance-scale stream-sediment-sample data available for Alaska (at about 1 stream-sediment sample per 11.5 km^2) is probably sufficient to identify relatively large copper-bearing deposits; however, it will less accurately (and incompletely) reflect possible small sources of Ag, Co, Ge, or Ga because these critical elements are concentrated in relatively small high-grade lenses within these deposits.

Mineral-Resource-Potential Estimation Method

Scoring schema used to evaluate copper potential in carbonate rocks is complicated by the ubiquitous occurrence of copper (particularly chalcopyrite) in many different deposit types (for example,

volcanogenic massive sulfides, porphyry systems, etc.). The scoring system used here was designed to avoid possible "false-positive indications" associated with other copper-bearing deposit types. That schema minimizes the influence of copper itself and, instead, emphasizes features distinctive to carbonate rocks and the unique critical-element signatures of carbonate-hosted Cu deposits.

Seven types of data were used to score the resource potential of carbonate-hosted Cu deposits in Alaska: (1) lithology, particularly the presence of carbonate host rocks, (2) presence of known (ARDF-record) deposits and occurrences of Cu in sedimentary rocks, particularly carbonates, or Cu in basalt or greenstone, (3) mineralogy of heavy-mineral concentrates derived from stream sediment, (4) abundance of Cu in stream-sediment samples, (5) abundances of Co, Ag, Ge, and Ga in stream-sediment samples, (6) abundance of Cu in sedimentary or metasedimentary rocks, and (7) abundance of Co, Ag, Ge, and Ga in sedimentary or metasedimentary rocks (table 9).

Lithology

Rock-type information, derived from previously published map-unit descriptions, is included in the digital database of the "Geologic Map of Alaska" (Wilson and others, 2015). All map units that contain carbonate rocks were identified and assigned to one of three groups: (1) "Carbonates, major," (2) "Carbonates, minor or incidental," or (3) "Carbonates, indeterminate." "Major" indicates that carbonate rocks constitute at least 33 percent of the map unit; "minor or incidental" indicates that carbonate rocks make up between 10 and 33 percent of the unit; and "indeterminate" indicates that carbonate rocks are included in the unit description but their abundance is not indicated (appendix D). The minimum area considered necessary to contain an economic deposit of carbonate-hosted Cu is 5 km^2. Accordingly, each HUC underlain by at least 5 km^2 of any "Carbonates, major" unit received 5 points. The HUCs that are underlain by less than 5 km^2 of "Carbonates, major" or by any areal extent of "Carbonates, minor or incidental" or "Carbonates, indeterminate" received 1 point (table 9).

Alaska Resource Data File

The Alaska Resource Data File (ARDF) keyword list and scoring criteria for carbonate-hosted Cu deposits was designed to include any occurrences that are consistent with either the Kennecott or Kipushi deposit type, as well as to minimize inclusion of other unrelated, although numerous and widespread, copper occurrences. Highest scores were assigned to ARDF records that correspond to either basaltic Cu- or Kipushi-type deposits (model numbers 23 and 32c, respectively, of Cox and Singer, 1986). Negative scores were assigned to HUCs that contain ARDF records indicative of other deposit types or model numbers (for example, porphyry Cu deposits, volcanic-hosted massive sulfide deposits, or Cu-skarn deposits). No value was assigned to ARDF records classified as polymetallic-replacement deposits or polymetallic veins (model numbers 19a and 22c, repectively, of Cox and Singer, 1986) because of ambiguities associated with their classification. In several ARDF records, polymetallic-replacement-deposit and (or) polymetallic-vein occurrences are described near clusters of Cu-mineral occurrences in carbonate host rocks. Note that models 19a and 22c (Cox and Singer, 1986) are broad descriptions not sufficiently distinctive to determine whether they represent unique deposit types or are parts of larger mineralizing systems. The assignment of zero to records that refer to these model types allows for this possible overlap by assigning neither positive nor negative values.

The ARDF records that indicate Cu and (or) Co as a main commodity received 3 points, whereas those that list any element (for example, Au, Cr, Mo) that is unlikely to occur in a carbonate-hosted Cu deposit received –3 points. Negative scores were also assigned to ARDF records that contain certain keywords (for example, "porphyry," "rhyolite") that are typical of deposits unlikely to be associated with Kennecott- or Kipushi-type deposits (appendix C). The overall ARDF-record keyword rankings produced maximum scores of 23; all the highest scores correspond to occurrences classified as either basaltic Cu- or Kipushi-type.

A score of 3 was assigned to each HUC that contains one or more ARDF records having a keyword score of at least 4 (that is, 4–23). A score of 1 was assigned to each HUC that contains one or more ARDF records having keyword model scores of between 1 and 3, and a score of 0 was assigned to any HUC that contains only ARDF records having keyword score results of less than 1.

Heavy-Mineral-Concentrate Mineralogy

The HUCs that include one or more HMC samples containing copper cobalt sulfides, copper silicate minerals, copper sulfides and (or) oxides, cuprite, or enargite (that is, abundance value is not null in the database) received 2 points for each mineral present. The HUCs having HMCs that contain just chalcopyrite received only 1 point because chalcopyrite is widespread and not unique to carbonate-hosted Cu deposits. The HMC point totals for each HUC are additive for each mineral present; consequently, for any HUC, the maximum score that can be derived from HMC mineralogy is 11 (table 9). In order to emphasize the heavy minerals that are distinctive to the Kipushi- and Kennecott-type copper deposits, no points were assigned for the two Cu minerals that are most commonly identified in HMC samples, malachite and azurite.

Stream-Sediment Geochemistry

The HUCs that contain one or more stream-sediment samples having copper values in the 98th percentile or greater (≥150 ppm) received 2 points; those containing one or more sediment samples that have copper values of at least 50 ppm but less than 150 ppm received 1 point.

Trace metals that are distinctive to copper deposits in carbonate rocks were weighted heavily because copper itself is a constituent of so many different deposit types. The HUCs that contain one or more stream-sediment samples that have Co, Ge, Ga, and (or) Ag concentrations in the 91st percentile or greater (≥36 ppm, ≥3 ppm, ≥30 ppm, ≥0.4 ppm, respectively), received 2 points each for Ga and Ge and 1 point each for Co and Ag. For any HUC, the maximum possible score derived from stream-sediment chemical data is, therefore, 8 points: 2 points for Cu, and 6 points for the trace metals (table 9). In each HUC, the score of the sample having the largest point value was assigned as the score for the entire HUC. This approach eliminates potential bias that can arise from large numbers of samples having been collected in a particular HUC.

Rock Geochemistry

Geochemical data for sedimentary and metasedimentary rocks from both the AGDB2 and the ADGGS databases were also used to quantify the prospectivity of individual HUCs. Those containing sedimentary- or metasedimentary-rock samples that have at least 5,000 ppm Cu received 2 points, whereas those containing rock samples that have at least 1,000 ppm but leas than 5,000 ppm Cu received 1 point. In order to prevent overvaluing the more heavily sampled HUCs, only the sample that had the greatest measured Cu concentration contributed to an individual HUC's score.

The HUCs received additional points when one or more rock samples contained at least 45 ppm Co, at least 3 ppm Ge, at least 35 ppm Ga, and (or) at least 1 ppm Ag. These lower limits were established by Huyck (1990), who examined trace-element abundances in black shales, the sedimentary-rock type that has the highest background contents of these four elements. Our scoring thresholds were designed to award points only when values exceed those of "metalliferous" black shales (Huyck, 1990). Presumably, these elevated concentrations are achieved only with epigenetic addition of trace metals. Accordingly, the HUCs received 1 point each for anomalous Co or Ag abundances and 2 points each for anomalous Ga or Ge concentrations. As with the other scoring components, only the sample having the highest score contributed to each HUC score. Trace-metal geochemical data can contribute as much as 6

points to the score of a single HUC, and the maximum score derived from rock-geochemical data is 8 (table 9).

Results and Discussion

Summing all scoring factors results in a maximum HUC score of 35 points for this deposit type; however, the actual maximum point total tabulated in Alaska is 14. A total score of 14 was achieved by only three HUCs, two in the Kennecott district (in the McCarthy quadrangle) and one in the Talkeetna Mountains quadrangle. All three highest scoring HUCS are underlain by rocks of the Wrangellia terrane (plate 8). Relative mineral resource potential for each HUC was established using the parameters described above (table 10): HUCs that have scores of at least 4 were classified as having Low *potential* for carbonate-hosted copper deposits; those that contain at least 5 km^2 of "Carbonates, major" host rocks received 5 points, which places them in the Medium *potential* category, even if the remaining six parameters contributed nothing to the final scores. Numerous tests of the scoring schema indicate that the presence of a carbonate host-rock unit is the best single predictor of potential for known deposits and major prospects of carbonate-hosted Cu in Alaska. Many basaltic copper-type mineral occurrences are located outside major carbonate-rock terranes, and, although they identify copper-mineralizing systems, the presence of "Carbonates, major" as a host-rock unit marks a clear distinction between the general evidence of a mineralizing system and the HUCs having true potential for economic deposits of this type.

Composite scores of at least 5 were subdivided into Medium (5–7 points) and High *potential* (≥8 points) groups; the cutoff at 7 points was based on trial-and-error runs that accounted for both the distribution of total point values and the location of known occurrences (plate 8). Assigned *certainty* values for each HUC increase with the number of data types available, regardless of whether the data contributed to the HUC's resource potential score (table 10).

Carbonate-hosted Cu deposit resource *potential* and *certainty* were established for each HUC (plate 7; appendix E). A total of 601 HUCs (3.5 percent) have High *potential* for Cu deposits in carbonate rocks (almost 70 percent of these have High *certainty*), and 1,848 HUCs (nearly 11 percent) have Medium *potential*. The remaining 14,728 HUCs (nearly 86 percent) include about 61 percent that have Low *potential* and almost 25 percent that have Unknown *potential* (because no applicable data are available). Large areas that have very little data that are pertinent to assessing carbonate-hosted Cu deposit potential include (1) the Yukon and Kuskokwim River delta region, (2) most of the Aleutian Island chain and other islands, and (3) several national parks in southern and southeastern Alaska. Carbonate rocks are mostly absent in the Aleutian Islands; consequently, the lack of data is of little concern. The Yukon and Kuskokwim River delta region may include carbonate rocks in the subsurface, but overlying rocks and surficial deposits limit the likelihood of finding economic deposits in this region. In contrast, several of the national park and preserve areas in southern Alaska, for which Earth science data are essentially absent, do include generally prospective geologic terranes. Consequently, some regions that have Unknown *potential* might transition to Medium or High *potential* tracts when additional data become available. Many parts of northern Alaska that have prospective geology or evidence for mineralizing systems, as well as those identified as having High or Medium *potential*, are currently withdrawn from mineral entry because they are in national parks and preserves.

The GIS-based resource analysis identified several generally well-defined areas that have High *potential* for carbonate-hosted Cu deposits in Alaska (plate 8). From north to south within the state, these include (1) an area in the far-northeastern Brooks Range underlain by carbonate rocks of the Neoproterozoic Katakturuk Dolomite that have High *potential* for Kennecott-type copper deposits, (2) an enigmatic northern foreland terrane that extends nearly the full length of the Brooks Range, (3) parts of the Central Belt of the Brooks Range as defined by Till and others (2008), and the southern flank of the Brooks Range, including the Cosmos Hills where the Ruby Creek deposit is located, (4) two discrete

areas on the Seward Peninsula where Cu occurs in carbonates of the Nome Complex of Till and others (2014), and (5) the Wrangellia terrane in southern and southeastern Alaska, where the Kennecott deposits are located (plate 8). Each of these areas, as well as several areas that are coincident with scattered high-rated HUCs that have poorly defined geologic relations.

Neoproterozoic Rocks of the Northeastern Brooks Range

In the northeastern Brooks Range, an east-west-oriented fold-and-thrust belt exposes Neoproterozoic metasedimentary rocks in the cores of anticlines. The Shublik Mountains occurrence at Nanook Creek (from the ARDF) contains copper in basalt breccia of the Mount Coplestone Volcanics and in the overlying Katakturuk Dolomite. The Katakturuk Dolomite contains rocks appropriate for lithologic assignment to the "Carbonates, major" group; accordingly, areas underlain by these rocks, exposed in tens of nearby HUCs, have Medium *potential*. The area is also underlain by Paleozoic carbonate rocks, although none are known to be mineralized. The Itkilyariak Creek occurrence, about 35 miles east-northeast of Nanook Creek, contains native copper in amygdules. Macdonald (2011, p. 381) suggested that similar rocks are common to basalts of the Mount Coplestone Volcanics, exposed across large parts of this region; such features are also characteristic of basaltic-copper-deposit-type mineralizing systems (Cox, 1986a). Sparse stream-sediment samples in this area (most HUCs contain only 5 to 8 samples) do not contain anomalous Cu or accessory metals, and sparse sedimentary- and metasedimentary-rock samples collected in these HUCs also do not have high copper or trace-metal values. Heavy-mineral assemblages were not quantified for stream-sediment samples collected in this area.

Neoproterozoic rocks on the east side of the Canadian Rockies contain a stratabound Cu-mineralizing system (known as the Redstone copper belt, in Northwest Territories), hosted in Tonian (1,000–850 Ma) carbonate and red clastic sedimentary rocks (Ruelle, 1982). The Nularvik unit within the Katakturuk Dolomite was recently correlated with worldwide Marinoan (650–635 Ma [timescale of Knoll and others (2006)]; Smith, 2009) "cap carbonates" by Macdonald (2011). If this is a valid correlation, parts of the Mount Coplestone Volcanics of northeastern Alaska, exposed beneath the Katakturuk Dolomite, must be roughly age-equivalent to sedimentary rocks that host mineralization in the Redstone copper belt. Although native-Cu occurrences in the Mount Coplestone Volcanics identify a basaltic Cu-mineralizing system, the Katakturuk Dolomite is the unit most likely to contain economic-Cu deposits because these carbonate rocks directly overlie the volcanic rocks that are the source of mineralizing fluids and metals, analogous to rocks of the Chitistone Limestone that host the mineral-rich veins of Kennecott district. This part of Alaska is little explored, in part because most of it is within the Arctic National Wildlife Refuge, which prohibits exploration or mineral entry.

Northern Foreland of the Brooks Range

A terrane that contains scattered High *potential* HUCs extends along the northern foreland of the Brooks Range (plate 8), but most copper concentrations in stream-sediment and rock samples from this area are generally low; in addition, no ARDF records indicate the presence of carbonate-hosted Cu deposits. Cobalt is the most common of the targeted trace metals in stream-sediment samples in this area. A few rock samples that contain 2,000 ppm Cu concentrations also contain associated trace metals, including Co, Ag, and Ga. Most rock samples that have anomalous metal abundances are described as "chert or jasperoid", which may include silicified carbonate rocks.

The high-scoring HUCs in the northern foreland of the Brooks Range are primarily underlain by slope carbonate facies rocks of the Carboniferous Lisburne Group, which are viable hosts for copper mineralization. In the western Brooks Range, sedimentary exhalative (sedex) Zn-Pb-Ag deposits (for example, Red Dog, Lik) are hosted by deeper water facies rocks of the Lisburne Group. For comparison, at Mount Isa (Australia), conformable Pb-Zn-Ag sedex orebodies in off-shelf shale facies rocks are

associated with a large cobalt-producing, epigenetic, silica-rich, copper orebody that cuts the adjacent shelf carbonate rocks (Finlow-Bates and Stumpfl, 1979). Hitzman (1986) considered the Ruby Creek deposit in the southern Brooks Range to be directly comparable to the silica-dolomite-hosted copper orebody at Mount Isa; rocks of the northern foreland of the Brooks Range may contain similar mineralization.

Central Belt of the Brooks Range and the Cosmos Hills

The Central Belt of the Brooks Range (Till and others, 2008) and the Cosmos Hills, separated by the Schist Belt and Ambler Lowlands, contain a remarkable number of Cu mineral occurrences in carbonate rocks, including the Ruby Creek deposit in the Cosmos Hills (plate 8).

Both areas are underlain by extensive Paleozoic carbonate rocks, commonly hundreds of meters thick. The age ranges and characteristics of carbonate rocks in these two areas are not well understood. Carbonate rocks of the Central Belt of the Brooks Range include early Paleozoic and also extensive Devonian carbonate rocks. Carbonate-rock-bearing geologic units that host mineral occurrences in this terrane include the Devonian Skajit Limestone; the Beaucoup Formation; Devonian metaigneous and metasedimentary rocks that lie conformably below the Hunt Fork Shale, a possible correlative of the Beaucoup Formation; and, in the western Brooks Range, Devonian carbonate rocks that overlie Ordovician carbonate rocks and underlie the Hunt Fork Shale (Folger and Schmidt, 1986; Dumoulin and Harris, 1987).

Rocks in the Cosmos Hills, separated from Central Belt rocks by Paleozoic metapelitic and metavolcanic schists, resemble the Central Belt rocks. Similar to the Central Belt, the Cosmos Hills sequence includes Silurian carbonate (A.G. Harris, USGS, unpub. data, 1991 [fossil report, table A-1, Ambler River quadrangle]), as well as Devonian carbonate rocks (see Hitzman, 1986, and references therein).

Mineral occurrences in the Central Belt and Cosmos Hills are also similar. Chalcopyrite, the dominant copper sulfide mineral, is often accompanied by precipitation of quartz as veins and (or) replacements of carbonate host rocks. These mineral occurrences are distinct from copper skarns because they include no calc-silicate or magnesium silicate alteration minerals. Many occurrences in limestone or dolostone immediately underlie argillitic units (primarily the Late Devonian Hunt Fork Shale) that might have formed permeability boundaries that constrained upward hydrothermal fluid flow. Mineralized rock that has these characteristics has been identified at the Peak, Sheep Creek, and Beaucoup Creek occurrences, (plate 8), as well as nearly 20 additional occurrences throughout the Central Belt. However, many ARDF records of occurrences in the Central Belt either have been identified as “polymetallic veins” or “polymetallic replacements” (Cox and Singer, 1986) or were assigned no deposit model designation and, thus, may not be Kipushi-type carbonate-hosted copper deposits.

The Ruby Creek ore system is reasonably classified as Kipushi-type on the basis of available information, although the characteristics and timing of mineralization relative to orogeny do not appear exactly commensurate with its assignment to that deposit type. Recent studies of Kipushi-type deposits in Africa have suggested that these deposits formed from hydrothermal fluids of such extreme salinity that they must have dissolved preexisting evaporate deposits, possibly including potash salts (Chetty and Frimmel, 2000; Heijlen and others, 2006); however, no salt beds or high-salinity rocks are known in the Ruby Creek area. At Kipushi, ore deposition occurred no less than 300 million years after host-rock deposition, following collisional orogeny. The age and details of ore deposition at Ruby Creek are not well known. A rhenium-osmium (Re-Os) date of Ruby Creek ore yielded an age of 384±4.2 Ma (Middle Devonian [timescale of the International Commission on Stratigraphy, 2013]) (Selby and others, 2009), indicating that ore deposition occurred shortly after host-rock deposition. Ore deposition at Ruby Creek following the Jurassic-Cretaceous Brookian orogeny would be more analogous to ore genesis at Kipushi.

The Schist Belt between the Cosmos Hills and the Central Belt contains numerous Kuroko-type volcanogenic massive sulfide deposits hosted in bimodal metavolcanic rocks that are younger than the Cosmos Hills carbonate sequence. However, the relative ages of mineralization and geologic relations between these rock sequences at the time of mineralization are unknown.

Resource potential scores for the carbonate-hosted Cu deposits in the Central Belt and Cosmos Hills areas were derived from all data types except HMC mineral identification data, which was not available for this area.

Throughout the Central Belt, most HUCs that have High *potential* include sedimentary or metamorphic rocks having Cu grades in excess of 1 percent; numerous samples contain 2 to 5 percent Cu, and a few exceed 20 percent Cu. These samples commonly have high Co and (or) Ag abundances as well. Sediment samples that have at least 150 ppm Cu are common, and many have elevated Co and Ag abundances. Several tens of Cu mineral occurrences, including 10 classified as Kipushi-type, contribute to the high potential scores for Central Belt HUCs.

Paleozoic schists and carbonate rocks of the Central Belt are intruded by the Devonian-aged Igikpak and Arrigetch plutons, as well as other similar granitic plutons that have skarn zones, some of which include copper- and tin- or tungsten-enriched rocks near their contacts (Newberry and others, 1986). Although skarn occurrences were deliberately excluded from the ARDF-record keyword counts, their erosion contributes to high copper values in downstream sediment samples that may have contributed to overrepresentation of the associated Medium and High *potential* HUCs. As many as two-thirds of the high-rated HUCs in the central Survey Pass and northwestern Chandalar quadrangles may reflect skarn mineralization.

Nome Complex of the Seward Peninsula

In two parts of the Seward Peninsula, Nome Complex rocks (Till and others, 2014) host clusters of Cu occurrences in carbonate rocks, although none have been classified as Kipushi-type. Historically, a few of these occurrences produced small tonnages of copper ore. These two areas are delineated by HUCs that have High *potential*; most of these potential ratings also have High *certainty* (plate 8). Other parts of the eastern Seward Peninsula contain scattered base-metal mineralization, including possible sedex occurrences (Slack and others, 2014) and lead-zinc-bearing quartz veins that have locally high Ag abundances. The coincidence of Cu occurrences in carbonate rocks and possible sedex occurrences is similar to that in the western Brooks Range (plate 8). Most Nome Complex Cu occurrences are in discordant zones that cut pure carbonate host rocks immediately overlying schists. Stratigraphic relations in rocks associated with these occurrences are poorly defined. Till and others (2014) concluded that vertical stacking within the Nome Complex is tectonic and that the Ordovician to Devonian Mixed Unit, rich in marble and locally mineralized, is overturned throughout the Seward Peninsula, as well as that the younger Calcareous Metasiliceous Unit is beneath the Mixed Unit.

Resource potential scores for HUCs on the Seward Peninsula were derived from all data types except HMC mineral identification data. In all cases, the carbonate-rock-bearing unit that contributed to the HUC score is the Mixed Unit of the Nome Complex. High *potential* HUCs on the Seward Peninsula contain rock samples that have at least 1 percent Cu and elevated abundances of Co and (or) Ag. Many sediment samples have at least 150 ppm Cu, and some include elevated abundances of Co, Ag, and Ga, in various combinations.

Wrangellia Terrane

The Wrangellia terrane in south-central Alaska is defined as late Paleozoic metaigneous and metasedimentary rocks overlain by the thick, massive, Middle to Late Triassic Nikolai Greenstone, itself overlain by the Late Triassic (late Carnian to Norian) Chitistone Limestone (Jones and others, 1977). The type section of the Wrangellia terrane (Wrangell Mountains, McCarthy quadrangle) includes the

carbonate-hosted Cu deposits of the Kennecott district. Paleomagnetic studies of the Nikolai Greenstone have demonstrated that Wrangellia terrane rocks are allochthonous to Alaska and originated far south of their present positions (Hillhouse, 1977); paleontologic studies have suggested an origin in near-equatorial paleolatitudes (Hallam, 1986). Wrangellia terrane rocks are found in fault-bounded blocks that extend from Vancouver Island in western Canada to Chichagof Island in southeastern Alaska, as well as from the Chilkat Peninsula in southeastern Alaska (Plafker and Hudson, 1980) northwestward through southwestern Yukon, Canada, to the central Alaska Range and westward from the Wrangell Mountains into the Mount Hayes and Talkeetna Mountains quadrangles (Jones and others, 1977; Nokleberg and others, 1992; Schmidt and others, 2003) (plate 8). Each segment of Wrangellia terrane in Alaska includes many HUCs that have High *potential* for carbonate-hosted Cu deposits (plates 7, 8).

The Nikolai Greenstone is critical to the genesis of Kennecott-type Cu deposits in carbonate rocks (plate 8). The greenstone contains numerous basaltic-copper-type mineral occurrences whose formation probably was approximately coeval with Kennecott-type deposit formation. A potassium-argon whole-rock date on a greenstone (Silberman and others, 1980) and subsequent structural studies (Price and others, 2014) suggest an Early Cretaceous age for peak (prehnite-pumpellyite facies) metamorphism and genesis of both types of mineralization.

Formation of both Kennecott-type and basaltic-copper mineralization was related to burial and to diagenesis and (or) metamorphism of the intrinsically high-Cu flood basalts of the Nikolai Greenstone. Similar processes have been documented in many other places in the world within subaerial flood basalts. In the Nikolai-correlative Karmutsen Group basalts on Vancouver Island, very early copper redistribution and hematite deposition occurred within individual flows, possibly accompanying fumarolic activity within just days after eruption (Surdam, 1968). These early processes altered rock-forming igneous iron and titanium minerals to hematite, and native Cu and prehnite precipitated in vesicles of adjacent basalt. Low-grade native-Cu mineralization of this type is common in flood-basalt provinces.

In the Keweenaw district (on Michigan's "Upper Peninsula"), higher grade, economic native-Cu deposits formed at maximum temperatures of 350 °C in brecciated and amygdular flow tops, in interflow conglomerates, and, less commonly, in veins within the Portage Lake Volcanics; mineralization is associated with prehnite-pumpellyite-facies and epidote-bearing greenschist-facies metamorphism (Stoiber and Davidson, 1959). In detail, metamorphic isograds and associated metallic mineral assemblages crosscut layering in flows and conglomerates at a low angle. Copper was leached during dewatering of the lavas in the deeper part of the volcanic pile. Dewatered fluid migrated up dip and deposited Cu where conditions were sufficiently reducing (Bornhorst and others, 1986). Oxidation potential required for the Cu mobilization that accompanied burial metamorphic conversion of pumpellyite to epidote would have been provided by early hematite. Thus, only subaerially erupted basalt released Cu to the mineralizing solutions. Farther southwest along the Keweenaw Peninsula, ore-grade stratabound copper deposits formed in the nearest reducing environment upsectionward, in black-to-gray, organic-rich siltstone and shale at the White Pine and Copperwood deposits (Ensign and others, 1968). In the Wrangell Mountains, the nearest reducing environment upsectionward from the Nickolai Greenstone was in the overlying carbonate rocks of the Chitistone Limestone, which host the Kennecott-type deposits.

The Nikolai Greenstone is 3.5 to 4 km thick in both the Wrangell Mountains (McCarthy quadrangle) and Clearwater Mountains (eastern part of the Healy quadrangle) (Greene and others, 2008). Basaltic-Cu occurrences indicative of dewatered rocks of the Nikolai Greenstone are scattered across all exposures of greenstone in the Wrangellia terrane. Overall, scores that define HUCs that have High *potential* largely correspond to the presence of basaltic-Cu occurrences, although most HUCs that have high potential for carbonate-rock-hosted copper also include more than 5 km^2 of a "Carbonates, major" host-rock unit. Most high potential HUCs also contain sediment samples that have at least 150

ppm Cu, high Co, or high Ag abundances, and many include sedimentary or metamorphic rocks that have more than 1 percent Cu. In the Mount Hayes and Healy quadrangles, chalcopyrite identified in HMC samples also contributes to higher scores. The limiting factor and most important indicator of high potential for carbonate-hosted copper deposits is the presence of a substantial area underlain by "Carbonates, major" rocks.

Where the Wrangellia terrane abuts the Denali Fault, HUCs that have High *potential* extend southwestward into the west-central Talkeetna Mountains (plates 7, 8) (Schmidt and others, 2003). The HUCs that have high potential for carbonate-hosted copper deposits also are north and west of the Denali Fault (plate 8), across the Healy quadrangle, the southwestern part of the Mount McKinley quadrangle, the northeastern part of the McGrath quadrangle, the northwestern part of the Talkeetna quadrangle, and the eastern part of the Lime Hills quadrangle, where rocks of the Wrangellia terrane and the Nikolai Greenstone have not been identified. The High *potential* scores for these areas are derived from a different combination of factors than the high potential scores associated with the Wrangellia terrane. North and west of the Denali Fault, none of the scoring reflects the basaltic-Cu mineral occurrences that characterize the HUCs of the Wrangellia terrane. Chalcopyrite observed in HMC contributes significantly to northern and western HUCs that have high scores, but they may reflect mineral deposit types that are significantly different than those affiliated with flood basalt. North and west of the Denali Fault, the carbonate unit that contributes to the high scores is the calcareous sedimentary rocks unit (mapped as "Tcs", *in* Csejtey and others, 1992), a sequence at least 1,000 m thick of calcareous siliciclastic mudrocks and sandstones overlain by shallow-shelf and intertidal carbonates. Scattered Late Triassic subaqueous pillow basalts and related diabasic intrusions are the only mafic rocks that underlie the High *potential* terrane north and west of the Denali Fault. Few sediment samples from this area have more than 100 ppm Cu; in addition, rock samples generally contain more than 200 ppm and only rarely as much as 2,000 ppm Cu, which contrasts strongly with numerous rock samples from the Wrangellia terrane that contain more than 2 percent Cu.

Most known mineral occurrences in the High *potential* terrane north and west of the Denali Fault have been classified as volcanogenic massive sulfide deposits, including some Besshi-type deposits (that is, dominated by sedimentary rocks rather than volcanic rocks). However, the presence of a carbonate-rock host unit in a HUC, together with a single sample that is anomalous in Cu, can lead to a High *potential* rating, which may result in the inclusion of some High *potential* HUCs that actually correspond to Cu-skarn potential (for example, in the Chulitna Mountains) (plate 8; see also Hawley and Clark, 1974).

Other Areas in Alaska that have High Potential for Cu(-Co-Ag-Ge-Ga) Deposits

One area west of Cook Inlet that is underlain by the Cottonwood Bay Greenstone, which is not part of Wrangellia, contains a HUC that has High *potential* for carbonate-hosted copper (plate 8). In the eastern part of the Iliamna quadrangle, the Cottonwood Bay Greenstone is massive, as much as 600 m thick, locally porphyritic, locally amygdular (having heulandite fillings), and metamorphosed to epidote-amphibolite facies (Detterman and Reed, 1980). Most Cu-bearing mineral occurrences in the area are well described as Cu- or Cu-Fe- or Fe-skarns related to Cretaceous or Tertiary intermediate-composition to felsic intrusions. Both the greenstone and minor Triassic carbonate rocks form roof pendants within the Alaska-Aleutian batholith. An ARDF record of one Cu occurrence, the Durand (Durant), consists of a 10-foot-thick quartz vein that contains chalcopyrite and pyrite and cuts the Cottonwood Bay Greenstone; the occurrence was categorized as a polymetallic-vein-type deposit but could be classified as basaltic-Cu-type.

Beyond the Wrangellia terrane and the northeastern Brooks Range, only two Alaskan mineral occurrences have been classified as basaltic-Cu-type. At Kivivik in the northwestern Baird Mountains quadrangle, chalcopyrite and pyrite fill vesicles in epidote-altered, orange-weathering basalt. The other

occurrence classified as basaltic Cu is in the Selawik Hills; this occurrence may be related to nearby postbasalt intrusions.

Several areas that contain HUCs having High *potential* for carbonate-hosted Cu deposits have no associated basaltic Cu deposits; these HUCs coincide with places where more than 5 km^2 of "Carbonates, major" lithologic units are present that contain one or more stream-sediment or rock samples that have high Cu content. These characteristics, however, are also consistent with Cu-bearing skarns, which, using the scoring schema described above, cannot be differentiated from carbonate-hosted Cu deposits; thus, the presence of skarns cannot be ruled out as the cause of some of these high-scoring HUCs. For example, rock samples in the Limestone Mountains (in the Medfra quadrangle) that have high Cu abundances are located adjacent to Jurassic intrusive rocks (plate 8). Consequently, the associated High *potential* HUCs may reflect Cu-skarn or porphyry Cu mineralization, rather than carbonate-hosted Cu deposits. This same ambiguity pertains to scattered HUCs (1) across central Alaska, westward from the Yukon-Tanana terrane, (2) in the western Alaska Range, (3) in the Ahklun Mountains, in southwestern Alaska, and (4) in southeastern Alaska.

Chapter 5. Sandstone-Hosted U(-V-Cu) Deposits

By Bronwen Wang, Douglas B. Yager, and Timothy S. Hayes

Deposit-Group Characteristics

Sandstone-hosted uranium (ssU) deposits are epigenetic deposits that form in sandstone that ranges in age from Carboniferous to Holocene. Most sandstone-hosted uranium deposits are one of four types—basal, tabular, roll front, and tectonolithologic (table 1; see also Cuney and Kyser, 2009). Regardless of type, ssU deposits probably form by processes that can be generalized as (1) oxidative dissolution and mobilization of uranium from source rocks, commonly granite or tuff, (2) transport of soluble uranyl (U^{6+}) complexes through an oxidized nonmarine-sandstone aquifer, and (3) reduction and precipitation as (U^{4+}) minerals where transporting fluids encounter reduced host rocks, typically containing carbonized plant matter, that are laterally continuous with or are below the aquifer in which uranium was transported (Guilbert and Park, 1986; Cuney and Kyser, 2009).

Although resource potential for all types of ssU deposits was evaluated, basal-type deposits are probably most likely in Alaska because the most common geologic setting for ssU deposits in Alaska is basal sediments on granites rich in HFSE, as exemplified by the Death Valley deposit on the eastern Seward Peninsula. Basal-type deposits are typically found in poorly consolidated, highly permeable, fluvial to lacustrine carbonaceous gravels and sand deposited in paleovalleys directly incised in basement rocks, generally granitic, and capped by plateau basalts or impermeable sediments. Uranium is leached from the granitic basement rocks and precipitates by reaction with organic matter during groundwater percolation (Cuney and Kyser, 2009). Trace elements associated with the basal-type ssU deposits include V, Cu, Fe, Mo, Pb, Zn, Ag, Cd, Cr, Co, Ni, Se, and Sr (Dahlkamp, 1993). Limited data from the Death Valley deposit suggest that Sr, Ba, P, As, and Mo are positively correlated with the U mineralization, whereas V and Mn appear to be negatively correlated (Dickinson and others, 1987). The V content varies from less than 30 ppm to 300 ppm in the U-bearing sedimentary rocks, but, in the highly mineralized rock, the slightly mineralized mudstone, and the nonmineralized mudstone, it averages less than 30, 101, and 128 ppm, respectively.

Previous Uranium-Resource Studies in Alaska

Resource investigations of uranium and other radioactive materials in Alaska began in the 1940s (Wedow and others, 1951; White and West, 1953; Killeen and Ordway, 1955; Robinson and others, 1955; West and Benson, 1955; Houston and others, 1958; Freeman, 1963; Matzko and Freeman, 1963). Early work suggested that the most prospective areas for radioactive mineral commodities are on the Seward Peninsula and in southeastern Alaska (MacKevett, 1963; Eakin, 1969, 1975; Eakin and Forbes, 1976; Johnson and others, 1978: Miller and Johnson, 1978). From 1973 to 1984, stream-sediment, water, and bedrock samples were collected under the auspices of the National Uranium Resource Evaluation (NURE) as part of a reconnaissance uranium-resource assessment. NURE was a U.S. Department of Energy program designed to acquire and compile Earth science information required to establish the magnitude and distribution of uranium resources in the United States and to identify areas favorable for the occurrence of uranium deposits. In support of this effort, Eakin and Forbes (1976) published an investigation of Alaska's uranium potential that highlighted regions containing major sedimentary basins and associated felsic intrusive rocks and described the economic geology, radiometric surveys and investigations, and uranium-resource potential. Follow-up reconnaissance studies of sedimentary rocks in the Copper River Basin and Chitina River Valley (in south-central Alaska) and in the Nenana coal field in central Alaska were conducted in recognition of their

favorability for associated uranium deposits (Eakin and others, 1977; Dickinson, 1978; Dickinson and Campbell, 1978; Dickson, 1982). Additional studies of favorable sedimentary host rocks were conducted around the state, including in northeastern Alaska (Huffman and others, 1982; Huffman, 1985) and south-central Alaska (Dickinson, 1977; Dickinson and Skipp, 1990; Dickinson, 1995; Dickinson and others, 1995).

Weakly developed uranium mineralization in the Tertiary continental sedimentary rocks of the Kootznahoo Formation in southeastern Alaska (Dickinson and Campbell, 1982; Dickinson and Vuletich, 1990) and in the Tertiary nonmarine sedimentary rocks in the northwestern Yukon Flats basin (Barker, 1981a) has been reasonably well described. The Kootznahoo Formation is mainly arkosic sandstone and conglomerate and lesser amounts of coal and shale. Early diagenesis under nonmarine fluvial and paludal conditions produced sideritic concretions and cement. Local uplift recharged these alluvial aquifers with oxygenated meteoric groundwater. Uranium mineralization is associated with carbonaceous material in uplifted areas. These parts of the Kootznahoo Formation contain as much as 93 ppm U (Dickinson and Pierson, 1988), and they are considered to be favorable uranium-mineralization hosts but are probably too small to contain commercially viable deposits (Dickinson and Vuletich, 1990). Tertiary sedimentary rocks of the Yukon Flats basin contain nonmarine sediments that include lignitic and coaly materials, felsic tuffs, and tuffaceous sediments, which also constitute a favorable host rock (Barker, 1981a). Outcrops along Coal Creek in the Yukon Flats contain 20 to 50 ppm U (Barker, 1981a). Most of the Yukon Flats basin is beneath surficial deposits and very little is known about its subsurface geology (Barker, 1981a).

Limited industrial uranium exploration has been completed in Alaska, and only the Ross Adams deposit in southeastern Alaska has produced uranium ore. The Ross Adams deposit was mined between 1957 and 1971, producing 79,500 metric tons of ore (ARDF; http://ardf.wr.usgs.gov/). Uranium is associated with the U-Th-REE peralkaline granite that underlies Bokan Mountain (MacKevett, 1963; Staatz, 1978; Thompson, 1997; Dostal and others, 2014). MacKevett (1963) identified the following four modes of uranium-thorium accumulation at Bokan Mountain: (1) U-Th-bearing zircon, uranothorite, and xenotime that are syngenetic accessory minerals in the peralkaline granite; (2) veins that contain uranothorite and uranoan thorianite of hydrothermal origin, which is the dominant occurrence of U-Th in the area; (3) disseminated primary uraninite, uranothorite, uranoan thorianite(?), brannerite, ellsworthite, and secondary beta-uranophane in pegmatite and aplite dikes; and (4) a single occurrence of hydrothermal allanite that occupies interstices in clastic metasedimentary rocks. However, the allanite occurrence was subsequently restudied and is now considered to be similar to other dike prospects near Bokan Mountain (Warner and Barker, 1989).

The Death Valley deposit (ARDF record BN089), located in the Boulder Creek Basin in the southeastern part of the Seward Peninsula is the best described ssU deposit in Alaska (plate 10). The deposit was discovered in 1977 by airborne radiometric survey and was subsequently sampled by shallow excavation and 65 core and rotary drill holes between 1978 and 1981. In an incompletely defined, 3-m thick body that is less than 1,280 m long and has an unknown width, the average grade is 0.27 percent U_3O_8 (2,290 ppm U). Calculated resources are about 1,000,000 lbs (~454 metric tons) U_3O_8 (Dickinson and others, 1987). The host rocks are early Eocene carbonaceous arkosic sandstones of fluvial or colluvial origin deposited in a graben formed on granitic bedrock. The underlying Late Cretaceous granite, part of the Darby pluton, also forms the western upthrown block of the graben and mountains that rise immediately to the west. Basalt, coal, and laminated, sideritic, lacustrine mudstone and turbidite deposits are interlayered with the sandstone. An early Eocene basalt flow dammed the ancestral river valley, forming a lake in which lacustrine sediments were deposited (Dickinson and others, 1987). Primary epigenetic mineralization likely formed during the Eocene; the Darby pluton is the uranium source rock. Primary mineralization probably developed when uranium was dissolved from the granite by oxidizing recharge water, carried eastward from the Darby pluton, and deposited where

groundwater encountered a reducing environment associated with carbonaceous Tertiary sedimentary rocks (Dickinson and others, 1987). Mineralized rocks are fairly widespread in the subsurface and are present both above and below the Eocene basalt and lacustrine rocks. Uranium minerals in the primary ore are coffinite [tetragonal $U(SiO_4)\cdot nH_2O$] in the reduced zones and autunite [tetragonal $Ca(UO_2)_2(PO_4)_2\cdot 10\text{-}12H_2O$] where the primary ore is oxidized. Secondary supergene enrichment is related to present surface exposures and is thought to be ongoing because recent mudflows and soils are mineralized (Dickinson and others, 1987). The most abundant uranium mineral in the secondarily enriched rock is meta-autunite [tetragonal $Ca(UO_2)_2(PO_4)_2\cdot 6H_2O$].

Mineral-Resource-Potential Estimation Method

Scoring for sandstone-hosted uranium was based on host-rock-favorability and U-mineralization indicators. Both were considered equally diagnostic. Host-rock-favorability indicators were the presence of sandstone and coal. Evidence of U-mineralization includes (1) uranium distribution (abundances in stream-sediment and sedimentary-rock samples), (2) radioactivity, and (or) (3) locations of known or possible ssU occurrences or prospects (according to ARDF records). Aerial gamma-ray survey data was used to identify areas of radiogenic rock.

Lithology

The distribution of potentially favorable sandstone rock units were derived from the "Geologic Map of Alaska" (Wilson and others, 2015), using the search terms in appendix D in this report; however, the search terms were derived from the map-unit descriptions in Wilson and others (2015). In order to include areas where sandstone units may be covered by surficial deposits, a buffer of 3 km that extends from mapped sandstone units into adjacent surficial deposits was applied.

Many ssU deposits in North America, including the Death Valley deposit in Alaska (plate 10), are hosted in Tertiary arkosic sandstone (Guilbert and Park, 1986; Cuney and Kyser, 2009). The HUCs that contain arkosic sandstone received 4 points, and those that have either Tertiary or Cretaceous and Tertiary sandstone received 3 points (table 11). The HUCs that contain all other sandstone types received 2 points, and those containing unconsolidated sediments within the 3-km-wide buffer area received 1 point. The point value for the most prospective rock type in each HUC was assigned to the entire HUC. The maximum possible score that is based on sandstone host rock is 4 (table 11).

Coal

To identify HUCs that might contain solid organic matter, coal-bearing rock units were identified from Merritt and Hawley's (1986) "Map of Alaska's Coal Resources." The HUCs that have either Tertiary or Cretaceous and Tertiary coal-bearing rock units received 2 points, and all other HUCs that have coal-bearing units received 1 point (table 11).

Alaska Resource Data File

Alaska Resource Data File (ARDF) records were evaluated for ssU occurrences using keywords and associated scores (appendix C). The results of the keyword search were further limited to only those records that have U as a "main" or "other" commodity. These records were reviewed individually and retained for scoring if (1) the reported deposit-type model is ssU or roll front, (2) no deposit type was identified and lode, granite, vein, dike, phosphates, or skarn were absent from the descriptive fields, or (3) the deposit type indicated is placer that has U present as either a major or minor commodity. For the state of Alaska, six ARDF records indicate that sandstone-hosted uranium or roll front as the deposit type; each of the associated HUCs received 4 points. All other retained ARDF records received 2 points; a maximum value of 2 points per HUC was possible (table 11).

Stream-Sediment and Sedimentary-Rock Geochemistry

Geochemical data for sedimentary rock and stream sediments was evaluated and scored. Sedimentary-rock analysis is the most direct indication of the uranium content in the potential host rocks; however the quantity and spatial distribution of available sedimentary-rock data is more limited than that of stream-sediment data. In sedimentary rocks, both U and V contents were independently scored; however, in stream-sediment samples, only U content was scored (table 11).

The HUCs that contain one or more sedimentary-rock samples having U contents in the 98th percentile or higher for uranium (≥33 ppm) received 5 points; those in which sedimentary-rock samples have U contents between the 91st and 98th percentile values (≥10 but <33 ppm) received 3 points. The HUCs that have one or more sedimentary-rock samples having V contents in the 98th percentile value (≥1,500 ppm) or higher received 2 points; those in which sedimentary-rock samples have V contents between the 91st and 98th percentile values (≥390 but <1,500 ppm) received 1 point. The scores for U and V were added, giving the sedimentary-rock geochemical score. Thus, the highest possible sedimentary-rock geochemical score for ssU is 7.

HUCs that contain a stream-sediment sample that has a U content in the 98th percentile value or higher (≥21.8 ppm) received 5 points; those containing a stream-sediment sample that has a U content between the 91st and 98th percentile values (≥6.3 but <21.8 ppm) received 3 points; and those containing a stream-sediment sample that has a U content between the 75th and 91st percentile values (≥3.6 but <6.3 ppm) received 1 point (table 11).

For both the sedimentary-rock and stream-sediment data, the HUCs that contain multiple samples received the scores that correspond to the sample having the highest score. The two geochemistry datasets were scored independently; therefore, a HUC received 7 points if it contained sedimentary-rock samples in which the U and V contents were in the 98th percentile or higher. The HUC would also receive 5 points if the U content in a stream-sediment sample was in the 98th percentile or higher.

Aerial Gamma-Ray Survey Data

Aerial gamma-ray survey data depict the spatial distribution of naturally occurring radioactive ^{238}U decay across large parts of Alaska (Duval, 2001); the resulting uranium abundance data are reported in equivalent U (eU), in ppm. The HUCs that contain measured radioactivity of at least 5 eU received 2 points, and HUCs that contain between 2 and 5 eU received 1 point (table 11). The maximum score assigned to each HUC corresponds to the maximum eU value measured anywhere within the HUC.

Results and Discussion

The maximum score attainable using the scoring schema (table 11) for ssU deposits is 24; however, no HUC received the maximum score. Scores ranged from 0 to 19, and scores of 11 or more were assigned High *potential*. The HUCs that had scores of 6–10 and 0–5 were assigned Medium and Low *potential*, respectively. *Certainty* classification was based on the number of datasets that contributed (six possible) to resource potential scores (table 12): High *certainty* was assigned when five or six datasets contributed to the total score; Medium *certainty* was assigned when four datasets contributed to the score; and Low *certainty* was assigned when 3 or fewer datasets contributed to the score. A value of Unknown *potential* was assigned to HUCs that (1) lacked stream-sediment data and had a total score of zero or (2) lacked stream-sediment data and the total score was completely based on the lithology or the lithology plus the presence of coal.

Several refinements to the ssU scoring procedure and *certainty* classification were made subsequent to publication of the Bureau of Land Management's Central Yukon Planning Area resource

assessment (Jones and others, 2015). Scores for sedimentary-rock-sample geochemistry were increased from 2 to 5 for samples that had U contents in the 98th percentile or higher; similarly, scores were increased from 1 to 3 for samples between the 91st and 98th percentile. Scores for V contents that were both in the 98th percentile or higher and between the 91st and 98th percentiles were included for the sedimentary-rock scores. Thus, the total sedimentary-rock-geochemistry score for a HUC reflects both the U and the V content of the rocks. Scores for stream-sediment samples whose U contents were either in the 98th percentile or higher or between the 91st and 98th percentiles were also increased from 3. These changes were made so that the scores of data types that are indicative of U mineralization were similarly weighted to the scores derived from those indicative of host-rock setting. The changes allowed the elimination of the previously used special requirement that a host-rock setting have some evidence of U mineralization in order to receive a Medium *potential* classification. In addition, the igneous-rock indicator of U sources was eliminated because it is largely redundant with the more spatially extensive airborne-radiometric-survey dataset. Finally, the distinction between Low and Medium *certainty* was increased from a score of 2 to a score of 3 because host-rock favorability scores always contribute to the *certainty* determination.

Relative mineral-resource potential for each HUC was established using the parameters described above (plate 9; appendix E). Statewide, 0.15 percent of all HUCs have High *potential* for ssU. Of the HUCs that have High *potential*, 92 percent have High *certainty* and 8 percent have Medium *certainty*. Of the 7.05 percent of all HUCs that were assigned Medium *potential*, 4.57, 2.31, and 0.17 percent had High, Medium, and Low *certainty*, respectively. Low *potential* for ssU was assigned to 75.53 percent of all HUCs; of these, 19.94, 36.01 and 19.58 percent have High, Medium, and Low *certainty*, respectively. The *potential* of 17.26 percent of the HUCs is Unknown.

The HUCs that have High *potential* are scattered across the state (plate 10). The HUCs that have both High *potential* and High *certainty* are located in the Darby Mountains on the Seward Peninsula; along the Kokrines-Hodzana trend; in the Yukon-Tanana uplands; in the northern and western Alaska Range; around Prince William Sound; and in southeastern Alaska. The HUCs in the Port Camden–southeastern Keku Strait area, which contains sedimentary rocks of the Kootznahoo Formation (Dickinson and Vuletich, 1990), and in the Upper Tubutulik River area, which contains the Death Valley deposit, were classified as High *potential* and High *certainty*. These HUCs scored 19 points if they had five datasets contributing and 15 points if they had six datasets contributing. Isolated HUCs that have both High *potential* and High *certainty* have scores between 11 and 13; these HUCs typically have total sedimentary-rock scores from 3 to 5; at least one stream-sediment sample that has U content at the 91st percentile or higher (≥6.3 ppm); either arkosic or Tertiary or Cretaceous and Tertiary sandstones; Tertiary coal units; and either favorable ARDF records or airborne radiometric equivalent uranium (eU) greater than 2. Two HUCs have High *potential* and Medium *certainty*: one is in arkosic sandstone along the coast in the Point Hope quadrangle; the other is in the sedimentary rocks near the Kiligwa River in the Howard Pass quadrangle. Both have sedimentary-rock scores greater than 5, indicating that U and V are present, and both have at least one stream-sediment sample that has a U content in the 75th percentile or higher. The HUCs that have Medium *potential* often cluster around those that have High *potential* (plate 10). The Medium *potential* HUCs typically have host rock sandstone not distinguished as arkosic or Tertiary or Cretaceous and Tertiary, as well as stream-sediment U contents in the 91st percentile or higher and airborne radiometric eU score of between 2 and 5.

General concepts concerning the formation of ssU deposits have not changed significantly since the 1970s. Most of the stream-sediment data used in this assessment were derived from investigations in the 1950s and the sampling conducted in 1973–84 as part of the NURE program. Consequently, the resulting potential map strongly resembles that of Eakin and Forbes (1976), which focused on host-rock favorability, coupled with regional uranium studies (Freeman, 1963; MacKevett, 1963; Eakin, 1975; Barker and Clautice, 1977; Dickinson, 1977,1978, 1995; Barker, 1981a; Dickson, 1982; Dickinson and

Morrone, 1982; Huffman and others, 1982; Huffman, 1985; Dickinson and Skipp, 1990; Dickinson and Vuletich, 1990; Dickinson and others, 1995). For example, we determined that *potential* for ssU deposits in most of the Copper River Basin is Low, which is consistent with earlier work that concluded that the area contains favorable host rocks (Eakin and Forbes, 1976), but evidence of U mineralization is minimal (Eakin, 1977). Conversely, the large area of HUCs that is coincident with areas of High *potential* and is contiguous to areas of Medium *potential*, including parts of the Yukon-Tanana uplands and the north flank of the Alaska Range, was previously identified as containing favorable host rocks and airborne-radiometric-survey characteristics that are consistent with elevated U contents in rock, stream-sediment, and (or) surface-water samples (Eakin and Forbes, 1976; Barker and Clautice, 1977; Dickson, 1982; Dickinson and Pierson, 1988). Similarly, areas that have High and Medium *potential* on the Seward Peninsula and in the Hogatza igneous belt were also identified as prospective for ssU deposits during earlier investigations (Eakin and Forbes, 1976; Miller and Johnson, 1978; Johnson and others, 1978); however, prospective areas within the Kokrines-Hodzana belt were not identified in previous studies, although the upland areas in the Yukon Flats region have been mentioned as possible source areas for potential uranium mineralization (Eakin and Forbes, 1976; Barker, 1981a).

Considerable ambiguity attends the study of ssU resource potential in Alaska. The large regions beneath surficial cover and the limited subsurface information from major sedimentary basins, as well as the structural complexity and the metamorphism, all complicate the assessment of ssU potential in Alaska. Therefore, to better characterize areas that have High and Medium *potential* for ssU deposits, future work in Alaska should include more detailed work to delineate extent and characteristics of the sedimentary-basin rocks.

Chapter 6. Sn-W-Mo(-Ta-In-Fluorspar) Deposits Associated with Specialized Granites

By Susan M. Karl, Erin Todd, Keith A. Labay, and Nora B. Shew

Deposit-Group Characteristics

Specialized granites that have Sn-W-Mo(-Ta-In-fluorspar) concentrations have a range of compositions, which reflect the many factors that influence the genesis and crystallization of felsic to silicic granites and associated mineralization. The diverse compositions of granites associated with Sn, W, and, to a lesser degree, Mo deposits tend to form relatively small-volume intrusions. In general, concentrations of these elements are found in deposits that are derived from late-stage, highly evolved magmas and magmatic fluids. The deposits are found in stockworks, breccia pipes, veins, dikes, and greisens, in cupolas of the granitic bodies and in adjacent host rocks, often recording multiple episodes of intrusion. The small size of these granitic bodies contrasts with the much larger size of intrusive complexes that host porphyry Cu deposits. Intrusive rocks associated with porphyry Sn, W, and Mo deposits also are more differentiated and more silicic, and they also have low sulfidization states relative to those associated with porphyry Cu and porphyry Cu-Au(±Mo) deposits (Seedorff and others, 2005). Although Mo is a common constituent of intermediate-composition igneous rocks that host porphyry Cu deposits, our GIS analysis of Sn-W-Mo(-Ta-In-fluorspar) deposits associated with specialized granites is designed to exclude porphyry Cu(-Mo) deposits and to focus on Mo deposits associated with highly evolved granitic rocks.

Economic concentrations of Sn, W, Mo, Ta, and In (with or without fluorspar) are mainly associated with peraluminous granites (Černý and others, 2005). These granites have high aluminum saturation index (ASI) values and commonly contain aluminous minerals, including combinations of biotite, muscovite, garnet, topaz, tourmaline, cordierite, andalusite, and sillimanite. In addition, some Sn, W, and (or) Mo deposits are associated with pegmatites (Černý and others, 2005). Pegmatite dikes or bodies that contain elevated concentrations of Sn, Ta, W, Mo, Cs, and Li are classified as lithium-cesium-tantalum pegmatites, and they typically are associated with highly fractionated, weakly to strongly peraluminous granites (Černý and others, 2005).

Fluorine (F) and H_2O are important agents for transport and concentration of many incompatible elements, including Sn, In, Ta, and W, in late-stage magmatic fluids (Dobson, 1982; Swanson and others, 1990; Keppler, 1993; Černý and others, 2005; Johan and others, 2012). Enrichment in F is attributed to protracted differentiation of a relatively primitive melt (Černý, 1991; Černý and others, 2005). High volatile contents in near-solidus melts may result in some rocks in which it is difficult to distinguish magmatic versus aqueous fluid effects (see Černý and others, 2005, and references therein). Consequently, we include magmatic and potentially hydrothermal, granite-peripheral deposits such as veins, greisens, and skarns in this analysis.

Most economically productive tin deposits consist of Sn-greisens, Sn-veins, Sn-polymetallic veins, or skarns, but porphyry Sn deposits are also important (Sillitoe and others, 1975; Grant and others, 1980) (table 1). Greisens associated with evolved granites typically consist of quartz, Fe-Li micas, fluorite, topaz, and cassiterite, with or without wolframite, scheelite, molybdenite, and pyrite, and they form in the apical parts of hydrothermally altered granite cupolas (greisen) and (or) in altered wall rocks that host evolved granitic intrusions (exogreisen) (Hudson and Reed, 1997). Quartz, muscovite, and Li-rich annite [monoclinic $K(Fe^{2+}, Li, Al)_3(AlSi_3O_{10})(OH)_2$] (formerly, "zinnwaldite") are characteristic of Sn-greisens (Černý and others, 2005); other common minerals in greisens include tourmaline, beryl, andalusite, garnet, axinite, and fluorite. Porphyry Sn granites are typically quartz- and

feldspar-porphyritic, peraluminous, ilmenite-series granites that contain high levels of Li, Rb, B, Cs, and Sn, with quartz-sericite-tourmaline alteration, and cassiterite as the dominant ore mineral (Lehman and others, 2000).

Tungsten concentrations are most commonly found in veins and greisens at contacts with highly evolved granites (Werner and others, 1998; Richards and others, 2003) (table 1) and, less commonly, in porphyry deposits. Tungsten, molybdenum, indium, and tantalum may also be present in Sn-greisens. Sn-skarns often contain W; however, W-skarns do not necessarily contain Sn, and they do commonly contain Mo (Newberry, 1998). Porphyry W deposits can be associated with both oxidized (magnetite-series) and reduced (ilmenite-series) granitic rocks, but porphyry W deposits are rare (Seedorff and others, 2005). Tungsten enrichment is inferred to result from extended melt fractionation; however, in granites that have associated scheelite skarns, W concentrations are not known to be elevated relative to W concentrations in other granitic rocks (Newberry and Swanson, 1986; Černý and others, 2005). Fluorspar is commonly found with Sn and W in vein, greisen, and skarn deposits that are associated with highly evolved granites. The Mount Pleasant deposit in New Brunswick, Canada (table 1), is an example of a porphyry W-Mo deposit in a F-rich, high-silica[4]-feldspar porphyry that has late-stage Sn-, Zn-, and Cu-sulfide veins, W-Mo stockworks, granite-porphyry breccias, and dikes of granite porphyry that locally contain significant concentrations of indium (Sinclair and others, 2006). Indium is known to be associated with late fractionated phases of ilmenite-series granites; in Japan, late-stage cassiterite-wolframite (Sn-W) quartz veins associated with ilmenite-series granites contain as much as 0.8 percent indium; some granites in this belt also have associated W-skarn deposits (Ishihara and others, 2006).

Molybdenum is mined principally from the following three types of deposits: (1) Climax-type deposits that are associated with high-K aluminous granites and rhyolite porphyries that contain more than 73 weight percent SiO_2 and in which Mo is the principal commodity (White and others, 1981); (2) porphyry Cu(-Mo) systems from which Mo is recovered as a byproduct of large-tonnage, low-grade copper deposits (Seedorff and others, 2005); and (3) low-F, arc-related porphyry Mo deposits that are most commonly associated with I-type calc-alkaline quartz monzonites to granites that have SiO_2 contents between 65 to 77 weight percent and that are characterized by a lack of recoverable Cu (Theodore, 1986; Ludington and Plumlee, 2009; Taylor and others, 2012). The arc-related porphyry Mo deposits are associated with late-stage silicic alteration, replacement mineralization, breccia pipes, stockworks, and veins; quartz and potassium feldspar are the dominant gangue minerals in these deposits (Seedorf and Einaudi, 2004). This deposit type may be an end member of the alkali-feldspar rhyolite-granite (Climax-type) porphyry Mo model (Seedorf and Einaudi, 2004; Taylor and others, 2012). In this analysis, we applied a scoring method that focuses on Climax-type and low-F, arc-related porphyry deposits in which Mo is a dominant commodity, and it excludes porphyry Cu deposits in which Mo is a byproduct.

Mineral-Resource-Potential Estimation Method

To estimate mineral resource potential for Sn-W-Mo(-Ta-In-fluorspar) deposits associated with specialized granites in Alaska, the following six criteria were considered: (1) presence of appropriate mineral occurrences, deposits, or mines, (2) rock types, derived from the "Geologic Map of Alaska" (Wilson and others, 2015), (3) the presence of "specialized" granite compositions, as indicated by element ratios, (4) stream-sediment geochemical data, (5) heavy-mineral-concentrate (HMC) data, and (6) aerial gamma-ray survey data. The significance and application of these criteria (table 13) are

[4] 74 to 77 percent SiO_2.

described below. The scoring schema for the specialized granite is designed to identify high-silica alkali-feldspar rhyolite-granite porphyry Mo (Climax-type) deposits (White and others, 1981) and low-F, arc-related porphyry Mo (Quartz Hill-type) deposits (Ashleman and others, 1997; Taylor and others, 2012), as well as to exclude porphyry Cu(-Mo) deposits (Cox, 1986b; Ashleman and others, 1997); however, Mo enrichments might unintentionally foster inclusion of areas prospective for porphyry Cu deposits.

The scoring method for the Sn-W-Mo(-Ta-In-fluorspar) deposit group involves adding the total scores derived for each dataset parameter. As with previous models, the highest value for each evaluated parameter is applied to assign the score for that HUC; multiple scores for a given parameter within a HUC are not cumulative. In the scoring method created for this deposit group, stream-sediment geochemical data has the most comprehensive and systematic coverage for the state, and the data contributed a maximum of 9 points, or about 36 percent, to the HUC resource *potential* scores. Igneous-rock geochemistry, the best available predictor of appropriate igneous rock types, accounted for a maximum of 5 points, or about 20 percent, of the *potential* score. Other spatially quantifiable physical data, such as heavy-mineral-concentrate mineralogy, heavy-mineral-concentrate geochemistry, and scored ARDF records, are important predictors, but they contributed a maximum of 3 points, or about 12 percent apiece, to the *potential* score because of limited geographic coverage, which can skew results. Map-unit lithology data have broad geographic coverage but lack precision at the scale of a HUC, so this data contributed a maximum of 1 point, or 4 percent, of the total *potential* score. Although airborne gamma-ray survey data have broad state coverage, they are not a strong predictor for the commodities of interest and so only contributed a maximum of 1 point, or 4 percent, of the total score for resource *potential* in a HUC.

The HUC-based scoring schema for Sn-W-Mo(-Ta-In-fluorspar) deposits described above yields a maximum value of 25 points for resource *potential* (table 13). Total scores for HUCs were subdivided at natural statistical breaks (Jenks, 1967) method into Low, Medium, and High *potential* categories; the resulting score ranges are 0–2, 3–7, and 8–25 points, respectively (table 14). *Certainty* values were assigned on the basis of the number of datasets that contributed to HUC *potential* total scores; Low, Medium, and High *certainty* scores correspond to contributions of 0–1, 2–3, and 4–5 datasets, respectively (table 14). The sixth dataset, map-unit lithology, was not considered to be sufficiently precise geospatially to contribute to *certainty* in a specific HUC.

Lithology

Igneous rock names derived from the “Geologic Map of Alaska” (Wilson and others, 2015) were used to identify areas of igneous rocks that are permissive for Sn-W-Mo(-T-In-fluorspar) deposits. These names were extracted from map-unit descriptions, which indicate those units in which felsic and (or) silicic igneous rocks constitute at least 33 percent of the mapped unit. These igneous rock map-unit descriptions are generalized and the units cover large areas, and so the lithology assignments are unreliable at the scale of a HUC. Consequently, map lithology contributed one point to resource *potential* scores (table 13), and they provided no contribution to *certainty* scores (table 14).

Alaska Resource Data File

Descriptive fields contained in Alaska Resource Data File (ARDF) mineral-occurrence records were scored relative to selected keywords. Such keywords include those for individual elements and commodities (such as Sn, W, Mo, Ta, In, fluorspar), various minerals (such as fluorite, cassiterite, zinnwaldite, scheelite, wolframite), alteration assemblages (such as tourmaline-muscovite-quartz), alterations (such as tourmalinized, sericitized), and deposit models (such as Sn replacement, W veins, porphyry Mo) (appendix C). When fluorite is specified in an ARDF record, it provides an indication of fluorine in a HUC because fluorine abundance in rock and stream-sediment samples were not routinely

or reliably determined, and also the number of HMC samples is limited. Cumulative keyword points for each HUC contributed to net scores in the ARDF records; statistical analysis and verification by inspection suggested that net scores of 4 or more represent favorable occurrences for the specialized-granite deposit group. Results of the ARDF-record scoring were reviewed to ensure that known occurrences received appropriate scores and that occurrences that are unlikely to contain Sn, W, Ta, Mo, In, and (or) fluorspar mineralization were not inappropriately ranked. Many ARDF-record localities that received high keyword scores correspond to placer deposits, which are useful because placer cassiterite or scheelite deposits, like HMC mineral data, are evidence for the possible presence of a nearby igneous-related deposit that contains those minerals. ARDF-record keyword scores of 20 or higher correspond to mineral occurrences that contain keyword points for multiple ARDF record categories, which suggests resource potential. Natural statistical breaks in ARDF-record score distributions were applied, and these breaks suggest that localities having scores of 4 to 19 have moderate potential for a deposit and, thus, were assigned 1 point, and localities having scores of 20 or higher had relatively high potential and, thus, received 3 points (table 13). Although some HUCs contain more than one ARDF-record locality, the maximum score for an individual ARDF-record locality defines the score for the HUC. Consequently, the maximum ARDF-record score for any HUC is 3 points. The presence of an ARDF record in a HUC, regardless of score, positive or zero, contributed 1 point to the *certainty* total, whereas HUCs that contain no ARDF records received a null score and, thus, no points toward the number of datasets used to calculate *certainty*.

Igneous-Rock Geochemistry

Igneous-rock geochemical data were used to identify rock types that are permissive for Sn-W-Mo(-Ta-In-fluorspar) deposits, particularly those indicative of specialized granite. Specialized granites have distinct compositions that are relatively easy to identify. Geochemical analyses of nearly 49,000 igneous-rock samples from across the state locally provide more precise compositional information than does the "Geologic Map of Alaska" (Wilson and others, 2015), especially given the compositional complexity of many intrusions and the general lack of detailed geologic mapping. Discriminating specialized granites using geochemical data has three advantages, (1) geochemical data provide an objective test of compositional criteria, (2) geochemical data are spatially referenced to particular small intrusions and dikes that are not typically delineated on the geologic map but may potentially have associated Sn-W-Mo mineralization, and (3) rock samples correspond to discrete locations within HUCs, providing geospatial precision. Consequently, igneous-rock geochemistry was more heavily weighted than geologic-map-derived lithologic characterizations in identification of favorable rock types in Alaska.

Three components, each based on igneous-rock geochemical criteria, were used to identify specialized-granite composition parameters (table 13). The first scoring component applies the alumina saturation index (ASI) in combination with molar Al/[Na+K] (ANK) (Maniar and Piccoli, 1989) to determine whether the rock is peraluminous. The second scoring component is the Ga/Al ratio, calculated as 10,000Ga/Al. Ga/Al ratio values greater than 2.6 distinguish alkaline and subalkaline igneous rock types (Whalen and others, 1987) and can serve as a crude proxy of fluorine contents. The Ga/Al ratio has only been calibrated for intermediate and felsic rock compositions (Whalen and others, 1987), and, because highly fractionated igneous rocks were the target of this deposit model, scoring of both the ASI and Ga/Al ratio were limited to igneous rocks that contain more than 65 weight percent SiO_2 (table 13). The third scoring component pertains to igneous-rock SiO_2 content, with rocks containing more than 73 weight percent SiO_2 being considered prospective. The cutoff at 73 weight percent silica reflects the average silica composition of different suites of late-orogenic, postorogenic, and anorogenic granite (Rogers and Greenberg, 1990), as well as silica values for granite porphyries

associated with Mo deposits at Climax (White and others, 1981) and Quartz Hill (Ashleman and others, 1997).

In Alaska, nonsystematic and incomplete rock sampling compromise the utility of these metrics. As explained earlier, geochemical composition, when available, is more robust than map-unit descriptions for identification of appropriate rock types that are potentially associated with this deposit group. The HUCs that contain rock samples having peraluminous compositions received 2 points. Similarly, HUCs that contain rock samples that have greater than 65 weight percent SiO_2 and Ga/Al ratio values greater than 2.6 received 2 points. The HUCs that contain samples having SiO_2 contents greater than 73 weight percent received 1 point. Maximum possible HUC scores for *potential* derived from igneous-rock geochemical data is, therefore, 5 points (table 13). All HUCs for which igneous-rock geochemical data is available received 1 point toward HUC *certainty* scores.

Stream-Sediment Geochemistry

Abundances of In, Mo, Sn, Ta, and W in stream-sediment samples were statistically evaluated and scored at the 91st and 98th percentiles (table 13). As previously stated, in HUCs that contain multiple samples, the highest value for an element of interest was used to assign a score. Stream-sediment samples that had concentrations of W, In, and Ta in the 91st percentile or higher received 1 point. Those samples that had Sn and Mo abundances between the 91st and 98th percentile values received 2 points, whereas those abundances at or above the 98th percentile values received 3 points. The scores are additive, and the maximum score for resource *potential* derived from stream-sediment-sample data in a HUC is 9. All HUCs that contain non-null geochemical data for stream-sediment samples received 1 point toward the *certainty* score. If a HUC lacks a sample, then it has a null score and, thus, received no *certainty* points.

Heavy-Mineral-Concentrate Data

Statewide, the HMC dataset contains records for 18,137 samples for mineralogy and 49,783 samples for chemistry. These samples are important because they unequivocally indicate the presence of Sn-, W-, Mo-, In-, and Ta-bearing minerals or fluorite in a HUC. HMC data are contained in the AGDB2, and they include mineralogic and geochemical information. Estimates of relative abundances of minerals, which range from “trace” to “abundant”, were not applied for scoring because mineral abundance evaluations are inconsistently assigned. The HUCs containing HMC samples that have Sn- or Mo-bearing minerals, such as cassiterite or molybdenite, received 3 points, whereas those containing samples that have scheelite, wolframite, or fluorite received 2 points, and those containing samples that have possible deposit-associated minerals, including columbite, thorite, or uranothorite, received 1 point. Because of the limited amount of data available for HMC, the maximum score assigned for HMC mineral-content data is 3 points (table 13).

The HMC geochemical data also contributed to HUC resource *potential* scores. Because of the limited data available, all geochemical data were scored; however, statistics were run separately on “best value” data and stepwise semi-quantitative emission-spectroscopy data (for samples that lacked any other type of geochemical data). Stepwise data are provided as ranges of values that cannot be compared to discrete analyzed values that are determined by XRF or ICP-MS methods. Approximate 80th percentile values were determined for each data subset and scored as listed in table 13. These scores were weighted to emphasize relative significance for the specialized-granite deposit group. For example, In values are rare and, consequently, important if present. The HUCs containing samples that have W abundances higher than the 80th percentile value received 1 point; those containing samples that have Sn abundances higher than the 80th percentile value received 2 points; and those containing samples that have Mo, In, or Ta abundances higher than the 80th percentile value received 3 points. The HMC geochemical data provided a maximum of 3 points to a HUC *potential* score (table 13). All HUCs for

which HMC data are available received 1 point toward its *certainty* score (table 14); HUCs that contain no samples did not receive a point for *certainty*.

Aerial Gamma-Ray Survey Data

In aerial gamma-ray surveys, equivalent thorium (eTh) concentrations were determined by proxy from gamma-rays emitted by radioactive ^{208}Tl, the daughter product of ^{232}Th decay. These data help identify igneous rocks that have potential for Sn, W, and Ta deposits because these elements are often associated with Th, which is an incompatible element that is commonly concentrated in late-stage magmatic fluids similar to the minerals of interest (Černý and others, 2005). As previously noted, aerial radiometric Th values correlate with Th concentrations in stream-sediment samples, which suggests that radiometric surveys can define areas that are sources for Th- and rare-metal-enriched igneous rocks. The HUCs that have Th values at the 75th percentile value (~6 ppm eTh; Duval, 2001) or higher received 1 point; anomalous Th abundances received relatively limited weighting because elevated Th concentrations do not necessarily correspond to elevated Sn, W and (or) Ta abundances. The HUC scores derived from radioactivity data were assigned a single value calculated from the average radioactivity value measured within a HUC (table 13).

Results and Discussion

Relative mineral-resource potential for each HUC was established using the parameters described above (tables 13, 14; plate 11; appendix E). A total of 1,024 HUCs (7 percent of Alaskan HUCs) have High *potential* for Sn-W-Mo(-Ta-In-fluorspar) mineral deposits, 401 of which also have High *certainty*; 3,564 HUCs (26 percent) have Medium *potential*, and 9,176 HUCs (67 percent) have Low *potential*. A total of 3,413 HUCs either lacked any data that were pertinent to resource potential or lacked any stream-sediment data and, therefore, received a resource potential score of zero; these HUCs were classified as having Unknown *potential* (colored gray on plates 11,12).

The distribution of HUCs that have High *potential* for Sn-W-Mo(-Ta-In-fluorspar) deposits correlates with certain Alaskan magmatic belts (Wilson and others, 2015; see also plate 12, this report). The scattered distribution of high-scoring HUCs reflects the compositional variability within these belts, as well as inhomogenous and discontinuous data availability. Peripheral to these belts, high-scoring HUCs may represent concentrations of Sn, W, Ta, Mo, In, and F hosted in dikes, veins, greisens, stockworks, or small plugs that are mostly too small to be shown on regional geologic maps. Because of these factors, the scored HUCs may be the best available approximation the distribution of specialized granites that have potential to contain Sn-W-Mo(-Ta-In-fluorspar) deposits.

Known Sn-W-Mo(-Ta-In-Fluorspar) Mineralization Associated with Specialized Granites in Alaska

Deposits and occurrences of Sn, W, and Mo are widely distributed in Alaska, but only a few are economically significant (table 1). Magmatic belts in Alaska that contain peraluminous granites and associated Sn-W-Mo mineralization include the Brooks Range (Newberry and others, 1986), the Darby-Hogatza igneous belt (Miller and Elliott, 1969), the Kokrines-Hodzana belt (Ruby batholith) (Barker and Foley, 1986), the Kuskokwim–White Mountains belt (Warner and others, 1988; Burleigh, 1992a,b), the Alaska Range (Reed, 1978), and the Coast Range batholith in southeastern Alaska (Newberry and Brew, 1989; Ashleman and others, 1997; see also plate 12, this report). Intrusive complexes in these areas are compositionally and texturally diverse. In these intrusive complexes, highly fractionated granites intrude less-fractionated phases of granite, and they locally have coeval volatile-rich phases of granite that contain high concentrations of incompatible elements; these highly fractionated granites either were emplaced at shallow depths as small stocks and dikes or were erupted in volcanic complexes (Arth and others, 1989a,b; Moll-Stalcup and Arth, 1989).

Most lode-Sn deposits in Alaska are found in greisens, which were divided by Hudson and Reed (1997) into the following three types: (1) those that replace felsic dikes and plugs adjacent to mineralizing granites, (2) those that form adjacent to, and below, the upper contacts of mineralizing granites, and (3) those that dip steeply downward into the source granite. Alaska contains a globally recognized province of Sn-bearing granites and associated Sn occurrences, located in the Lost River–Kougarok belt (Hudson and Arth, 1983; Hudson and Reed, 1997) on the northwestern part of the Seward Peninsula (plate 12). Most of the lode-Sn produced in Alaska was derived from the Lost River district. The Lost River mine was developed on a meter-scale, cassiterite-rich felsic intrusion, the Cassiterite Dike, which was extensively altered and replaced by quartz-topaz-fluorite greisen that contains disseminated cassiterite and sulfide minerals (Sainsbury, 1964). The altered dike is cut by sulfide-rich veinlets that contain cassiterite and wolframite. In addition to the mineralized dike, the upper part of a granite cupola at Lost River is replaced by Sn-rich quartz-topaz-tourmaline and muscovite-quartz±tourmaline greisens (Dobson, 1982). Steeply dipping greisens (Hudson and Reed, 1997) are also common in the Lost River district; these consist of locally sheeted, cassiterite-bearing quartz-topaz zones hosted in source granites. Fluids exsolved from a buried granite cupola that intruded limestone also produced the Lost River skarn deposit, formed by multiple episodes of Sn mineralization (Dobson, 1982). The first episode of skarn formation represents early anhydrous skarn development that was subsequently overprinted and increased in size by hydrous-skarn formation. Postskarn fluorite-mica veins that contain cassiterite and wolframite extend outward several hundred meters from the skarn. The destruction of early anhydrous skarn by hydrous skarn and the ensuing hydrothermal processes remobilized and concentrated tin (Dobson, 1982). Rocks near the upper contact of zinnwaldite granite at Kougarok, on the Seward Peninsula (plate 12), are altered to Sn-mineralized quartz-tourmaline-topaz greisen, and dikes and plugs that are peripheral to the granite are greisenized (Puchner, 1986). In the central Brooks Range, Devonian batholiths include evolved specialized granites that intrude carbonate rocks, and they have associated greisen and skarn deposits (Newberry and others, 1986). ARDF-record occurrences near Mount Hecht and Ernie Lake, in the central Brooks Range (plate 12), consist of cassiterite and fluorite disseminated in pale-green to white fluorite-muscovite granite orthogneiss; these are classified as porphyry Sn(?) deposits. Steeply dipping greisen deposits are associated with Sithylemenkat, in the Ruby batholith within the Kokrines-Hodzana magmatic belt (Barker and Foley, 1986); Lime Peak, in the White Mountains area (Warner and others, 1998); Ohio Creek, in the Alaska Range; and Sleitat in southwestern Alaska (Hudson and Reed, 1997). The Sleitat system contains all three greisen types (Burleigh, 1991).

In the Kuskokwim–White Mountains area (plate 12), a Late Cretaceous magmatic belt includes tourmaline granites that have associated Au and Ag-Sn (locally ±W, ±Mo, and rarely In) greisens, silicified breccias, and quartz veins that contain cassiterite (for example, Win, Won, Bismarck, Ganes Creek, Tolstoi, and Konechney ARDF-record localities; Bundtzen and Miller, 1997). These are locally intruded by evolved Sn-, U-, and REE-bearing volcanic rocks, such as those at Mount Sischu (Miller and others, 1980), and 55-Ma granitic plugs, such as those in the Tofty area (Reifenstuhl and others, 1998).

In the southern part of the Yukon-Tanana uplands, the Banner prospect consists of Au-Ag-Sn-bearing greisens and veins associated with a 90-Ma quartz porphyry intrusion (Freeman, 2011).

Specialized granites in the northern Alaska Range include the Ohio Creek prospect, which consists of Sn-greisen and wodginite-tourmaline-muscovite Ag-, Sn-, W-, Mn-, and Nb-enriched pegmatites associated with Late Cretaceous or early Tertiary granite (Hawley and others, 1978), and the Green Spike porphyry Sn prospect that consists of quartz veins containing cassiterite, chalcopyrite, molybdenite, pyrite, and sphalerite hosted by Oligocene rhyolite (Balen and others, 1991). In southeastern Alaska, Groundhog Basin contains early Miocene Sn-bearing granite and rhyolite

porphyry, as well as associated Sn-skarn and replacement deposits that are cut by quartz veins containing Mo, fluorite, and topaz and by joints coated with molybdenite (Newberry and Brew, 1989).

Tungsten Deposits and Occurrences in Alaska

Although porphyry W deposits are rare (Seedorff and others, 2005), the Yukon-Tanana uplands in the Fairbanks area (plate 12) contains granite porphyries that have associated W mineralization (Newberry and others, 1990). Scheelite skarns and veins (Stepovich and Spruce Hen mines, table 1; plate 12) are associated with apliltic or pegmatitic ilmenite-series granites that are part of the larger tonalite-to-granite igneous complex near Fairbanks (Newberry and Swanson, 1986); these associated granites, pegmatites, veins, and skarns may also contian concentrations of In, on the basis of stream-sediment geochemical data. Late Cretaceous plutons and early Tertiary rhyolite porphyries in the Yukon-Tanana uplands are associated with polymetallic hydrothermal veins that contain Ag, Au, Sn, W, Mo, and REE, in host rocks that include Devonian plutons, greisens, and skarns (Newberry and Solie, 1995). The host rocks to the specialized granites in the Yukon-Tanana uplands, Seward Peninsula, and Brooks Range, as well as in the Kokrines-Hodzana belt, are also tectonically shortened pericratonic terranes, suggesting that similar factors may have contributed to the formation of the specialized granites and associated mineralization in these areas.

Molybdenum Deposits and Occurrences in Alaska

Known localities of Mo mineralization in Alaska are widely scattered. They include deposits which are associated with high-silica granite (according to the geochemical database) and biotite quartz monzonite on Saint Lawrence Island, as well as with the Darby-Hogatza igneous belt (plate 12), of Middle to Late Cretaceous age, that may be examples of low-F, arc-related porphyry Mo mineralization described by Taylor and others (2012). Both of these intrusive complexes contain associated quartz veins and silicified breccia zones rich in fluorite, Sn, W, Ag, Pb, and Zn (Bundtzen and others, 1994). A porphyry Mo deposit of probable Tertiary age at Bear Mountain, in the Porcupine area (plate 12), transitions upwards to a W-topaz-rich zone capped by massive silica (Barker and Swainbank, 1986). The Mike prospect, on the Alaska Peninsula, is a Pliocene dacite porphyry Mo prospect that is also moderately rich in Cu (Nokleberg and others, 1987). Miss Molly, in the western Alaska Range (plate 12), consists of two intersecting sheeted sets of quartz-molybdenite-pyrite-sericite(-fluorite) veinlets and thin veins that cut coarse, equigranular biotite granite: no local porphyry intrusions are known near this locality (Fernette and Cleveland, 1984), but these veinlets probably represent either Climax-type or low-fluorine arc-related porphyry Mo mineralization.

The best known porphyry Mo deposit in Alaska is the Oligocene Quartz Hill deposit in the Coast Mountains in southeastern Alaska (Ashleman and others, 1997). Intrusive rocks at Quartz Hill consist of an early epizonal granite intruded by porphyritic rhyolite plugs and dikes and associated breccia pipes. Mineralization consists of a well-developed stockwork of quartz-molybdenite veinlets, which are rich in Mo and W but low in Sn, Cu, Pb, and Zn; the stockwork, which has a surface expression of 2.8×1.5 km, cuts the composite Quartz Hill granite-rhyolite-porphyry stock to as much as a 1,000 m depth (Ashleman and others, 1997). The Burroughs Bay deposit, located between Groundhog Basin and Quartz Hill (plate 12), is hosted within pegmatitic granite, and it consists of Mo-bearing aplite dikes and quartz-molybdenite stockwork veins (Hudson and others, 1981). Emplacement of these siliceous stocks and dikes was structurally controlled and took place along the western margin of tectonically thickened pericratonic terranes that host the Late Cretaceous to early Tertiary Coast batholith arc complex (Ashleman and others, 1997) after the regional transition from a contractional tectonic setting to dextral transpression (Plafker and Berg, 1994).

Areas in Alaska that have High Potential for Sn-W-Mo(-Ta-In-Fluorspar) Deposits Associated with Specialized Granites

The areas that stand out as having the highest potential for Sn-W-Mo(-Ta-In-fluorspar) mineralization in Alaska include each of the following areas that contain known Sn, W, or Mo mineralization: (1) the Lost River–Kougarok area, (2) the Darby-Hogatza belt, (3) the Porcupine area, (4) the Kokrines-Hodzana terrane, (5) the Kuskokwim–White Mountains belt, (6) the Yukon-Tanana uplands, (7) the western Alaska Range, (8) the northern Alaska Range, and (9) the Coast Mountains (plate 12). High-scoring HUCs are also scattered across areas not previously known to have high concentrations of Sn-W-Mo(-Ta-In-fluorspar), and some are in places where ARDF-record localities for these commodities are rare or absent.

The HUCs that have the highest *potential* scores, each receiving 22 points (appendix E), include (1) the Jimmy Lake ARDF-record occurrence in the western Alaska Range, and (2) the Green Spike prospect in the northern Alaska Range. HUCs that have scores between 20 and 22 points are mainly in the western Alaska Range and the White Mountains; a few more of these are located in the Yukon-Tanana uplands, and one is at Sithylemenkat (plate 12). HUCs that have scores between 17 and 19 points are dominantly located in the western Alaska Range. Most of these HUCs had null (lacking deposits or occurrences) or zero (deposits or occurrences that lack the target commodities) ARDF-record scores and have Medium *certainty* assignments; the high scores for these HUCs are based mainly on geochemical parameters and HMC mineralogy.

Scattered HUCs that have 17 to 19 points for resource *potential* are also located in the Kokrines Hills, the White Mountains, the Yukon-Tanana uplands, the northern Alaska Range, the Coast Mountains, the Darby Mountains, and the southwestern part of the Kuskokwim Mountains. Many of these HUCs also had low or null ARDF-record scores and Medium *certainty* assignments. These areas that have High *potential* scores and Medium *certainty*, on the basis of limited data, are prime candidates for further investigation.

Areas having Medium and Low *potential* scores that are based on very little available data might become higher *potential* areas when additional data become available. In some cases, the combination of different datasets can suggest the presence of appropriate rocks in areas of poor exposure. In some of these areas, which include the Seward Peninsula, the Kaiyuh Mountains, the area between the Kuskokwim Mountains and the White Mountains, and the eastern Alaska Range, stream-sediment samples contain high concentrations of Sn, W, Mo, Ta, and (or) In, which suggests the presence of evolved granitic rocks where none are well documented. The quality of land-use planning decisions will be enhanced by acquisition of additional data in areas where the *certainty* of the resource *potential* estimate is Low or Medium.

Mineral exploration targets are best defined in areas indicated by the GIS analysis to have high *potential*. Consideration of multiple data types demonstrate that parts of Alaska contain evolved intrusive rocks and stream-sediment samples that have high concentrations of Sn, W, Mo, Ta, and In where few or no mineral occurrences are known. Consequently, these areas may be underexplored for Sn, W, Mo, and (or) fluorite potential. Historically, Ta and In have not been targets of exploration in Alaska, but prospects may be identified during additional investigation of specialized granites and associated mineralization. Areas that have high scores for igneous-rock- and stream-sediment-sample geochemistry, as well as HMCs that contain the appropriate minerals, in which the origins of anomalies are unknown or poorly defined should be prioritized for additional study.

Summary

A data-driven GIS process was used to screen and investigate the mineral resource potential for six deposit-type groups in Alaska. One or more examples of each deposit group, which may contain resources of one or more critical minerals, had previously been identified in Alaska. The six deposit-type groups investigated include (1) REE-Th-Y-Nb(-U-Zr) deposits associated with peralkaline to carbonatitic intrusive rocks, (2) placer and paleoplacer Au deposits, (3) PGE(-Co-Cr-Cu-Ni-Ti-V) deposits associated with mafic to ultramafic intrusive rocks, (4) carbonate-hosted Cu(-Co-Ag-Ge-Ga) deposits, (5) sandstone-hosted U(-V-Cu) deposits, and (6) Sn-W-Mo(-Ta-In-fluorspar) deposits associated with specialized granites. For each of these groups, newly assembled datasets were used to refine an appropriate favorability scoring scheme so that known high potential areas (in particular, those that contain ARDF-record deposits and occurrences of the type under consideration) were identified. The method was tested and then applied statewide. For each of the six deposit groups, some areas newly recognized as having high potential for additional deposits were identified and described.

The resource-estimation process employed provides the means to assemble and analyze disparate datasets in a geospatial environment in order to quantify mineral-resource prospectivity across broad areas, in this case, the state of Alaska. Some data types are better adapted for use in this kind of analysis than others. For example, with regard to scoring schemes that favored certain types of igneous rocks, individual samples that have whole-rock and trace-element geochemical data constitute better data than those for generalized geologic map units, and scoring schemes could be weighted to address the robustness of datasets with both *potential* and *certainty* scores.

The data on which this resource potential estimate is based are not systematically or continuously distributed across the area that was evaluated. In particular, the number and spatial distribution of geochemistry sample localities differ significantly among different parts of the state (Granitto and others, 2013). In some areas, ARDF records cluster around known occurrences, prospects, or mines, and (or) they cluster in areas that have the best access, such as along roads or rivers. In order to develop consistent resource-potential scores, methods were employed that were designed to equalize potentially skewed scores resulting from uneven sampling, such as choosing the single highest element value in HUCs that contain multiple stream-sediment samples.

The ability and opportunity to analyze and query the scoring results has been preserved by providing all of the data used to develop individual scoring components and score results for each deposit group (appendix E). For those datasets such as the AGDB2, ADGGS geochemical data, and ARDF that are publicly available, individual users can easily recompile the applied data and evaluate sampling trends for comparison to our results. Similarly, interested parties can integrate additional data with the datasets and apply different scoring methods to evaluate other types of inquiries for resource potential.

Each of the scoring schemes reported here was developed by trial and error. The time required to change the scoring schema and run a different estimate is relatively minor. Our approach promotes iterative data evaluation, which should result in ever-improving resource estimates.

Each of the data layers used here consists of data that had been collected and reported previously. Industry and agency geologists have had access to much of these data for years, although not in a digital format suitable for geospatial manipulation. Although coverage for Alaska is spotty and incomplete, a huge amount of data is available to synthesize. This study provides a new way to analyze large spatial datasets in combination and may result in identification of new areas for mineral exploration, new discoveries, and new insights into trends of mineral belts, tectonic settings, and ore-forming processes. Augmenting the available data with new information will undoubtedly contribute to a sharper focus for future exploration and resource assessment.

Identification of areas that deserve additional study is an important outgrowth of this analytical process. In particular, HUCs rated as having High *potential* and Low or Medium *certainty* are places

that merit additional sampling and investigation. Future geologic investigations should prioritize areas that either have relatively high *potential* based on limited available data or are adjacent to such areas. These areas might also benefit from the use of new exploration methods and types of data acquisition that would complement the currently available datasets. Land-use-planning decisions will benefit most from acquisition of new data in areas that have low degrees of certainty because the lack of relevant data precludes accurate assessment of mineral potential. Mineral-exploration targets are most confidently pursued in areas of known potential, but underexplored areas that lack data collected with previously unavailable technology and analytical tools may hold the greatest rewards. Although true for all six groups of deposit-types, such an approach is particularly pertinent to REE and PGE exploration, which include important commodities that were not previously targets for exploration.

Data Resources

Alaska Resource Data File (ARDF) – http://ardf.wr.usgs.gov/

Alaska Geochemical Database, Version 2.0 (AGDB2) – http://pubs.usgs.gov/ds/759/

National Uranium Resource Evaluation (NURE) Hydrogeochemical and Stream Sediment Reconnaissance data – http://pubs.usgs.gov/of/1997/ofr-97-0492/

Alaska Division of Geological & Geophysical Surveys (ADGGS) WebGeochem Geochemical Sample Analysis Search – http://www.dggs.alaska.gov/webgeochem/

Alaska Aerial Gamma-Ray Surveys – http://pubs.usgs.gov/of/2001/of01-128/

Map of Alaska's Coal Resources (Merritt and Hawley, 1986) – http://www.dggs.dnr.state.ak.us/pubs/pubs?reqtype=citation&ID=2636

Geologic Map of Alaska (Wilson and others, 2015) – http://dx.doi.org/10.3133/sim3340

References Cited

Ames, D.E., Davidson, A., and Wodicka, N., 2008, Geology of the giant Sudbury polymetallic mining camp, Ontario, Canada: Economic Geology, v. 103, no. 5, p. 1057–1077.

Angiboust, Samuel, Fayek, Mostafa, Power, I.M., Camacho, Alfredo, Calas, Georges, and Southam, Gordon, 2012, Structural and biological control of the Cenozoic epithermal uranium concentrations from the Sierra Peña Blanca, Mexico: Mineralium Deposita, v. 47, no. 8, p. 859–874.

Arbogast, B.F., 1990, Quality assurance manual for the Branch of Geochemistry, U.S. Geological Survey: U.S. Geological Survey Open-File Report 90–668, 184 p.

Arbogast, B.F., ed., 1996, Analytical methods manual for the Mineral Resource Surveys Program, U.S. Geological Survey: U.S. Geological Survey Open-File Report 96–525, 248 p.

Armbrustmacher, T.J., 1989, Minor element content, including radioactive elements and rare-earth elements, in rocks from the syenite complex at Roy Creek, Mount Prindle area, Alaska: U.S. Geological Survey Open-File Report 89–0146, 11 p.

Arth, J.G., Criss, R.E., Zmuda, C.C., Foley, N.K., Patton, W.W., Jr., and Miller, T.P., 1989a, Remarkable isotopic and trace element trends in potassic through sodic Cretaceous plutons of the Yukon-Koyukuk Basin, Alaska, and the nature of the lithosphere beneath the Koyukuk terrane: Journal of Geophysical Research—Solid Earth, v. 94, no. B11, p. 15,957–15,968.

Arth, J.G., Zmuda, C.C., Foley, N.K., Criss, R.E., Patton, W.W., Jr., and Miller, T.P., 1989b, Isotopic and trace element variations in the Ruby batholith, Alaska, and the nature of the deep crust beneath the Ruby and Angayucham terranes: Journal of Geophysical Research—Solid Earth, v. 94, no. B11, p. 15,941–15,955.

Ashleman, J.C., Taylor, C.D., and Smith, P.R., 1997, Porphyry molybdenum deposits of Alaska, with emphasis on geology of the Quartz Hill deposit, southeastern Alaska, *in* Goldfarb, R.J., and Miller, L.D., eds., Mineral deposits of Alaska: Economic Geology Monograph 9, p. 334–354.

Athey, J.E., Harbo, L.A., Lasley, P.S., and Freeman, L.K., 2013, Alaska's mineral industry, 2012: Alaska Division of Geological & Geophysical Surveys Special Report 68, p. 61.

Bailey, D., 1987, Mantle metasomatism—Perspective and prospect: Geological Society of London Special Publications, v. 30, no. 1, p. 1–13.

Bailey, D., 1989, Carbonate melt from the mantle in the volcanoes of south-east Zambia: Nature, v. 338, p. 415–418.

Baker, T., 2002, Emplacement depth and carbon dioxide-rich fluid inclusions in intrusion-related gold deposits: Economic Geology, v. 97, no. 5, p. 1111–1117.

Balen, M.D., and others, 1991, Executive summary of the Bureau of Mines investigations in the Valdez Creek mining district, Alaska: U.S. Bureau of Mines Special Publication 1991, 43 p.

Barker, J.C., 1981a, Coal and uranium investigation of the Yukon Flats Cenozoic basin: U.S. Bureau of Mines Open-File Report 140-81, 63 p.

Barker, J.C., 1981b, Mineral investigations in the Porcupine River drainage, Alaska: U.S. Bureau of Mines Open-File Report 27-81, 201 p.

Barker, J.C., 1985, Sampling and analytical results of a mineral reconnaissance in the Selawik Hills area, northwestern Alaska: U.S. Bureau of Mines Open File Report 43-85, 67 p.

Barker, J.C., 1991, Investigation of rare-earth elements and zirconium in the Windy Fork peralkaline pluton, west-central Alaska: U.S. Bureau of Mines Field Report, 36 p.

Barker, J.C., and Clautice, K.H., 1977, Anomalous uranium concentrations in artesian springs and stream sediments in the Mount Prindle area, Alaska: U.S. Bureau of Mines Open-File Report 130-77, 19 p.

Barker, J.C., and Foley, J.Y., 1986, Tin reconnaissance of the Kanuti and Hodzana Rivers uplands, central Alaska, U.S. Bureau of Mines Information Circular 9104, 27 p.

Barker, J.C., and Swainbank, R.C., 1986, A tungsten-rich porphyry molybdenum occurrence at Bear Mountain, northeast Alaska: Economic Geology, v. 81, no. 7, p. 1753–1759.
Barker, J.C., and Van Gosen, B.S., 2012, Alaska's rare earth deposit and resource potential: Mining Engineering, January 2012, p. 20–32.
Barker, S.L.L., Hickey, K.A., Cline, J.S., Dipple, G.M., Kilburn, M.R., Vaughan, J.R., and Longo, A.A., 2009, Uncloaking invisible gold: Use of nanoSIMS to evaluate gold, trace elements, and sulfur isotopes in pyrite from Carlin-type gold deposits: Economic Geology, v. 104, no. 7, p. 897–904.
Barnes, S.J., Godel, Belinda, Gürer, Derya, Brenan, J.M., Robertson, Jesse, and Paterson, David, 2013, Sulfide-olivine Fe-Ni exchange and the origin of anomalously Ni rich magmatic sulfides: Economic Geology, v. 108, no. 8, p. 1971–1982.
Barnes, S.-J., and Lightfoot, P.C., 2005, Formation of magmatic nickel- sulfide deposits and processes affecting their copper and platinum group element contents, *in* Hedenquist, J.W., Thompson, J.F.H., Goldfarb, R.J., and Richards, J.P., eds., Economic Geology One Hundredth Anniversary Volume, 1905–2005: Littleton, Colorado, Society of Economic Geologists, p. 179–213.
Bea, F., 1996, Residence of REE, Y, Th and U in granites and crustal protoliths—Implications for the chemistry of crustal melts: Journal of Petrology, v. 37, no. 3, p. 521–552.
Beaty, D.W., Landis, G.P., and Thompson, T.B., eds., 1990, Carbonate-hosted sulfide deposits of the Central Colorado mineral belt: Economic Geology Monograph 7, 424 p.
Begg, G.C., Hronsky, J.A.M., Arndt, N.T., Griffin, W.L., O'Rielly, S.Y., and Hayward, Nick, 2010, Lithospheric, cratonic, and geodynamic setting of Ni-Cu-PGE sulfide deposits: Economic Geology, v. 105, p. 1057–1070.
Bierlein, F.P., and Maher, S., 2001, orogenic disseminated gold in phanerozoic fold belts -- examples from Victoria, Australia and elsewhere: Ore Geology Reviews, v. 18, p. 113-148.
Belasky, Paul, Stevens, C.H., and Hanger, R.A., 2002, Early Permian location of western North American terranes based on brachiopod, fusulinid, and coral biogeography: Palaeogeography, Palaeoclimatology, and Palaeocology, v. 179, p. 245–266.
Bell, Keith, ed., 1989, Carbonatites—Genesis and evolution: London, Unwin Hyman Ltd., 618 p.
Bell, Keith, and Simonetti, Antonio, 2010, Source of parental melts to carbonatites—Critical isotopic constraints: Mineralogy and Petrology, v. 98, p. 77–89.
Bentzen, E.H., II, Ghaffari, Hassan, Galbraith, Les, Hammen, R.F., Robinson, R.J., Hafez, S.A., and Srikant Annavarapu, R., 2013, Preliminary economic assessment—Bokan Mountain rare earth element project, near Ketchikan, Alaska: Tetra Tech, Inc., technical report prepared for Ucore Rare Metals, March 4, 2013, 229 p., accessed June 11, 2013, at http://www.sedar.com.
Berger, B.R., and Henley, R.W., 1989, Advances in the understanding of epithermal gold-silver deposits, with special reference to the western United States, *in* Keays, R.R., Ramsay, W.R.H., and Groves, D.I., eds., The geology of gold deposits—The perspective in 1988: Economic Geology Monograph 6, p. 405–423.
Berger, V.I., Singer, D.A., and Orris, G.J., 2009, Carbonatites of the world, explored deposits of Nb and REE—Database and grade and tonnage models: U.S. Geological Survey Open-File Report 2009–1139, 17 p. and database, http://pubs.usgs.gov/of/2009/1139/.
Bernstein, L.R., and Cox, D.P., 1986, Geology and sulfide mineralogy of the Number One Orebody, Ruby Creek copper deposit, Alaska: Economic Geology, v. 81, p. 1675–1689.
Bittenbender, P.E., Bean, K.W., Kurtak, J.M., and Deininger, J., Jr., 2007, Mineral assessment of the Delta River mining district area, east-central Alaska: U.S. Bureau of Land Management, Alaska Technical Report 57, 676 p.
Blatt, H., Tracy, R.J., and Owens, B., 2006, Petrology—Igneous, sedimentary, and metamorphic (3d ed.): New York, W.H. Freeman and Company, 533 p.

Blevin, P.L., and Chappell, B.W., 1992, The role of magma sources, oxidation states and fractionation in determining the granite metallogeny of eastern Australia: Transactions of the Royal Society of Edinburgh: Earth Sciences, v. 83, no. 1–2, p. 305–316.
Bliss, J.D., ed., 1992, Developments in mineral deposit modeling: U.S. Geological Survey Bulletin 2004, 168 p.
Bluemel, Britt, Leijd, Magnus, Dunn, Colin, Hart, C.J.,R. Saxon, Mark, and Sadeghi, Martiya, 2013, Biogeochemical expression of rare earth element and zirconium mineralization at Norra Kärr, southern Sweden: Journal of Geochemical Exploration, v. 133, p. 15–24.
Blundy, Jonathon, and Wood, Bernard, 2003, Mineral-melt partitioning of uranium, thorium and their daughters: Reviews in Mineralogy and Geochemistry, v. 52, no. 1, p. 59–123.
Bornhorst, T.J., Kaliokoski, J.O., and Paces, J.B., 1986, The Keweenaw native-copper district, *in* Brown, A.C., and Kirkham, R.V., eds., Field Trip 1, Guidebook—Proterozoic sediment-hosted stratiform copper deposits of Upper Michigan and Belt Supergroup of Idaho and Montana: Ottawa, Ontario, Canada, Geological Association of Canada, Ottawa 86 Committee, p. 21–36.
Boyle, D.R., 1982, The formation of basal-type uranium deposits in south central British Columbia: Economic Geology, v. 77, no. 5, p. 1176–1209.
Boyle, D.R., 1985, Geologic environments for basal-type uranium deposits in sedimentary host rocks, *in* Finch, W.I., and Davis, J.F., eds., Geological environments of sandstone-type uranium deposits: Vienna, Austria, International Atomic Energy Agency IAEA-TECDOC-328, p. 363–382.
Boyle, D.R., and Ballantyne, S.B., 1980, Geochemical stidoes of uranium dispersion in south-central British Columbia: CIM Bulletin, p. 89 –108.
Bundtzen, T.K., and Miller, M.L., 1997, Precious metals associated with Late Cretaceous-Early Tertiary igneous rocks of southwestern Alaska, *in* Goldfarb, R.J., and Miller, L.D., eds., Mineral Deposits of Alaska: Economic Geology Monograph 9, p. 242–286.
Bundtzen, T.K., Swainbank, R.C., Clough, A.H., Henning, M.W., and Hansen, E.W., 1994, Alaska's Mineral Industry, 1993: Alaska Division of Geological & Geophysical Surveys Special Report 48, 84 p.
Burleigh, R.E., 1991, Evaluation of the tin-tungsten greisen mineralization and associated granite at Sleitat Mountain, southwestern Alaska: U.S. Bureau of Mines Open-File Report 35-91, 41 p.
Burleigh, R.E., 1992a, Examination of the Win tin prospect, west-central Alaska: U.S. Bureau of Mines Open-File Report 92-92, 23 p.
Burleigh, R.E., 1992b, Tin mineralization at the Won prospect, west-central Alaska: U.S. Bureau of Mines Open-File Report 85-92, 21 p.
Burton, P.J., 1981, Radioactive mineral occurrences, Mount Prindle area, Yukon-Tanana uplands, Alaska: Fairbanks, University of Alaska, M.S. thesis, 72 p.
Cabri, L.J., 2002, The platinum-group minerals: Canadian Institute of Mining, Metallurgy, and Petroleum Special Volume 54, p. 13–129.
Castor, S.B., 2008, The Mountain Pass rare-earth carbonatite and associated ultrapotassic rocks, California: Canadian Mineralogist, v. 46, no. 4, p. 779–806.
Černý, Petr, 1991, Rare-element granitic pegmatites, Part I—Anatomy and internal evolution of pegmatitic deposits: Geoscience Canada, v. 18, p. 49–67.
Černý, Petr, Blevin, P.L., Cuney, Michel, and London, David, 2005, Granite-related ore deposits, *in* Hedenquist, J.W., Thompson, J.F.H., Goldfarb, R.J., and Richards, J.P., eds., Economic Geology One Hundredth Anniversary Volume, 1905–2005: Littleton, Colo., Society of Economic Geologists, p. 337–370.
Chao, E.C.T., Back, J.M., Minkin, J.A., Tatsumoto, M., Wang Junwen, Conrad, J.E., McKee, E.H., Hou Zonglin, Meng Qingrun, and Huang Shengguang, 1997, The sedimentary carbonate-hosted giant

Bayan Obo REE-Fe-Nb ore deposit of Inner Mongolia, China—A cornerstone example for giant polymetallic ore deposits of hydrothermal origin: U.S. Geological Survey Bulletin 2143, 65 p.
Chetty, D., and Frimmel, H.E., 2000, The role of evaporites in the genesis of base metal sulphide mineralisation in the Northern Platform of the Pan-Africa Damara Belt, Namibia: Geochemical and fluid inclusion evidence from carbonate wall rock alteration: Mineralium Deposita, v. 35, p. 364–376.
Clemens, J.D., and Wall, V.J., 1984, Origin and evolution of a peraluminous silicic ignimbrite suite—The Violet Town Volcanics: Contributions to Mineralogy and Petrology, v. 88, no. 4, p. 354–371.
Cobb, E.H., comp., 1972, Metallic mineral resources map of the Nulato quadrangle, Alaska: U.S. Geological Survey Miscellaneous Field Studies Map MF–423, scale 1:250,000.
Cox, D.P., 1986a, Descriptive model of basaltic Cu, *in* Cox, D.P., and Singer, D.A., eds., Mineral deposit models: U.S. Geological Survey Bulletin 1693, p. 130.
Cox, D.P., 1986b, Descriptive model of porphyry Cu, *in* Cox, D.P., and Singer, D.A., eds., Mineral deposit models: U.S. Geological Survey Bulletin 1693, p. 76–81.
Cox, D.P., and Singer, D.A., eds., 1986, Mineral deposit models: U.S. Geological Survey Bulletin 1693, 379 p.
Csejtey, Béla, Jr., Mullen, M.W., Cox, D.P., and Stricker, G.D., 1992, Geology and geochronology of the Healy quadrangle, south-central Alaska: U.S. Geological Survey Miscellaneous Investigations Series Map I–1961, 2 sheets, scale: 1:250,000, pamphlet 64 p.
Cuney, M., and Kyser, T.K., 2009, Recent and not-so-recent developments in uranium deposits and implications for exploration: Mineralogical Association of Canada, Short Course Series, 257 p.
Czamanske, G.K., Haffty, Joseph, and Nabbs, S.W., 1981, Pt, Pd, and Rh analyses and beneficiation of mineralized mafic rocks from the La Perouse layered gabbro, Alaska: Economic Geology, v. 76, no. 7, p. 2001–2011.
Dahlberg, P.S., 2014, Bear Lodge project Canadian NI 43-101 Pre-feasiblity Study Report on the Reserves and Devilopment of the Bull Hill Mine Wyoming: Roche Engineering Technical Report prepared for Rare Element Resources, October 9, 2014, 475 p., accessed September 18, 2015, at http://www.sedar.com.
Dahlkamp, F.J., 1993, Uranium ore deposits: Berlin, Heidelberg, Spinger-Verlag, p. 58–135.
Dashevsky, S.S., 2002, Alaska Resource Data File, Norton Bay quadrangle, Alaska: U.S. Geological Survey Open-File Report 2002–75, 27 p., http://ardf.wr.usgs.gov/quads/html/NortonBay.html.
Davis, Bruce, Sim, Robert, and Austin, Jeff, 2014, NI 43-101 Technical Report on the Bornite Project, Northwest Alaska, USA: BD Resource Consulting, Inc., SIM Geological Inc., and International Metallurgical & Environmental Inc., technical report for NovaCopper, Inc., April 1, 2014, 142 p., accessed April 28, 2014, at www.novacopper.com/s/NewsReleases.asp?ReportID=645513&_Type=News-Releases&_Title=NovaCopper-Files-NI-43-101-Technical-Report-on-the-Bornite-Project-Alaska.
Detterman, R.L., and Reed, B.L., 1980, Stratigraphy, structure, and economic geology of the Iliamna quadrangle, Alaska: U.S. Geological Survey Bulletin 1368–B, p. B1–B86.
Dickinson, K.A., 1977, Uranium and thorium distribution in continental Teriary rocks of the Cook Inlet basin and some adjacent areas, Alaska, *in* Campbell, J.A., ed, Short papers of the U.S. Geological Survey uranium-thorium symposium, 1977: U.S. Geological Survey Circular 753, p. 70–72.
Dickinson, K.A., 1978, Uraninite in sideritic nodules from Tertiary continental sedimentary rocks in the Healy Creek basin area, central Alaska, *in* Johnson, K.M., and Williams, J.R., eds., The United States Geological Survey in Alaska—Accomplishments during 1978: U.S. Geological Survey Circular 804–B, p. 98–99.
Dickinson, K.A., 1979, Uraniferous phosphate occurrence on Kupreanof Island, southeast Alaska: U.S. Geological Survey Open-File Report 79–1316, 2 p.

Dickinson, K.A., 1995, Geology, geochemistry, and uranium favorability of the Tertiary Kenai Group in the Susitna Lowlands at the northern end of Cook Inlet Basin, Alaska: U.S. Geological Survey Bulletin 2098–A, p. A1–A33.
Dickinson, K.A., and Campbell, J.A., 1978, Epigenetic mineralization and areas favorable for uranium exploration in Tertiary continental sedimentary rock in south-central Alaska—A preliminary report: U.S. Geological Survey Open-File Report 78–757, 13 p.
Dickinson, K.A., and Campbell, J.A., 1982, The potential for uranium deposits in the Tertiary Kootznahoo Formation of the southern part of the Admiralty Trough, southeastern Alaska: U.S. Geological Survey Open-File Report 82–983, 18 p.
Dickinson, K.A., Campbell, J.A., and Dula, W.F., Jr., 1995, Geology, geochemistry, and uranium favorabiility of Tertiary continental sedimentary rocks in the northwestern part of the Cook Inlet area, Alaska: U.S. Geological Survey Bulletin 2098–B, p. B1–B37.
Dickinson, K.A., Cunningham, K.D., and Ager, T.A., 1987, Geology and origin of the Death Valley uranium deposit, Seward Peninsula, Alaska: Economic Geology, v. 82, no. 6, p. 1558–1574.
Dickinson, K.A., and Morrone, J.F., 1982, Distribution of uranium and thorium in the lower Tertiary Orca Group and related rocks in part of the Cordova quadrangle, southern Alaska: U.S. Geological Survey Open-File Report 82–1032, 10 p.
Dickinson, K.A., and Pierson, C.T., 1988, A statistical analysis of chemical and mineralogic data from the Tertiary Kootznahoo Formation in southeastern Alaska, with emphasis on uranium and thorium: U.S. Geological Survey Bulletin 1851, 21 p.
Dickinson, K.A., and Skipp, G.L., 1990, Clay mineral depositional facies and uranium resource potential in part of the Tertiary Kenai Group, Kenai Peninsula, Alaska, *in* Bradley, D.C., and Ford, A.B., eds., Geologic studies in Alaska by the U.S. Geological Survey, 1990: U.S. Geological Survey Bulletin 1999, p. 81–99.
Dickinson, K.A., and Vuletich, April, 1990, Diagenesis and uranium mineralization of the Lower Tertiary Kootzhahoo Formation in the northern part of Admiralty Trough, southeastern Alaska: U.S. Geological Survey Bulletin 1888, 12 p.
Dickson, R.K., 1982, Uranium mineralization in the Nenana Coal Field, Alaska, *in* Alaska Division of Geological & Geophysical Surveys, Short Notes on Alaskan Geology—1981: Alaska Division of Geological & Geophysical Surveys Geologic Report 73H, p. 37–42. doi:10.14509/441.
Dobson, D.C., 1982, Geology and alteration of the Lost River tin-tungsten-fluorine deposit, Alaska: Economic Geology, v. 77, no. 4, p. 1033–1052.
Dostal, Jaroslav, Karl, S.M., Keppie, Duncan, Kontak, D.J., and Shellnutt, J.G., 2013, Bokan Mountain peralkaline granitic complex, Alexander terrane (southeastern Alaska)—Evidence for Early Jurassic rifting prior to accretion with North America: Canadian Journal of Earth Sciences, v. 50, no. 6, p. 678–691.
Dostal, Jaroslav, Kontak, D.J., and Karl, S.M., 2014, The Early Jurassic Bokan Mountain peralkaline granitic complex (southeastern Alaska)—Geochemistry, petrogenesis and rare-metal mineralization: Lithos, v. 202–203, p. 395–412.
Dumoulin, J.A., and Harris, A.G., 1987, Lower Paleozoic rocks of the Baird Mountains quadrangle, western Brooks Range, Alaska, *in* Tailleur, I.L., and Weimer, Paul, eds., Alaskan North Slope geology: Bakersfield, Calif., Pacific Section, Society for Sedimentary Geology (SEPM) and Alaska Geological Society, v. 1, p. 311–336.
Duval, J.S., 2001, Aerial gamma-ray surveys in Alaska: U.S. Geological Survey Open-File Report 2001–128, 2 CD-ROMS.
Eakin, G.R., 1969, Uranium in Alaska: Alaska Division of Geological & Geophysical Surveys Geologic Report No. 38, 49 p.

Eakin, G.R., 1975, Uranium investigations in southeastern Alaska: Alaska Division of Geological & Geophysical Surveys Geologic Report No. 44, 62 p.
Eakin, G.R., 1977, Investigation of Alaska's uranium potential, Part 1—Reconnaissance Program, West-Central Alaska and Copper River Basin: Alaska Division of Geological & Geophysical Surveys Open-File Report 109, 66 p.
Eakin, G.R., and Forbes, R.B., 1976, Investigation of Alaska's uranium potential: Alaska Division of Geological & Geophysical Surveys Special Report 12, 372 p.
Eakin, G.R., Jones, B.K., and Forbes, R.B., 1977, Investigation of Alaska's uranium potential: Alaska Division of Geological & Geophysical Surveys Open-File Report 109, 213 p.
Eby, G.N., 1990, The A-type granitoids—A review of their occurrence and chemical characteristics and speculations on their petrogenesis: Lithos, v. 26, p. 115–134.
Eckstrand, O.R., 1985, Canadian mineral deposit types—A geological synopsis: Geological Survey of Canada Economic Geology Report 36, 86 p..
Eckstrand, O.R., and Hulbert, L.J., 2007, Magmatic nickel-copper-platinum group element deposits, *in* Goodfellow, W.D., ed., Mineral Deposits of Canada—A Synthesis of Major Deposit-Types, District Metallogeny, the Evolution of Geological Provinces, and Exploration Methods: Geological Association of Canada, Mineral Deposits Division, Special Publication 5, p. 205–222.
Economou, M.I., and Naldrett, A.J., 1984, Sulfides associated with podiform bodies of chromite at Tsangli, Eretria, Greece: Mineralium Deposita, v. 19, p. 289–297.
Ensign, C.O., Jr., White, W.S., Wright, J.C., Patrick, J.L., Leone, R.J., Hathaway, D.J., Trammell, J.W., Fritts, J.J., and Wright, T.L., 1968, Copper deposits in the Nonesuch Shale, White Pine, Michigan, *in* Ridge, J.D., ed., Ore Deposits of the United States, 1933–1967, the Graton-Sales Volume: New York, American Institute of Mining, Metallurgical, and Petroleum Engineers, p. 460–488.
Eppinger, R.G., 1993, Gold and cinnabar in heavy-mineral concentrates from stream-sediment samples from the western half of the Lime Hills 1°x3° quadrangle, Alaska, *in* Dusel-Bacon, C., and Till, A.B., eds., Geologic studies in Alaska by the U.S. Geological Survey, 1992: U.S. Geological Survey Bulletin 2068, p. 91–100.
Fernette, Gregory, and Cleveland, Gaylord, 1984, Geology of the Miss Molly molybdenum prospect, Tyonek C-6 quadrangle, Alaska, *in* Short notes on Alaskan Geology 1981–82: Alaska Division of Geological & Geophysical Surveys Professional Report 86, p. 35–41.
Finlow-Bates, T., and Stumpfl, E.F., 1979, The copper and lead-zinc-silver orebodies of Mt. Isa mine, Queensland—Products of one hydrothermal system: Annales de la Société Géologique de Belgique, v. 102, p. 497–517.
Flanigan, B.P., 1998, Genesis and mineralization of ore deposits in the Illinois Creek region, west central Alaska: Fairbanks, University of Alaska, M.S. thesis, 125 p.
Foley, J.Y., and Barker, J.C., 1984, Chromite deposits along the Border Ranges Fault, southern Alaska (in two parts)—1. Field investigations and descriptions of chromite deposits: U.S. Bureau of Mines Information Circular 8990, 58 p.
Foley, J.Y., and Barker, J.C., 1986, Uranium occurrences in the northern Darby Mountains—Seward Peninsula, Alaska: U.S. Bureau of Mines Information Circular 9103, p. 27.
Foley, J.Y., Light, T.D., Nelson, S.W., and Harris, R.A., 1997, Mineral occurrences associated with mafic-ultramafic and related alkaline complexes in Alaska, *in* Goldfarb, R.J., and Miller, L.D., eds., Mineral deposits of Alaska: Economic Geology Monograph 9, p. 396–449.
Folger, P.F., and Schmidt, J.M., 1986, Geology of the carbonate-hosted Omar copper prospect, Baird Mountains, Alaska: Economic Geology, v. 81, p. 1690–1695.
Force, E.R., 1991, Geology of titanium-mineral deposits: Geological Society of America Special Paper 259, 112 p.

Freeman, C.J., 2011, Geology and mineralization of the Richardson gold property, Richardson Mining District, Alaska: Geologic Report RC-11EXE1 by Avalon Development Corp. for Select Resources Corp., Inc., paging unknown, available at http://tri-valleycorp.com/docs/NI_43-101_Report.

Freeman, V.L., 1963, Examination of uranium prospects, 1956, *in* Contributions to the economic geology of Alaska: U.S. Geological Survey Bulletin 1155, p. 29–33.

Frimmel, H.E., Groves, D.I., Kirk, J., Ruiz, J., Chesley, J., and Minter, W.E.L., 2005, The formation and preservation of the Witwatersrand goldfields, the world's largest gold province, *in* Hedenquist, J.W., Thompson, J.F.H., Goldfarb, R.J., and Richards, J.P., eds., Economic Geology 100th Anniversary Volume: Littleton, Colo., Society of Economic Geologists, p. 769–797.

Frost, B.R., Barnes, C.G., Collins, W.J., Arculus, R.J., Ellis, D.J., and Frost, C.D., 2001, A geochemical classification for granitic rocks: Journal of Petrology, v. 42, no. 11, p. 2033–2048.

Frost, B.R., and Frost, C.D., 2008, A geochemical classification for feldspathic igneous rocks: Journal of Petrology, v. 49, no. 11, p. 1955–1969.

Frost, C.D., and Frost, B.R., 2011, On ferroan (A-type) granitoids—Their compositional variability and modes of origin: Journal of Petrology, v. 52, no. 1, p. 39–53.

Gamble, B.M., Reed, B.L., Richter, D.H., and Lanphere, M.A., 2013, Geologic map of the east half of the Lime Hills 1:250,000-scale quadrangle, Alaska: U.S. Geological Survey Open-File Report 2013–1090, scale 1:250,000, http://pubs.usgs.gov/of/2013/1090/.

Garnett, R.H.T., and Bassett, N.C., 2005, Placer deposits, *in* Hedenquist, J.W., Thompson, J.F.H., Goldfarb, R.J., and Richards, J.P., eds., Economic Geology One Hundredth Anniversary Volume 1905–2005: Littleton, Colo., Society of Economic Geologists, p. 813–843.

Ghaffari, Hassan, Morrison, R.S., de Ruijter, M.A., Živković, Aleksandar, Hantelmann, Tysen, Ramsey, Douglas, and Cowie, Scott, 2011, Preliminary assessment of the Pebble project, southwest Alaska: Wardrop technical report prepared for Northern Dynasty Minerals, Ltd., March 22, 2011, 529 p., accessed October 12, 2015, at http://www.sedar.com.

Goldfarb, R.J., Baker, T., Dubé, B., Groves, D.I., Hart, C.J.R., and Gosselin, P., 2005, Distribution, character, and genesis of gold deposits in metamorphic terranes, *in* Hedenquist, J.W., Thompson, J.F.H., Goldfarb, R.J., and Richards, J.P., eds., Economic Geology One Hundredth Anniversary Volume 1905–2005: Littleton, Colo., Society of Economic Geologists, p. 407–450.

Goudarzi, G.H., comp., 1984, Guide to preparation of mineral survey reports on public lands: U.S. Geological Survey Open-File Report 84–0787, 41 p.

Graham, G.E., Goldfarb, R.J., Miller, Marti, Gibler, Kati, and Roberts, Mike, 2013, Tectonic evolution and Cretaceous gold metallogenesis of southwestern Alaska, *in* Colpron, M., Bissig, T., Rusk, B.G., and Thompson, J.F.H., eds., Tectonics, metallogeny, and discovery—The North American Cordillera and similar accretionary settings: Society of Economic Geologists Special Publication Number 17, p. 169–200.

Granitto, Matthew, Bailey, E.A., Schmidt, J.M., Shew, N.B., Gamble, B.M., and Labay, K.A., 2011, Alaska Geochemical Database (AGDB)—Geochemical data for rock, sediment, soil, mineral, and concentrate sample media: U.S. Geological Survey Data Series 637, 31 p.

Granitto, Matthew, Schmidt, J.M., Shew, N.B., Gamble, B.M., and Labay, K.A., 2013, Alaska Geochemical Database, Version 2.0 (AGDB2)—Including "best value" data compilations for rock, sediment, soil, mineral, and concentrate sample media: U.S. Geological Survey Data Series 759, 20 p.

Grant, J.N., Halls, Christopher, Sheppard, S.M.F., and Avila, Waldo, 1980, Evolution of the porphyry tin deposits of Bolivia: Mining Geology Special Issue, no. 8, p. 151–173.

Gray, J.E., Theodorakos, P.M., Lee, G.K., Hageman, P.O., and Sutley, S.J., 1997, Analytical data of stream-sediment and heavy-mineral-concentrate samples from the Buckstock Mountains and surrounding areas, Sleetmute quadrangle, southwest Alaska: U.S. Geological Survey Open-File Report 97–743–A, 147 p.

Greene, A.R., Scoates, J.S., and Weis, Dominique, 2008, Wrangellia flood basalts in Alaska—A record of plume-lithosphere interaction in a Late Triassic accreted oceanic plateau: Geochemistry, Geophysics, Geosystems, v. 9, no. 12, 34 p., doi:10.1029/2008GC002092.
Groves, D.I., Goldfarb, R.J., Gebre-Mariam, M., Hagemann, S.G., and Robert, F., 1998, Orogenic gold deposits—A proposed classification in the context of their crustal distribution and relationship to other gold deposit types: Ore Geology Reviews, v. 13, p. 7–27.
Guilbert, J.M., and Park, C.F., 1986, The geology of ore deposits: New York, W.H. Freeman and Company, 985 p.
Hallam, A., 1986, Evidence of displaced terranes from Permian to Jurassic faunas around the Pacific margins: Journal of the Geological Society of London, v. 143, p. 209–216.
Hamilton, N.T.M., 1995, Controls on the global distribution of coastal titanium-zirconium placers: International Geology Review, v. 37, no. 9, p. 755–779.
Harper, J.R., 1990, Morphology of the Canadian Beaufort Sea coast: Marine Geology, v. 91, p. 75–91.
Harris, D.C., and Cabri, L.J., 1991, Nomenclature of platinum-group-element alloys—Review and revision: The Canadian Mineralogist, v. 29, no. 2, p. 231–237.
Harshman, E.N., 1972, Geology and uranium deposits, Shirley Basin area, Wyoming: U.S. Geological Survey Professional Paper 745, 82 p.
Hart, C.J.R., 2007, Reduced intrusion-related gold systems, *in* Goodfellow, W.D., ed., Mineral Deposits of Canada—A Synthesis of Major Deposit-Types, District Metallogeny, the Evolution of Geological Provinces, and Exploration Methods: Geological Association of Canada, Mineral Deposits Division, Special Publication No. 5, p. 95–112.
Hawley, C.C., and Clark, A.L., 1974, Geology and mineral deposits of the Upper Chulitna district, Alaska: U.S. Geological Survey Professional Paper 758–B, p. B1–B47.
Hawley, C.C., and others, 1978, Mineral appraisal of lands adjacent to Mt. McKinley National Park, Alaska—Contract No. JO166107: U.S. Bureau of Mines Open-File Report 24-78, 274 p., 12 sheets.
Hayes, T.S., 1982, Climate dependent geochemical mechanisms of copper, uranium, and vanadium transport and deposition in sandstone ores: Stanford, Calif., Stanford University, M.S. thesis, 148 p.
Heijlen, Wouter, Banks, D.A., Muchez, Phillippe, Stensgard, B.M., and Yardley, B.W.D., 2006, The nature of mineraliing fluids of the Kipushi Zn-Cu deposit, Katanga, Democratic Republic of Congo—Quantitative fluid inclusion analysis using laser ablation ICP-MS and bulk crush-leach methods: Economic Geology, v. 103, p. 1459–1482.
Helsel, D.R., 2012, Statistics for censored environmental data using Minitab and R (2d ed.): New York, John Wiley and Sons, 344 p.
Herreid, G.H., 1970, Geology of the Spirit Mountain nickel-copper prospect and surrounding area: Alaska Division of Mines and Geology Geologic Report 40, 19 p., 2 sheets, scale 1:31,680, doi:10.14509/369.
Hillhouse, J.W., 1977, Paleomagnetism of the Triassic Nikolai Greenstone, McCarthy quadrangle, Alaska: Canadian Journal of Earth Sciences, v. 14, p. 1578–2592.
Himmelberg, G.R., and Loney, R.A., 1981, Petrology of the ultramafic and gabbroic rocks of the Brady Glaier nickel-copper deposit, Fairweather Range, southeastern Alaska: U.S. Geological Survey Professional Paper 1195, 26 p.
Himmelberg, G.R., and Loney, R.A., 1995, Characteristics and petrogenesis of Alaskan-type ultramafic-mafic intrusions, southeastern Alaska: U.S. Geological Survey Professional Paper 1564, 47 p.
Hitzman, M.W., 1986, Geology of the Ruby Creek copper deposit, southwestern Brooks Range, Alaska: Economic Geology, v. 81, no. 7, p. 1644–1674.
Höll, R., Kling, M., and Schroll, E., 2007, Metallogenesis of germanium—A review: Ore Geology Reviews, v. 30, no. 3–4, p. 145–180.

Houston, J.F., Bates, R.G., Velikanje, R.S., and Wedow, Helmuth, Jr., 1958, Reconnaissance for radioactive deposits in southeastern Alaska, 1952: U.S. Geological Survey Bulletin 1058–A, 31 p.
Hudson, Travis, and Arth, J.G., 1983, Tin granites of Seward Peninsula, Alaska: Geological Society of America Bulletin, v. 94, no. 6, p. 768–790.
Hudson, Travis, Arth, J.G., and Muth, K.G., 1981, Geochemistry of intrusive rocks associated with molybdenite deposits, Ketchikan quadrangle, southeastern Alaska: Economic Geology, v. 76, p. 1225–1232.
Hudson, T.L., and Reed, B.L., 1997, Tin deposits in Alaska, *in* Goldfarb, R.J., and Miller, L.D., eds., Mineral deposits of Alaska: Economic Geology Monograph 9, p. 450–465.
Huffman, A.C., Kirk, A.R., and Molenaar, C.M., 1982, Uranium investigations—Northeastern Alaska, *in* Coonrad, W.L., ed., The United States Geological Survey in Alaska—Accomplishments during 1980: U.S. Geologial Survey Circular 844, p. 41–43.
Huffman, A.C., Jr., 1985, Uranium potential of the Cretaceous Nanushuk Group, North Slope, Alaska, *in* Huffman, A.C., Jr., ed., Geology of the Nanushuk Group and related rocks, North Slope, Alaska: U.S. Geological Survey Bulletin 1614, p. 121–123.
Hulbert, L.J., 1997, Geology and metallogeny of the Kluane mafic-ultramafic Belt, Yukon Territory, Canada—Eastern Wrangellia, a new Ni-Cu-PGE metallogenic terrane: Geological Survey of Canada Bulletin 506, 265 p.
Hulbert, L.J., Carne, R.C., Gregoire, D.C., and Paktunc, Dogan, 1992, Sedimentary nickel, zinc, and platinum-group-element mineralization in Devonian black shales at the Nick Property, Yukon, Canada—A new deposit type: Exploration and Mining Geology, v. 1, no. 1, p. 39–62.
Huyck, H.L.O., 1990, When is a metalliferous black shale not a black shale?, *in* Grauch, R.I., and Huyck, H.L.O., eds., Metalliferous black shales and related ore deposits—Proceedings, 1989 United States Working Group Meeting, International Geological Correlation Program Project 254: U.S. Geological Survey Circular 1058, p. 42–56.
International Commission on Stratigraphy, 2013, International Chronostratigraphic Chart (v. 2013/01): International Commission on Stratigraphy, http://www.stratigraphy.org/ICSchart/ChronostratChart2013-01.pdf.
Irvine, T.N., and Baragar, W.R.A., 1971, A guide to the chemical classification of the common volcanic rocks: Canadian Journal of Earth Sciences, v. 8, no. 5, p. 523–548.
Ishihara, Shunso, Hoshino, Kenichi, Murakami, Hiroyasu, and Endo, Yuji, 2006, Resource evaluation and some genetic aspects of indium in the Japanese ore deposits: Resource Geology, v. 56, no. 3, p. 347–364.
Jenks, G.F., 1967, The data model concept in statistical mapping: International yearbook of cartography, v. 7, no. 1, p.186–190.
Johan, Zdenek, Strnad, Ladislav, and Johan, Vera, 2012, Evolution of the Cínovec (Zinnwald) granite cupola, Czech Republic—Composition of feldspars and micas, a clue to the origin of W, Sn mineralization: Canadian Mineralogist, v. 50, no. 4, p. 1131–1148.
Johnson, B.R., Miller, T.P., and Karl, Susan, 1978, Uranium-thorium investigations of the Darby pluton, Seward Peninsula, Alaska*, in* Johnson, K.M., and Williams, J.R., eds., The United States Geological Survey in Alaska—Accomplishments during 1978: U.S. Geological Survey Circular 804–B, p. B68–B70.
Jones, D.L., Silberling, N.J., Coney, P.J., and Plafker, George, 1987, Lithotectonic terrane map of Alaska (west of the 141st meridian): U.S. Geological Survey Miscellaneous Field Studies Map MF–1874–A, scale: 1:2,500,000.
Jones, D.L., Silberling, N.J., Csejtey, Béla, Jr., Nelson, W.H., and Blome, C.D., 1980, Age and structural significance of ophiolite and adjoining rocks in the Upper Chulitna district, south-central Alaska: U.S. Geological Survey Professional Paper 1121–A, p. A1–A21.

Jones, D.L., Silberling, N.J., and Hillhouse, John, 1977, Wrangellia—A displaced terrane in northwestern North America: Canadian Journal of Earth Sciences, v. 14, p. 2565–2577.
Jones, J.V., III, Karl, S.M., Labay, K.A., Shew, N.B., Granitto, Matthew, Hayes, T.S., Mauk, J.L., Schmidt, J.M., Todd, Erin, Wang, Bronwen, Werdon, M.B., and Yager, D.B., 2015, GIS-based identification of areas with mineral resource potential for six selected deposit groups, Bureau of Land Management Central Yukon Planning Area, Alaska: U.S. Geological Survey Open-File Report 2015–1021, 78 p., 5 appendixes, 12 plates, scale 1:3,825,000, http://dx.doi.org/10.3133/ofr20151021.
Kamona, A.F., and Günzel, A., 2007, Stratigraphy and base metal mineralization in the Otavi Mountain Land, northern Namibia—A review and regional interpretation: Gondwana Research, v. 11, no. 3, p. 396–413.
Kampunzu, A.B., Cailteux, J.L.H., Kamona, A.F., Intiomale, M.M., and Melcher, F., 2009, Sediment-hosted Zn–Pb–Cu deposits in the Central African Copperbelt: Ore Geology Reviews, v. 35, no. 3, p. 263–297.
Kaufman, D.S., and Hopkins, D.M., 1989, Late Cenozoic geologic controls on placer-gold distribution in the Nome nearshore area, *in* Dover, J.H., ed., Geologic studies in Alaska by the U.S. Geological Survey, 1988: U.S. Geological Survey Bulletin 1903, p. 26–45.
Keith, T.E.C., Page, N.J., Oscarson, R.L., and Foster, H.L., 1987, Platinum-group element concentrations in a biotite-rich clinopyroxenite suite, Eagle C-3 quadrangle, Alaska, *in* Hamilton, T.D., and Galloway, J.P., eds., Geologic studies in Alaska by the U.S. Geological Survey during 1986: U.S. Geological Survey Circular 998, p. 62–66.
Kelley, K.D., Lang, J.R., and Eppinger, R.G., 2013, The giant Pebble Cu-Au-Mo deposit and surrounding region, southwest Alaska—Introduction: Economic Geology, v. 108, no. 3, p. 397–404.
Kelly, W.C., and Rye, R.O., 1979, Geologic, fluid inclusion, and stable isotope studies of the tin-tungsten deposits of Panasqueira, Portugal: Economic Geology, v. 74, no. 8, p. 1721–1822.
Keppler, H., 1993, Influence of fluorine on the enrichment of high field strength trace elements in granitic rocks. Contributions to Mineralogy and Petrology, v. 114, p. 479 - 488.
Keppler, H., 2003, Water solubility in carbonatite melts: American Mineralogist, v.88, p. 1822–1824.
Killeen, P.L., and Ordway, R.J., 1955, Radioactivity investigations at Ear Mountain, Seward Peninsula, Alaska, 1945: U.S. Geological Survey Bulletin 1024–C, 94 p.
Kimball, A.L., Still, J.C., and Rataj, J.L., 1978, Mineral resources, *in* Brew, D.A., Johnson, B.R., Grybeck, Donald, Griscom, Andrew, Barnes, D.F., Kimball, A.L., Still, J.C., and Rataj, J.L., Mineral resources of the Glacier Bay National Monument Wilderness Study Area: U.S. Geological Survey Open-File Report 78–494, p. C-1–C-375.
Knoll, A.H., Walter, M.R., Narbonne, G.M., and Christie-Blick, N., 2006, The Ediacaran Period—A new addition to the geologic time scale: Lethaia, v. 39, p. 13–30.
Kogarko, L.N., Lahaye, Y., and Brey, G.P., 2010, Plume-related mantle source of super-large rare metal deposits from the Lovozero and Khibina massifs on the Kola Peninsula, eastern part of Baltic Shield—Sr, Nd and Hf isotope systematics: Mineralogy and Petrology, v. 98, no. 1–4, p. 197–208.
Kooiman, G.J.A., McLeod, M.J., and Sinclair, W.D., 1986, Porphyry tungsten-molybdenum orebodies, polymetallic veins and replacement bodies, and tin-bearing greisen zones in the Fire Tower Zone, Mount Pleasant, New Brunswick: Economic Geology, v. 81, no. 6, p. 1356–1373.
Kwak, T.A.P., 1987, W-Sn skarn deposits and related metamorphic skarns and granitoids: Developments in Economic Geology 24, 468 p.
Kwak, T.A.P., and Askins, P.W., 1981, Geology and genesis of the F-Sn-W (-Be-Zn) skarn (wrigglite) at Moina, Tasmania: Economic Geology, v. 76, no. 2, p. 439-467.
Le Bas, M.J., Keller, J., Tao Kejie, Wall, F., William, C.T., and Zhang Peishan, 1992, Carbonatite dykes at Bayan Obo, Inner Mongolia, China: Mineralogy and Petrology, v. 46, no. 3, p. 195–228.

Le Bas, M.J., Le Maitre, R.W., Streckeisen, A., and Zanettin, B., 1986, A chemical classification of volcanic rocks based on the total alkali silica diagram: Journal of Petrology, v. 27, no. 3, p. 745–750.
Lehman, B., Dietrich, A., Heinhorst, J., Metrich, N., Mosbah, M., Palacios, C., Schneider, H.-J., Wallianos, A., Webster, J., and Winkelman, L., 2000, Boron in the Bolivian tin belt: Mineralium Deposita, v. 35, p. 223–232.
Le Maitre, R.W., 2002, Igneous rocks, a classification and glossary of terms—Recommendations of the International Union of Geological Sciences Subcommission on the systematics of igneous rocks (2d ed.): Cambridge, United Kingdom, Cambridge University Press, 236 p.
Li, Chusi, Ripley, E.M., and Naldrett, A.J., 2009, A new genetic model for the giant Ni-Cu-PGE sulfide deposits associated with the Siberian flood basalts: Economic Geology, v. 104, no. 2, p. 291–301.
Linnen, R.L., Samson, I.M., Williams-Jones, A.E., and Chakhmouradian, A.R., 2014, Geochemistry of the rare-earth element, Nb, Ta, Hf, and Zr deposits, chap. 21 *in* Holland, H.D., and Turekian, K.K., eds., Treatise on Geochemistry (2d ed.), vol. 13: Oxford, United Kingdom, Elsevier, p. 543–568.
Loney, R.A., and Himmelberg, G.R., 1989, The Kanuti ophiolite, Alaska: Journal of Geophysical Research—Solid Earth, v. 94, no. B11, p. 15,869–15,900.
Long, K.R., Van Gosen, B.S., Foley, N.K., and Cordier, Daniel, 2010, The principal rare earth elements deposits of the United States—A summary of domestic deposits and a global perspective: U.S. Geological Survey Scientific Investigations Report 2010–5220, 96 p., http://pubs.usgs.gov/sir/2010/5220/.
Lottermoser, B.G., 1990, Rare-earth element mineralization within the Mt. Weld carbonatite laterite, Western Australia: Lithos, v. 24, p. 151–167.
Ludington, Steve, Hammarstrom, Jane, and Piatak, Nadine, 2009, Low-fluorine stockwork molybdenite deposits: U.S. Geological Survey Open-File Report 2009–1211, 9 p., http://pubs.usgs.gov/of/2009/1211/.
Ludington, Steve, and Plumlee, G.S., 2009, Climax-type porphyry molybdenum deposits: U.S. Geological Survey Open-File Report 2009–1215, 16 p., http://pubs.usgs.gov/of/2009/1215/.
Macdonald, F.A., 2011, The Hula Hula Diamictite and Katakturuk Dolomite, Arctic Alaska, *in* Arnaud, E., Halverson, G.P., and Shields-Zhou, G., eds., The geological record of Neoproterozoic glaciations: Geological Society of London Memoir 36, p. 379–387.
MacKevett, E.M., Jr., 1963, Geology and ore deposits of the Bokan Mountain uranium-thorium area, southeastern Alaska: U.S. Geological Survey Bulletin 1154, 125 p.
MacKevett, E.M., Jr., Cox, D.P., Potter, R.W., II, and Silberman, M.L., 1997, Kennecott-type deposits in the Wrangell Mountains, Alaska—High-grade copper ores near a basalt-limestone contact, *in* Goldfarb, R.J., and Miller, L.D., eds., Mineral deposits of Alaska: Economic Geology Monograph 9, p. 66–89.
Maniar, P.D., and Piccoli, P.M., 1989, Tectonic discrimination of granitoids: Geological Society of America Bulletin, v. 101, no. 5, p. 635–643.
Mariano, A.N., 1989, Economic geology of rare earth minerals, *in* Lipin, B.R., and Mackay, G.A., eds., Geochemistry and mineralogy of rare earth elements: Washington, D.C., Mineralogical Society of America, Reviews in Mineralogy, v. 21, p. 309–338.
Matzko, J.J., and Freeman, V.L., 1963, Summary of reconnaissance for uranium in Alaska, 1955, *in* Contributions to economic geology of Alaska: U.S. Geological Survey Bulletin 1155, p. 33–49.
Mavrogenes, J.A., and O'Neill, H.S.C., 1999, The relative effects of pressure, temperature and oxygen fugacity on the solubility of sulfide in mafic magmas: Geochimica et Cosmochimica Acta, v. 63, p. 1173–1180.
Mernagh, T.P., Wyborn, L.I.A., and Jagodzinski, E.A., 1998, 'Unconformity-related' U ± Au ± platinum-group-element deposits: Australian Geological Survey Organization, Journal of Australian Geology and Geophysics, v. 17, no. 4, p. 197–205.

Merritt, R.D., and Hawley, C.C., 1986, Map of Alaska's coal resources: Alaska Division of Geological & Geophysical Surveys Special Report 37, scale 1:2,500,000.
Mertie, J.B., Jr., 1976, Platinum deposits of the Goodnews Bay district, Alaska: U.S. Geological Survey Professional Paper 938, 42 p.
Middlemost, Eric, 1990, Mineralogy and petrology of the rauhaugites of the Mt. Weld carbonatite complex of Western Australia: Mineralogy and Petrology, v. 41, no. 2–4, p. 145–161.
Miesch, A.T., 1976, Sampling designs for geochemical surveys—Syllabus for a short course: U.S. Geological Survey Open-File Report 76–772, 128 p.
Miller, J.D., Jr., Green, J.C., Severson, M.J., Chandler, V.W., Hauck, S.A., Peterson, D.M., and Wahl, T.E., 2002, Geology and mineral potential of the Duluth complex and related rocks of northeastern Minnesota: Minnesota Geological Survey Report of Investigations 58, 207 p.
Miller, M.L., Bailey, E.A., Beischer, G.A., Bradley, D.C., Bundtzen, T.K., Goldfarb, R.J., Karl, S.M., Saltus, R.W., and Wang, B., 2006, USGS mineral resource studies in the Taylor Mountains quadrangle, southwestern Alaska—New "AMRAP": The Alaska Miner, v. 34, no. 2, p. 1–15.
Miller, T.P., and Elliott, R.L., 1969, Metalliferous deposits near Granite Mountain, eastern Seward Peninsula, Alaska: U.S. Geological Survey Circular 614, 19 p.
Miller, T.P., and Elliott, R.L., 1977, Progress report on uranium investigations in the Zane Hills area, west-central Alaska: U.S. Geological Survey Open-File Report 77–428, 12 p.
Miller, T.P., and Ferrians, O.J., Jr., 1968, Suggested areas for prospecting in the central Koyukuk River region, Alaska: US Geological Survey Circular 570, 12 p.
Miller, T.P., and Johnson, B.R., 1978, An occurrence of parsonite, a secondary uranium mineral, in alaskite of the Wheeler Creek pluton, *in* Johnson, K.M., ed., The United States Geological Survey in Alaska—Accomplishments during 1977: U.S. Geological Survey Circular 772–B, p. 42–44.
Miller, T.P., Moll, E.J., and Patton, W.W., Jr., 1980, Uranium-and thorium-rich volcanic rocks of the Sischu Creek area, Medfra quadrangle, Alaska: U.S. Geological Survey Open-File Report 80–803, 9 p.
Minter, W.E.L., 2006, The sedimentary setting of Witwatersrand placer mineral deposits in an Archean atmosphere, *in* Kesler, S.E., and Ohmoto, H., eds., Evolution of early Earth's atmosphere, hydrosphere, and biosphere—Constraints from ore deposits: Geological Society of America Memoir 198, p. 105–119.
Moll-Stalcup, Elizabeth, and Arth, J.G., 1989, The nature of the crust in the Yukon-Koyukuk province as inferred from the chemical and isotopic composition of five Late Cretaceous to Early Tertiary volcanic fields in western Alaska: Journal of Geophysical Research—Solid Earth, v. 94, no. B11, p. 15,989–16,020.
Monger, J.W.H., and Berg, H.C., 1987, Lithotectonic terrane map of western Canada and southeastern Alaska: U.S. Geological Survey Miscellaneous Field Studies Map MF–1874–B, scale 1:2,500,000.
Moroni, Marilena, Girardi, V.A.V., and Ferrario, Alfredo, 2001, The Serra Pelada Au-PGE deposit, Serra dos Carajás (Pará State, Brazil)—Geological and geochemical indications for a composite mineralising process: Mineralium Deposita, v. 36, no. 8, p. 768–785.
Naldrett, A.J., 2004, Magmatic sulfide deposits—Geology, geochemistry and exploration: Berlin, Springer-Verlag, 727 p.
Naldrett, A.J., Asif, Mohammed, Krstic, Sasa, and Li, Chusi, 2000, The composition of mineralization at the Voisey's Bay Ni-Cu sulfide deposit, with special reference to platinum-group elements: Economic Geology, v. 95, no. 4, p. 845–865.
Naldrett, A.J., and Barnes, S-.J., 1986, The behaviour of platinum group elements during fractional crystallization and partial melting with special reference to the composition of magmatic sulfide ores: Fortschritte der Mineralogie, v. 64, p. 113–133.

National Research Council, 2008, Minerals, critical minerals, and the U.S. economy: Washington, D.C., The National Academies Press, 264 p.
Nelson, C.H., and Hopkins, D.M., 1972, Sedimentary processes and distribution of particulate gold in the northern Bering Sea: U.S. Geological Survey Porfessional Paper 689, 27p, 1 sheet.
Newberry, R.J., 1998, W- and Sn-skarn deposits—A 1998 status report: Mineralogical Association of Canada Short Course Series, v. 26, p. 289–335.
Newberry, R.J., and Brew, D.A., 1989, Epigenetic hydrothermal origin of the Groundhog Basin-Glacier Basin silver-tin-lead-zinc deposits, southeastern Alaska, *in* Dover, J.H., and Galloway, J.P., eds., Geologic studies in Alaska by the U.S. Geological Survey, 1988: U.S. Geological Survey Bulletin 1903, p. 113–121.
Newberry, R.J., Burns, L.E., Swanson, S.E., and Smith, T.E., 1990, Comparative petrologic evolution of the Sn and W granites of the Fairbanks-Circle area, interior Alaska, *in* Stein, H.E., and Hannah, J.L., eds., Ore-bearing granite systems: Geological Society of America Special Paper 246, p. 121–142.
Newberry, R.J., Dillon, J.T., and Adams, D.D., 1986, Regionally metamorphosed, calc-silicate-hosted deposits of the Brooks Range, northern Alaska: Economic Geology, v. 81, no. 7, p. 1728–1752.
Newberry, R.J., and Solie, D.N., 1995, Data for plutonic rocks and associated gold deposits in Interior Alaska: Alaska Division of Geological & Geophysical Surveys Public Data File 95–25, 62 p.
Newberry, R.J., and Swanson, S.E., 1986, Scheelite skarn granitoids—An evaluation of the roles of magmatic source and process: Ore Geology Reviews, v. 1, no. 1, p. 57–81.
Nokleberg, W.J., Aleinikoff, J.N., Lange, I.M., Silva, S.R., Miyaoka, R.T., Schwab, C.E., and Zehner, R.E., with contributions for selected areas from Bond, G.C., Richter, D.H., Smith, T.E., and Stout, J.H., 1992, Preliminary geologic map of the Mount Hayes quadrangle, eastern Alaska Range, Alaska: U.S. Geological Survey Open-File Report 92–594, scale 1:250,000, pamphlet 39 p.
Nokleberg, W.J., Bundtzen, T.K., Berg, H.C., Brew, D.A., Grybeck, Donald, Robinson, M.S., Smith, T.E., and Yeend, Warren, 1987, Significant metalliferous lode deposits and placer districts of Alaska: U.S. Geological Survey Bulletin 1786, 104 p.
Northrop, H.R., Goldhaber, M.B., Landis, G.P., Unruh, J.W., Reynolds, R.L., Campbell, J.A., Wanty, R.B., Grauch, R.I., Whitney, Gene, and Rye, R.O., 1990, Genesis of the tabular-type vanadium-uranium deposits of the Henry Basin, Utah: Economic Geology, v. 85, no. 2, p. 215–269.
Notholt, A.J.G., Highley, D.E., and Deans, T., 1990, Economic minerals in carbonatites and associated alkaline igneous rocks: Institution of Mining and Metallurgy Transactions, Section B, Applied Earth Science, v. 99, p. B59–B80.
Nyman, M.W., Sheets, R.W., and Bodnar, R.J., 1990, Fluid-inclusion evidence for the physical and chemical conditions associated with intermediate-temperature PGE mineralization at the New Rambler Deposit, southeastern Wyoming: The Canadian Mineralogist, v. 28, no. 3, p. 629–638.
Patton, W.W., Jr., 1992, Ophiolite terrane of western Brooks Range, Alaska: U.S. Geological Survey Open-File Report 92–20D, 7 p.
Patton, W.W., Jr., and Moll-Stalcup, E.J., 2000, Geologic map of the Nulato quadrangle, west-central Alaska: U.S. Geological Survey Geologic Investigations Series Map I–2677, scale 1:250,000, pamphlet 41 p., http://pubs.usgs.gov/imap/i2677/.
Patton, W.W., Jr., Wilson, F.H., Labay, K.A., and Shew, Nora, 2009, Geologic map of the Yukon-Koyukuk Basin, Alaska: U.S. Geological Survey Scientific Investigations Map 2909, 2 sheets, scale 1:500,000, pamphlet 26 p., http://pubs.usgs.gov/sim/2909/.
Pearce, J.A., 1996, A user's guide to basalt discrimination diagrams, *in* Wyman, D.A., and Bailes, A.H., eds., Trace element geochemistry of volcanic rocks—Applications for massive sulphide exploration: Geological Association of Canada Short Course Notes 12, p. 79–113.
Pearce, J.A., Harris, N.B.W., and Tindle, A.G., 1984, Trace element discrimination diagrams for the tectonic interpretation of granitic rocks: Journal of Petrology, v. 25, no. 4, p. 956–983.

Phillips, G.N., and Hughes, M.J., 1996, The geology and gold deposits of the Victorian gold province: Ore Geology Reviews, v. 11, p. 255-302.
Philpotts, John, Taylor, Cliff, Evans, John, and Emsbo, Poul, 1993, Newly discovered molybdenite occurrences at Dora Bay, Prince of Wales Island, Southeast Alaska, and preliminary scanning electron microscope studies, *in* Dusel-Bacon, Cynthia, and Till, A.B., eds., Geologic Studies in Alaska by the U.S. Geological Survey, 1992: U.S. Geological Survey Bulletin 2068, p. 187–196.
Philpotts, J.A., Taylor, C.D., Tatsumoto, Mitsunobu, and Belkin, H.E., 1998, Petrogenesis of late-stage granites and Y-REE-Zr-Nb-enriched vein dikes of the Bokan Mountain stock, Prince of Wales Island, southeastern Alaska: U.S. Geological Survey Open-File Report 98–459, 71 p.
Piestrzyński, Adam, Pieczonka, Jadwiga, and Gluszek, Adam, 2002, Redbed-type gold mineralization, Kupferschiefer, south-west Poland: Mineralium Deposita, v. 37, p. 512–528.
Pilet, S., Bajerm, M.B., and Stolper, E.M., 2008, Metasomatized lithosphere and the origin of alkaline lavas: Science, v. 320, p. 916–919.
Plafker, George, and Berg, H.C., 1994, Overview of the geology and tectonic evolution of Alaska, *in* Plafker, G., and Berg, H.C., eds., The Geology of Alaska: Boulder, Colo., Geological Society of America, The Geology of North America, v. G-1, p. 989–1021.
Plafker, George, and Hudson, Travis, 1980, Regional implications of Upper Triassic metavolcanic and metasedimentary rocks on the Chilkat Peninsula, southeastern Alaska: Canadian Journal of Earth Sciences, v. 17, p. 681–689.
Pollard, P.J., 1995, A special issue devoted to the geology of rare metal deposits—Geology of rare metal deposits, an introduction and overview: Economic Geology, v. 90, no. 3, p. 489–494.
Portnov, A.M., 1987, Specialization of rocks toward potassium and thorium in relation to mineralization: International Geology Review, v. 29, no. 3, p. 326–344.
Preto, V.A., 1978, Setting and genesis of uranium mineralization at Rexspar: Canadian Institute of Mining and Metallurgy Bulletin, v. 71, no. 800, p. 82–88.
Pretorius, D.A., 1981, Gold and uranium in quartz-pebble conglomerate, *in* Skinner, B.J., ed., Economic Geology, Seventy-fifth Anniversary Volume, 1905–1980: Lancaster, Pa., Economic Geology Publishing Co., p. 117–138.
Price, J.B., Hitzman, M.W., Nelson, E.P., Humphrey, J.D., and Johnson, C.A., 2014, Wall-rock alteration, structural control, and stable isotope systematics of the high-grade copper orebodies of the Kennecott district, Alaska: Economic Geology, v. 109, no. 3, p. 581–620.
Puchner, C.C., 1986, Geology, alteration, and mineralization of the Kougarok Sn deposit, Seward Peninsula, Alaska: Economic Geology, v. 81, no. 7, p. 1775–1794.
Raimbault, Louis, Cuney, Michel, Azencott, Claude, Duthou, J.L., and Joron, J.L., 1995, Geochemical evidence for a multistage magmatic genesis of Ta-Sn-Li mineralization in the granite at Beauvoir, French Massif Central: Economic Geology, v. 90, no. 3, p. 548–576.
Rankin, A., 2005, Carbonatite-associated rare metal deposits; composition and evolution of ore-forming fluids—The fluid inclusion evidence, *in* Samson, I., and Linnen, R., eds, Rare element geochemistry and mineral deposits: Geological Association of Canada–Mineralogical Association of Canada Short Course Series, v. 17, p. 299–314.
Reed, B.L., 1978, Disseminated tin occurrence near Coal Creek, Talkeetna Mountains D-6 quadrangle, Alaska: U.S. Geological Survey Open-File Report 78–77, 8 p.
Reed, B.L., 1986, Descriptive model of Sn greisen deposits, *in* Cox, D.P., and Singer, D.A., eds., Mineral deposit models: US Geological Survey Bulletin 1693, p. 70.
Reed B.L., and Anderson, L.A., 1969, Aeromagnetic maps of part of the southern Alaska Range: U.S. Geological Survey Open-file Report 355, 2 sheets, scale 1:63,360, 6 p.
Reed, B.L., and Miller, T.P., 1980, Uranium and thorium content of some Tertiary granitic rocks in the southern Alaska Range: U.S. Geological Survey Open-file Report 80–1052, 16 p.

Reger, R.D., and Bundtzen, T.K., 1990, Multiple glaciation and gold-placer formation, Valdez Creek valley, western Clearwater Mountains, Alaska: Alaska Division of Geological & Geophysical Surveys, Professional Report 107, 29p.
Reifenstuhl, R.R., Dover, J.H., Newberry, R.J., Clautice, K.H., Liss, S.A., Blodgett, R.B., and Weber, F.R., 1998, Interpretive geologic bedrock map of the Tanana A-1 and A-2 quadrangles, central Alaska: Alaska Division of Geological & Geophysical Surveys Public-Data File 98-37B, v. 1.1, 17 p., scale 1:63,360.
Richards, J.P., Dang, T., Dudka, S.F., and Wong, M.L., 2003, The Nui Phao tungsten-fluorite-copper-gold-bismuth deposit, northern Vietnam—An opportunity for sustainable development: Exploration and Mining Geology, v. 12, no. 1–4, p. 61–70.
Richardson, D.G., and Birkett, T.C., 1996, Peralkaline rock-associated rare metals, *in* Eckstrand, O.R., Sinclair, W.D., and Thorpe, R.I., eds., Geology of Canadian mineral deposit types: Geological Survey of Canada, Geology of Canada Series no. 8, p. 523–540.
Richter, D.H., 1967, Geology of the Upper Slana-Mentasta Pass Area, southcentral Alaska: Alaska Division of Mines and Minerals Geologic Report 30, 30 p.
Robinson, G.D.,Wedow, Helmuth, Jr., and Lyons, J.B., 1955, Radioactivity investigations in the Cache Creek area, Yentna district, Alaska, 1945: U.S. Geological Survey Bulletin 1024–A, 23 p.
Roeske, S.M., Dusel-Bacon, C., Aleinikoff, J.N., Snee, L.W., and Lanphere, M.A., 1995, Metamophic and structural history of continental crust at a Mesozoic collisional margin, the Ruby terrane, central Alaska: Journal of Metamorphic Geology, v. 13, p. 25–40.
Rogers, J.J., and Greenberg, J.K., 1990, Late-orogenic, post-orogenic, and anorogenic granites—Distinction by major-element and trace-element chemistry and possible origins: The Journal of Geology, v. 98, no. 3, p. 291–309.
Rollinson, H.R., 1993, Using geochemical data—Evaluation, presentation, interpretation: New York, Longman Scientific and Technical, 352 p.
Roy, P.S., 1999, Heavy mineral beach placers in southeastern Australia—Their nature and genesis: Economic Geology, v. 94, no. 4, p. 567–588.
Ruelle, J.C.L., 1982, Depositional environments and genesis of stratiform copper deposits of the Redstone copper belt, Mackenzie Mountains, N.W.T., *in* Hutchinson, R.W., Spence, C.D., and Franklin, J.M., eds, Precambrian sulphide deposits: Geological Association of Canada Special Paper 25, p. 701–737.
Runnells, D.D., 1969, The mineralogy and sulfur isotopes of the Ruby Creek copper prospect, Bornite, Alaska: Economic Geology, v. 64, no. 1, p. 75–90.
Sainsbury, C.L., 1964, Geology of the Lost River mine area, Alaska: U.S. Geological Survey Bullletin 1129, 80 p.
Saltus, R.W., Riggle, F.E., Clark, B.T., and Hill, P.L., 1999, Merged aeroradiometric data for Alaska—A web site for distribution of gridded data and plot files: U.S. Geological Survey Open-File Report 99–0016, 13 p., http://pubs.usgs.gov/of/1999/ofr-99-0016/.
Salvi, S., and Williams-Jones, A.E., 2005, Alkaline granite-syenite deposits, *in* Linnen, R.L., and Samson, I.M., eds., Rare-element geochemistry and mineral deposits: Geological Association of Canada Short Course Notes 17, p. 315–341.
Schmidt, J.M., Werdon, M.B., and Wardlaw, Bruce, 2003, New mapping near Iron Creek, Talkeetna Mountains, indicates presence of Nikolai Greenstone: Alaska Division of Geological & Geophysical Surveys Professional Report 120 (Short Notes on Alaskan Geology, 2003), p. 101–108.
Schneider, Jens, Melcher, Frank, and Brauns, Michael, 2007, Concordant ages for the giant Kipushi base metal deposit (DR Congo) from direct Rb-Sr and Re-Os dating of sulfides: Mineralium Deposita, v. 42, p. 791–797.

Schulz, K.J., Chandler, V.W., Nicholson, S.W., Piatak, Nadine, Seal, R.R., II, Woodruff, L.G., and Zientek, M.L., 2010, Magmatic sulfide-rich nickel-copper deposits related to picrite and (or) tholeiitic basalt dike-sill complexes—A preliminary deposit model: U.S. Geological Survey Open-File Report 2010–1179, 25 p., http://pubs.usgs.gov/of/2010/1179/.

Seedorff, Eric, Dilles, J.H., Proffett, J.M., Jr., Einaudi, M.T., Zurcher, Lukas, Stavast, W.J.A., Johnson, D.A., and Barton, M.D., 2005, Porphyry deposits—Characteristics and origin of hypogene features, *in* Hedenquist, J.W., Thompson, J.F.H., Goldfarb, R.J., and Richards, J.P., eds., Economic Geology One Hundredth Anniversary Volume, 1905–2005: Littleton, Colo., Society of Economic Geologists, p. 251–298.

Seedorff, Eric, and Einaudi, M.T., 2004, Henderson porphyry molybdenum system, Colorado—I. Sequence and abundance of hydrothermal mineral assemblages, flow paths of evolving fluids, and evolutionary style: Economic Geology, v. 99, no. 1, p. 3–37.

Selby, David, Kelley, K.D., Hitzman, M.W., and Zieg, Jerry, 2009, Re-Os sulfide (bornite, chalcopyrite, and pyrite) systematics of the carbonate-hosted copper deposits at Ruby Creek, southwestern Brooks Range, Alaska: Economic Geology, v. 104, p. 437–444.

Shand, S.J., 1943, Eruptive rocks, their genesis, composition, and classification: New York, J. Wiley & Sons, 444 p.

Sheard, E.R., Williams-Jones, A.E., Heiligmann, Martin, Pederson, Chris, and Trueman, D.L., 2012, Controls on the concentration of zirconium, niobium, and the rare earth elements in the Thor Lake rare metal deposit, Northwest Territories, Canada: Economic Geology, v. 107, no. 1, p. 81–104.

Silberman, M.L., MacKevett, E.M., Connor, C.L., and Matthews, A., 1980, Metallogenic and tectonic significance of oxygen isotope data and whole-rock potassium-argon ages of the Nikolai Greenstone, McCarthy quadrangle, Alaska: U.S. Geological Survey Open-File Report 802019, 31 p.

Sillitoe, R.H., Halls, C., and Grant, J.N., 1975, Porphyry tin deposits in Bolivia: Economic Geology, v. 70, p. 913–927.

Sinclair, W.D., 2007, Porphyry deposits, *in* Goodfellow, W.D., ed., Mineral Deposits of Canada—A Synthesis of Major Deposit-Types, District Metallogeny, the Evolution of Geological Provinces, and Exploration Methods: Geological Association of Canada, Mineral Deposits Division, Special Publication No. 5, p. 223–243.

Sinclair, W.D., Kooiman, G.J.A., Martin, D.A., and Kjarsgaard, I.M., 2006, Geology, geochemistry and mineralogy of indium resources at Mount Pleasant, New Brunswick, Canada: Ore Geology Reviews, v. 28, no. 1, p. 123–145.

Singer, D.A., 1993, Basic concepts in three-part quantitative assessments of undiscovered mineral resources: Nonrenewable Resources, v. 2, no. 2, p. 69–81.

Singer, D.A., 2007, Estimating amounts of undiscovered mineral resources, *in* Briskey, J.A., and Schulz, K.J., eds., Proceedings for a workshop on deposit modeling, mineral resource assessment, and their role in sustainable development: U.S. Geological Survey Circular 1294, p. 79–84.

Singer, D.A., and Menzie, W.D., 2010, Quantitative mineral resource assessments—An integrated approach: Oxford, United Kingdom, Oxford University Press, 232 p.

Skirrow, R.G., Jaireth, Subhash, Huston, D.L, Bastrokov, E.N., Schofield, Anthony, van der Wielen, S.E., and Barnicoat, A.C, 2009, Urnaium mineral systems—Processes, exploarion criteria and a dew deposit framework: Geoscience Australia Record 2009/20, 44 p,

Slack, J.F., Till, A.B., Belkin, H.E., and Shanks, W.C.P., III, 2014, Late Devonian-Mississippian(?) Zn-Pb(-Ag-Au-Ba-F) deposits and related aluminous alteration zones in the Nome Complex, Seward Peninsula, Alaska, *in* Dumoulin, J.A., and Till, A.B., eds., Reconstruction of a Late Proterozoic to Devonian continental margin sequence—Its paleogeographic significance, and contained base-metal sulfide deposits: Geological Society of America Special Paper 506, p. 173–212.

Slingerland, R., and Smith, N.D., 1986, Occurrence and formation of water-laid placers: Annual Review of Earth and Planetary Sciences, v. 14, no. 1, p. 113–147.
Smith, A.G., 2009, Neoproterozoic timescales and stratigraphy: Geological Society of London SPecial Publications, v. 326, p. 27-54.
Solie, D.N., 1983, The Middle Fork plutonic complex, McGrath A-3 quadrangle, southwest Alaska: Alaska Division of Geological & Geophysical Surveys Report of Investigations 83-16, 20 p.
Solie, D., Bundtzen, T., Bowman, N., and Cruse, G., 1993, Land selection unit 18 (Melozitna, Ruby, Nulato, and Kateel River quadrangles)—References, DGGS sample locations, geochemical and major oxide data: Alaska Division of Geological & Geophysical Surveys Public-Data File 93-18, 20 p., scale 1:250,000.
Staatz, M.H., 1978, I and L uranium and thorium vein system, Bokan Mountain, southeastern Alaska: Economic Geology, v. 73, p. 512–523.
Staatz, M.H., 1981, Thorianite from the Hogatza placer, Alaska: U.S. Geological Survey Professionsal Paper 1161–Y, p. Y1–Y2.
Staatz, M.H., 1983, Geology and description of thorium and rare-earth deposits in the southern Bear Lodge Mountains, northeastern Wyoming: U.S. Geological Survey Professional Paper 1049–D, 52 p.
Staatz, M.H., 1992, Descriptive model of thorium-rare-earth veins, *in* Bliss, J.D., ed., Developments in mineral deposit modeling: U.S. Geological Survey Bulletin 2004, p. 13–15.
Staatz, M.H., Sharp, B.J., and Hetland, D.L., 1979, Geology and thorium resources of the Lemhi Pass thorium district, Idaho and Montana: U.S. Geological Survey Professional Paper 1049–A, 90 p.
Still, J.C., 1984, Copper, gold, platinum, and palladium sample results from the Klukwan mafic/ultramafic complex, Southeast Alaska: U.S. Bureau of Mines Open-File Report 84-21, 53 p.
Still, J.C., Hoekzema, R.B., Bundtzen, T.K., Gilbert, W.G., Wier, K.R., Burns, L.E., and Fechner, S.A., 1991, Economic geology of Haines-Klukwan-Porcupine area, southeastern Alaska: Alaska Division of Geological & Geophysical Surveys Report of Investigation 91-4, 156 p.
Stoiber, R.E., and Davidson, E.S., 1959, Amygdule mineral zoning in the Portage Lake Lava Series, Michigan copper district: Economic Geology, v. 54, p. 1250–1277, 1444–1460.
Surdam, R.C., 1968, Origin of native copper and hematite in the Karamutssen Group, Vancouver Island, B.C.: Economic Geology, v. 63, p. 961–966.
Swanson, S.E., Newberry, R.J., Coulter, G.A., and Dyehouse, T.M., 1990, Mineralogical variation as a guide to the petrogenesis of the tin granites and related skarns, Seward Peninsula, Alaska, *in* Stein, H.J., and Hannah, J.L., eds., Ore-bearing granite systems—Petrogenesis and mineralizing processes: Geological Society of America Special Paper 246, p. 143–160.
Sweetapple, M.T., and Collins, P.L.F., 2002, Genetic framework for the classification and distribution of Archean rare metal pegmatites in the North Pilbara Craton, Western Australia: Economic Geology, v. 97, no. 4, p. 873–895.
Szumigala, D.J., and Werdon, M.B., 2011, Rare earth elements—A brief overview including uses, worldwide resources and known occurrences in Alaska: Alaska Division of Geological & Geophysical Surveys Information Circular 61, 12 p.
Taggart, J.E., ed., 2002, Analytical methods for chemical analysis of geologic and other materials: U.S. Geological Survey Open-File Report 02–223, variously paged, http://pubs.usgs.gov/of/2002/ofr-02-0223/.
Taylor, B.E., 2007, Epithermal gold deposits, *in* Goodfellow, W.D., ed., Mineral Deposits of Canada—A Synthesis of Major Deposit-Types, District Metallogeny, the Evolution of Geological Provinces, and Exploration Methods: Geological Association of Canada, Mineral Deposits Division, Special Publication No. 5, p. 113–139.
Taylor, R.B., and Steven, T.A., 1983, Definition of mineral resource potential: Economic Geology, v. 78, p. 1268–1270.

Taylor, R.D., Hammarstrom, J.M., Piatak, N.M., and Seal, R.R., II, 2012, Arc-related porphyry molybdenum deposit model, chap. D *of* Mineral deposit models for resource assessment: U.S. Geological Survey Scientific Investigations Report 2010–5070–D, 64 p., http://pubs.usgs.gov/sir/2010/5070/d/.

Taylor, S.R., and McLennan, S.M., 1995, The geochemical evolution of the continental crust: Reviews of Geophysics, v. 33, no. 2, p. 241–265.

Theodore, T.G., 1986, Descriptive model of porphyry Mo, low-F, *in* Cox D.P., and Singer, D.A., eds., Mineral deposit models: U.S. Geological Survey Bulletin 1693, p. 120.

Thompson, T.B., 1988, Geology and uranium-thorium mineral deposits of the Bokan Mountain granite complex, southeastern Alaska: Ore Geology Reviews, v. 3, no. 1, p. 193–210.

Thompson, T.B., 1997, Uraniuim, thorium, and rare metal deposits of Alaska, *in* Goldfarab, R.J., and Miller, L.D., eds., Mineral deposits of Alaska: Economic Geology Monograph 9, p. 466–482.

Thorne, R.L., and Wells, R.R., 1956, Studies of the Snettisham magnetite deposit, southeastern Alaska: U.S. Bureau of Mines Report of Investigations 5195, 41 p.

Till, A.B., Dumoulin, J.A., Ayuso, R.A., Aleinikoff, J.N., Amato, J.M., Slack, J.F., and Shanks, W.C.P., III, 2014, Reconstruction of an early Paleozoic continental margin based on the nature of protoliths in the Nome Complex, Seward Peninsula, Alaska, *in* Dumoulin, J.A., and Till, A.B., eds., Reconstruction of a Late Proterozoic to Devonian continental margin sequence, northern Alaska—Its paleogeographic significance, and contained base-metal sulfide deposits: Geological Society of America Special Paper 506, p. 1–28.

Till, A.B., Dumoulin, J.A., Harris, A.G., Moore, T.E., Bleick, H.A., and Siwiec, B.R., 2008, Preliminary integrated geologic map databases for the United States—Digital data for the geology of the southern Brooks Range, Alaska: U.S. Geological Survey Open-File Report 2008–1149, 88 p., http://pubs.usgs.gov/of/2008/1149/.

Till, A.B., Dumoulin, J.A., Werdon, M.B., and Bleick, H.A., 2011, Bedrock geologic map of the Seward Peninsula, Alaska, and accompanying conodont data: U.S. Geological Survey Scientific Investigations Map 3131, 2 sheets, scale 1:500,000, pamphlet 75 p., http://pubs.usgs.gov/sim/3131/.

Tolstykh, N.D., Foley, J.Y., Sidorov, E.G., and Laajoki, K.V.O., 2002, Composition of the platinum-group minerals in the Salmon River placer deposit, Goodnews Bay, Alaska: Canadian Mineralogist, v. 40, no. 2, p. 463–471.

Tolstykh, N.D., Siderov, E.G., and Kozlov, A.P., 2004, Platinum-group minerals in lode and placer deposits associated with Ural-Alaskan-type Gal'moenan Complex, Koryak-Kamchatka platinum belt, Russia: Canadian Mineralogist, v. 42, p. 619–630.

Turner-Peterson, C.E., and Hodges, C.A., 1986, Descriptive model of sandstone U, *in* Cox, D.P., and Singer, D.A., eds., Mineral deposit models: U.S. Geological Survey Bulletin 1693, p. 209–210.

Upton, B.G.J., Emeleus, C.H., Heaman, L.M., Goodenough, K.M., and Finch, A.A., 2003, Magmatism of the mid-Proterozoic Gardar Province, South Greenland—Chronology, petrogenesis and geological setting: Lithos, v. 68, no. 1, p. 43–65.

U.S. Department of Energy, 2010, Critical materials strategy: U.S. Department of Energy report, 170 p., accessed July 5, 2011, at http://www.energy.gov/news/documents/criticalmaterialsstrategy.pdf.

Van der Poel, W.I., and Hinderman, T.K., 2000, Summary report on lode platinum exploration, Goodnews Bay, Alaska: Calista Native Corporation Technical Report on Goodnews Bay, Alaska, 15 p.

Van Gosen, B.S., Fey, D.L., Shah, A.K., Verplanck, P.L., and Hoefen, T.M., 2014, Deposit model for heavy-mineral sands in coastal environments: U.S. Geological Survey Scientific Investigations Report 2010–5070–L, 51 p., http://pubs.usgs.gov/sir/2010/5070/l/.

Van Treeck, C.J., 2009, Platinum group element enriched hydrothermal magnetite of the Union Bay Alaska-type ultramafic intrusion, Southeast Alaska: Fairbanks, University of Alaska, M.S. thesis, 188 p.
Vasyukova, Olga, and Williams-Jones, A.E., 2014, Fluoride–silicate melt immiscibility and its role in REE ore formation—Evidence from the Strange Lake rare metal deposit, Québec-Labrador, Canada: Geochimica et Cosmochimica Acta, v. 139, p. 110–130.
Verplanck, P.L., Van Gosen, B.S., Seal, R.R., and McCafferty, A.E., 2014, A deposit model for carbonatite and peralkaline intrusion-related rare earth element deposits: U.S. Geological Survey Scientific Investigations Report 2010–5070–J, 58 p., http://pubs.usgs.gov/sir/2010/5070/j/.
Wall, F., 2013, Rare earth elements, *in* Gunn, G., ed., Critical Metals Handbook: Oxford, United Kingdom, J.Wiley & Sons, p. 312–339.
Warner, J.D., and Barker, J.C., 1989, Columbium- and rare-earth element-bearing deposits at Bokan Mountaiin, Southeast Alaska: U.S. Bureau of Mines Open-File Report 33-89, 196 p.
Warner, J.D., Dahlin, D.C., and Brown, L.L., 1988, Tin occurrences near Rocky Mountain (Lime Peak) east-central Alaska: U.S. Bureau of Mines Information Circular 9180, 24 p.
Warner, J.D., Mardock, C.L., and Dahlin, D.C., 1986, A columbium-bearing regolith on Upper Idaho Gulch, near Tofty, Alaska: U.S. Bureau of Mines Information Circular 9105, 29 p.
Wedow, Helmuth, White, M.G., and Moxham, R.M., 1951, interim report on an appraisal of the uranium possibilities of Alaska: U.S. Geological Survey Open-File Report 52–165, 124 p.
Wenrich, K.J., 1985, Mineralization of breccia pipes in northern Arizona: Economic Geology, v. 80, no. 6, p. 1722–1735.
Werner, A.B.T., Sinclair, W.D., and Amey, E.B., 1998, International strategic minerals issues summary report-tungsten: U.S. Geological Survey Circular 930–O, 71 p.
West, W.S., and Benson, P.D., 1955, Investigations for radioactive deposits in southeastern Alaska: U.S. Geological Survey Bulletin 1024–B, 33 p.
Whalen, J.B., Anderson, R.G., Struik, L.C., and Villeneuve, M.E., 2001, Geochemistry and Nd isotopes of the François Lake plutonic suite, Endako batholith—Host and progenitor to the Endako molybdenum camp, central British Columbia: Canadian Journal of Earth Sciences, v. 38, no. 4, p. 603–618.
Whalen, J.B., Currie, K.L., and Chappell, B.W., 1987, A-type granites—Geochemical characteristics, discrimination and petrogenesis: Contributions to Mineralogy and Petrology, v. 95, no. 4, p. 407–419.
White, M.G., and West, W.S., 1953, Reconnaissance for uranium in the Lost River area, Seward Peninsula, Alaska, 1951: U.S. Geological Survey Circular 319, 4 p.
White, W.H., Bookstrom, A.A., Kamilli, R.J., Ganster, M.W., Smith, R.P., Ranta, D.E., and Steininger, R.C., 1981, Character and origin of Climax-type molybdenum deposits, *in* Skinner, B.J., ed., Economic Geology Seventy-fifth Anniversary Volume, 1905–1980: Lancaster, Pa., The Economic Geology Publishing Co., p. 270–316.
Wilson, F.H., Hults, C.P., Mull, C.G., and Karl, S.M., compilers, 2015, Geologic map of Alaska: U.S. Geological Survey Scientific Investigations Map 3340, 2 sheets, scale 1:1,584,000, pamphlet 196 p., http://dx.doi.org/10.3133/sim3340.
Winchester, J.A., and Floyd, P.A., 1977, Geochemical discrimination of different magma series and their differentiation products using immobile elements: Chemical Geology, v. 20, p. 325–343.
Winter, J.D., 2001, An introduction of igneous and metamorphic petrology: Prentice Hall, N.J., 697 p.
Yang, K.-F., Fan, H.-R., Santosh, M., Hu, F.-F., and Wang, K.-Y., 2011, Mesoproterozoic carbonatitic magmatism in the Bayan Obo deposit, Inner Mongolia, North China—Constraints for the mechanism of super accumulation of rare earth elements: Ore Geology Reviews, v. 40, no. 1, p. 122–131.
Yeend, W.E., 1986, Descriptive model of placer Au-PGE, *in* Cox, D.P., and Singer, D.A., eds., Mineral deposit models: U.S. Geological Survey Bulletin 1693, p. 261–263.

Yefimov, A.V., Borodayev, Yu.S., Mozgova, N.N., and Nenasheva, S.N., 1990, Bismuth mineralization of the Akchatau molybdenum-tungsten deposit, central Kazakhstan: International Geology Review, v. 32, no. 10, p. 1017–1027.

Yuan Zhongxin, Bai Ge, Wu Chenyu, Zhang Zhongqin, and Ye Xianjiang, 1992, Geological features and genesis of the Bayan Obo REE ore deposit, Inner Mongolia, China: Applied Geochemistry, v. 7, p. 429–442.

Zientek, M.L., 2012, Magmatic ore deposits in layered intrusions—Descriptive model for reef-type PGE and contact-type Cu-Ni-PGE deposits: U.S. Geological Survey Open-File Report 2012–1010, 49 p., http://pubs.usgs.gov/of/2012/1010/.

Zientek, M.L., Causey, J.D., Parks, H.L., and Miller, R.J., 2014, Platinum-group elements in southern Africa—Mineral inventory and an assessment of undiscovered mineral resources: U.S. Geological Survey Scientific Investigations Report 2010–5090–Q, 126 p., http://pubs.usgs.gov/sir/2010/5090/q/.

Zientek, M.L., Cooper, R.W., Corson, S.R., and Geraghty, E.P., 2002, Platinum-group element mineralization in the Stillwater Complex, Montana, *in* Cabri, L.J., ed., The geology, geochemistry, mineralogy and mineral beneficiation of platinum-group elements: Canadian Institute of Mining, Metallurgy and Petroleum Special Volume 54, p. 459–481.

Table 1. Mineral deposit groups and types in Alaska that were considered in this study, as well as their commodities, characteristics, representative localities, and references.

[Abbreviations: PGE, platinum group elements; REE, rare earth elements. --, not available]

Mineral deposit group	Commodities (critical elements in bold)	Deposit types	World examples	Alaska deposits[5] and occurrences	Ore deposit model references	Deposit and occurrence references[6]
REE-Th-Y-Nb(-U-Zr) deposits associated with peralkaline to carbonatitic igneous rocks	**REE, Th,** Y, **Nb**, U, Zr	Carbonatite	Bayan Obo, China; Mount Weld, Australia; Mountain Pass, California; Bull Hill, Wyoming	Tofty	Model 16 *in* Eckstrand (1985); model 10 *in* Cox and Singer (1986); Notholt and others (1990); Berger and others (2009); Verplanck and others (2014)	Yang and others (2011); Middlemost (1990); Castor (2008); Reifenstuhl and others (1998); Staatz (1983)
		Alkaline intrusive	Thor Lake, Canada; Lovozero, Russia	Windy Fork, Ruby batholith, Darby Mountains	Long and others (2010); Verplanck and others (2014)	Sheard and others (2012); Kogarko and others (2010); Barker (1991); Arth and others (1989a,b); Foley and Barker (1986)
		Syenite or peralkaline granite REE-Zr-U-Nb	Strange Lake, Canada; Ilimaussaq, Greenland; Norra Kärr, Sweden	Bokan Mountain*, Dora Bay, Roy Creek	Linnen and others (2014); Verplanck and others (2014)	Vasyukova and Williams-Jones (2014); Upton and others (2003); Bluemel and others (2013); Dostal and others
		Thorium-REE veins	Lemhi Pass, Idaho-Montana	Roy Creek, Dotson sheeted vein/dike system at Bokan Mountain	Staatz and others (1979); Staatz (1992); Bliss (1992)	Staatz and others (1979); Dostal and others (2014)
		Plutonic-volcanic U-REE	Nopal, Mexico; Rexspar, Canada	Selawik Hills, Sischu Mountain	Cox and Singer (1986)	Angiboust and others (2012); Preto (1978); Barker (1985); Miller and others (1980)
Placer and paleoplacer Au	Au, **PGE**, Ag, **Sn, W**, Cr, **Ti**	Alluvial placer	Castlemaine, Victoria, Australia	Fairbanks, Valdez Creek	Model 39a *in* Cox and Singer (1986)	Bierlein and Maher (2001); Nokleberg and others (1987); Reger and Bundtzen (1990)
		Alluvial paleoplacer	Ballarat, Victoria, Australia	Tofty district	Frimmel and others (2005)	Phillips and Hughes (1996); Garnett and Bassett (2005)
		Coastal placer	Richards Bay, South Africa	Nome	Model 39c *in* Cox and Singer (1986)	Van Gosen and others (2014); Nelson and Hopkins (1972)
PGE(-Co-Cr-Cu-Ni-Ti-V) deposits associated with mafic to ultramafic igneous rocks	**PGE**, Co, Cr, Cu, Ni, Ti, **V**	Alaska-Ural type PGE	Nizhny Tagil, Russia	Goodnews Bay, Union Bay	Model 9 *in* Cox and Singer (1986)	Naldrett (2004); Tolstykh and others (2002); Van der Poel and Hinderman (2000); Van Treeck (2009)
		Duluth-Noril'sk Cu-Ni-PGE	Noril'sk, Russia; Wellgreen, Yukon, Canada	Spirit Mountain (ARDF VA 080)*	Models 5a, 5b *in* Cox and Singer (1986); Zientek (2012)	Li and others (2009); Hulbert (1997); Herreid (1970)
		Synorogenic-synvolcanic Ni-Cu-PGE	Selebi-Phikwe, Botswana	Brady Glacier	Models 5a, 5b *in* Cox and Singer (1986); Schulz and others (2010)	Barnes and Lightfoot (2005); Himmelberg and Loney (1981)
		Fe-Ti-V-rich mafic to ultramafic rocks that have PGE (see also, table 6)	--	Klukwan, Snettisham	--	Still (1984); Thorne and Wells (1956)
Carbonate-hosted Cu(-Co-Ag-Ge-Ga) deposits	Cu, Ag	Kennecott type; related to basaltic copper	Keweenawan native-copper district, Michigan	Kennecott veins*	Model 10 *in* Eckstrand (1985); model 23 *in* Cox and Singer (1986)	MacKevett and others (1997): Price and others (2014)
	Cu, **Co, Ge, Ga**	Kipushi type	Kipushi, Democratic Republic of Congo; Tsumeb, Namibia	Ruby Creek*	Model 32c *in* Cox and Singer (1986)	Kampunzu and others (2009); Kamona and Günzel (2007); Schneider and others (2007)
Sandstone-hosted U(-V-Cu) deposits	U, **V,** Cu	Roll-front	Shirley Basin district, Wyoming	--	Model 30c *in* Cox and Singer (1986)	Harshman (1972)
		Tabular	Grants Belt, New Mexico; Uravan district, Colorado	--	Model 30c *in* Cox and Singer (1986)	Northrop and others (1990)
		Basal	Okanagan highlands, British Columbia, Canada	Death Valley (Boulder Creek)*	Model 6.4 *in* Eckstrand (1985)	Boyle (1982)
		Tectono-lithologic	Orphan mine, Arizona	--	Model 32e *in* Bliss (1992)	Wenrich (1985)
Sn-W-Mo(Ta-In-fluorspar) deposits associated with specialized granites	**Sn, W, Mo, F, In, Ta**	Sn-porphyry, -greisen, -skarn	Podlesi, Czech Republic; Beauvoir, France; Chlorolque, Bolivia; Macusani, Peru; Moina, Australia; Cinovec, Czech Republic; Akchatau and Kara Oba, Kazakhstan	Ruby batholith, Rocky Mountain, Mount Prindle, Groundhog Basin; Lost River*, Kougarok*, Sleitat*, Sithylemenkat	Grant and others (1980); models 14b, 15c *in* Cox and Singer (1986); Kwak (1987);	Černý and others (2005); Raimbault and others (1995); Hudson and Arth (1983); Newberry and others (1990); Newberry and Brew (1989); Kwak and Askins (1981); Yefimov and others (1990); Dobson (1982); Puchner (1986); Hudson and Reed (1997); Barker and Foley (1986)
		Sn-veins, Sn-polymetallic veins, pegmatites	Wodgina, Australia; Tanco, Canada	Waterpump Creek*,Won, McIntyre, Groundhog Basin*	Models 15b, 20b *in* Cox and Singer (1986)	Sweetapple and Collins (2002); Černý and others (2005); Flanigan (1998); Burleigh (1992a,b); Reifenstuhl and others (1998); Newberry and Brew (1989)
		W-skarn, -porphyry, -greisen, -vein	Pine Creek, California; Mactung, Canada; Mount Pleasant, Canada; Panasqueira, Portugal	Stepovich*, Spruce Hen*, Tanana*, Gillmore Dome	Models 14a, 15a *in* Cox and Singer (1986); Kwak (1987)	Kelly and Rye (1979); Kooiman and others (1986); Newberry and others (1990); Barker and Swainbank (1986)
		Climax-type Mo	Climax, Henderson, Colorado	Bear Mountain	Model 16 *in* Cox and Singer (1986); Seedorff and others (2005); Ludington and Plumlee (2009)	White and others (1981); Barker and Swainbank (1986)
		Porphyry Mo, low-F	Endako, Canada	Quartz Hill*, Nunatak	Model 21b *in* Cox and Singer (1986); Ludington and others (2009)	Whalen and others (2001); Ashleman and others (1997); Kimball and others (1978)

[5] Deposits indicated by an asterisk (*) are localities that have reported inventory or past production.

[6] References in this column contain maps or coordinates for specific deposits, occurrences, and (or) prospects worldwide and in Alaska. References are in the same order as localities listed in previous two columns.

Table 2. Scoring template for analysis of REE-Th-Y-Nb(-U-Zr) potential within each HUC in Alaska.

[Abbreviations: ADGGS, Alaska Division of Geological & Geophysical Surveys database; AGDB2, Alaska Geochemical Database, Version 2.0; AM, analytical method; ARDF, Alaska Resource Data File; ES_SQ, semiquantitative emission spectroscopy; Fe#, (FeO/[FeO + MgO]); HFSE, high field strength elements; HMC, heavy-mineral concentrate; HREE, heavy rare earth elements; HUC, hydrologic unit code; LREE, light rare earth elements; MALI, modified alkali-lime index; NURE, National Uranium Resource Evaluation database; pct, weight percent; ppm, concentration in parts per million; REE, rare earth elements. Components shown as "MALI displacement" indicate a MALI deviation from a published geochemical threshold; components shown as "Fe# displacement" indicate an Fe# deviation from a published geochemical threshold]

Category	Dataset/layer	Component	Selection and score
ARDF records	ARDF	REE model keywords[1]	3 points if REE keyword total score >21 2 points if REE keyword total score >9 *and* ≤21 1 point if REE keyword total score >3 *and* ≤9
Igneous-rock-sample geochemical data[2]	AGDB2 + ADGGS + literature	MALI displacement[3]	1 point if MALI value >0 *and* SiO_2 pct >56
		10,000×Ga/Al[4]	1 point if 10,000Ga/Al >2.6 *and* SiO_2 pct >60
		Fe# displacement[5]	1 point if Fe# displacement >0.05
		Nb/Y	1 point if Nb/Y ≥1
Lithology	Geologic map of Alaska (Wilson and others, 2015)	Alkaline granitic rocks, major component	1 point if present
Sediment-sample geochemical data[6]	AGDB2 + ADGGS + NURE	HFSE proxy element	1 point if Nb ppm ≥17.01 (≥91st percentile)
		LREE proxy element	2 points if Ce ppm ≥175 (≥98th percentile) 1 point if Ce ppm ≥105 *and* <175 (≥91st *and* <98th percentile)
		HREE proxy element	2 points if Yb ppm ≥8.7 (ppm ≥98th percentile) 1 point if Yb ppm ≥5.7 *and* <8.7 (≥91st *and* <98th percentile)
		Thorium	1 point if Th ppm ≥14 (≥91st percentile)
Heavy-mineral-concentrate-sample data	AGDB2—HMC mineralogy[7]	REE-bearing mineral	3 points if columbite, cyrtolite, or xenotime is present
		REE indicator mineral	2 points if monazite, fluorite, thorite, uranothorite, uraninite, or Th-rich mineral is present
		HFSE mineral	1 point if allanite or zircon is present
	AGDB2—HMC geochemical data[8]	HFSE proxy elements	1 point if Nb ppm >200 1 point if Th ppm >272 *and* Th ppm AM ≠ 'ES_SQ' 1 point if Th ppm >300 *and* Th ppm AM = 'ES_SQ'
		LREE proxy element	1 point if Ce ppm >1,210 *and* Ce ppm AM ≠ 'ES_SQ' 1 point if Ce ppm >5,000 *and* Ce ppm AM = 'ES_SQ'
		HREE proxy element	1 point if Yb ppm >45 *and* Yb ppm AM ≠ 'ES_SQ' 1 point if Yb ppm >60 *and* Yb ppm AM = 'ES_SQ'
Aeroradiometric data[9]	Aerial gamma-ray survey data	Th/K	2 points if Th/K >12 1 point if Th/K >5 *and* ≤12

[1]See appendix C for a list of REE keywords and the scoring template for ARDF records; maximum single score for a HUC contributes to the total score.

[2]Igneous-rock-sample geochemical-data scores are additive, for a possible total score of 4 for each HUC.

[3]Score applied only to igneous-rock samples that have SiO_2 weight percent >56.

[4]10,000Ga/Al scores applied only to igneous-rock samples that have SiO_2 weight percent >60.

[5]Calculated using the Fe# versus SiO_2 array proposed by Frost and Frost (2008).

[6]Maximum single score for each element in a HUC is used. Element scores are additive, for a possible total score of 6 points.

[7]Maximum possible score is 3 points.

[8]Maximum possible score is 3 points.

[9]Mean score for each HUC contributes to the total score. Data from Duval (2001).

Table 3. Mineral resource potential versus certainty classification matrix for REE-Th-Y-Nb(-U-Zr) deposits in Alaska.

[Abbreviations: c, certainty; HUC, hydrologic unit code; p, potential; REE, rare earth elements]

REE-Th-Y-N-(-U-Zr)	Estimated certainty[1,2]				
	Low	Medium	High		
Unknown (Total score = 0 *and* no sediment samples in HUC *or* aerial gamma-ray survey is only dataset represented *and* no sediment samples in HUC)	Total score ≥7 (p) 1–2 datasets not null (c)	Total score ≥7 (p) 3–4 datasets not null (c)	Total score ≥7 (p) 5 datasets not null *or* Total score = 0 (c)	High	Estimated potential[1]
	Total score 3–6 (p) 1–2 datasets not null (c)	Total score 3–6 (p) 3–4 datasets not null (c)	Total score 3–6 (p) 5 datasets not null *or* Total score = 0 (c)	Medium	
	Total score 0–2 (p) 1–2 datasets not null (c)	Total score 0–2 (p) 3–4 datasets not null (c)	Total score 0–2 (p) 5 datasets not null *or* Total score = 0 (c)	Low	

[1]Abbreviations (p) and (c) in cells denote which components contribute to assignment of *potential* and *certainty*, respectively.

[2]Lithology dataset is used to calculate *potential*, but not *certainty*.

Table 4. Scoring template for analysis of placer and paleoplacer Au potential within each HUC in Alaska.

[Abbreviations: ARDF, Alaska Resource Data File; AGDB2, Alaska Geochemical Database, Version 2.0; ADGGS, Alaska Division of Geological & Geophysical Surveys database; HUC, hydrologic unit code; NURE, National Uranium Resource Evaluation database; NHD, National Hydrography Dataset; PLACER_TOTAL, total score from keywords in ARDF records; ppm, concentration in parts per million]

Category	Dataset/layer	Component	Selection and score
ARDF records	ARDF	Placer model keywords[1]	10 points if PLACER_TOTAL >0 *and* <20 12 points if PLACER_TOTAL ≥20 *and* <26 14 points if PLACER_TOTAL ≥26 *and* <35 16 points if PLACER_TOTAL ≥35 *and* <40 18 points if PLACER_TOTAL ≥40 *and* <50 20 points if PLACER_TOTAL ≥50
Heavy-mineral-concentrate-sample mineralogy[2]	AGDB2	Gold	10 points if present
		Cassiterite	1 point if present
		Powellite	1 point if present
		Scheelite	1 point if present
		Cinnabar	1 point if present
		Monazite	1 point if present
		Thorite	1 point if present
Sediment-sample geochemical data[3]	AGDB2 + ADGGS + NURE	Au	3 points if Au ppm ≥0.008 (75th percentile)
		Ag	3 points if Ag ppm ≥0.15 (75th percentile)
		Ti	1 point if Ti ppm ≥0.57 (75th percentile)
		W	1 point if W ppm ≥2.0 (75th percentile)
Lithology—igneous[4]	Geologic map of Alaska (Wilson and others, 2015)	Plutonic major component of map unit	3 points if present
		Plutonic minor component of map unit	2 points if present
		Hypabyssal igneous map unit	2 points if present
		Volcanic igneous map unit	1 point if present
		Metaigneous map unit	1 point if present
Lithology—sedimentary[4]	Geologic map of Alaska (Wilson and others, 2015)	Placer and anthropogenic deposits	5 points if present
		High-level gravel	5 points if present
		Older surficial deposits, undivided	3 points if present
Downstream of HUC that has high *potential*[5]	NHD	Medium or low *potential* HUC downstream and adjacent to HUC that has high *potential*	6 points if present
		Low *potential* HUC downstream and adjacent to HUC that has medium *potential*	3 points if present

[1]See appendix C for a list of placer model keywords and the scoring template for ARDF records.

[2]If Au is not null, only use the highest value of 10; otherwise, score is additive for other possible minerals.

[3]Scores are additive, for a maximum possible total score of 8.

[4]If more than one lithologic type is present, only use the type that has the highest value each for igneous and sedimentary. Igneous and sedimentary values are then summed for a total lithology score; maximum possible score is 8.

[5]Downstream analysis excludes HUCs that have high potential; if more than one type of segment is present, only use the type that has the highest value.

Table 5. Mineral resource potential versus certainty classification matrix for placer and paleoplacer Au deposits in Alaska.

[Abbreviations: ARDF, Alaska Resource Data File; c, certainty; HUC, hydrologic unit code; p, potential]

Placer Au	Estimated certainty[1]				
	Low	Medium	High		
Unknown (Total score = 0 *and* no sediment samples in HUC)	ARDF-record score ≥12 *or* heavy-mineral-concentrate score = 10 *or* Total score ≥16 (p) ARDF-record score = 12 or 14 *or* 1–3 datasets not null (c)	ARDF-record score ≥12 *or* heavy-mineral-concentrate score = 10 *or* Total score ≥16 (p) ARDF-record score = 16 *or* 4 datasets not null (c)	ARDF -record score ≥12 *or* heavy-mineral-concentrate score = 10 *or* Total score ≥16 (p) ARDF-record score ≥18 *or* 5 datasets not null (c)	High	Estimated potential[1]
	Total score 6–15 (p) 1–2 datasets not null (c)	Total score 6–15 (p) ARDF-record score = 10 *or* 3–4 datasets not null (c)	Total score 6–15 (p) 5 datasets not null (c)	Medium	
	Total score 1–5 (p) 1–2 datasets not null (c)	Total score 1–5 (p) 3–4 datasets not null (c)	Total score 1–5 (p) *and* 5 datasets not null (c) *or* Total score = 0 *and* sediment data points in HUC (p,c)	Low	

[1]Abbreviations (p) and (c) in cells denote which components contribute to assignment of *potential* and *certainty*, respectively.

Table 6. Platinum group element (PGE) ore deposit types in Alaska that were considered in this study, as well as their representative localities and references.

[Abbreviations: MUM, mafic to ultramafic; PGE, platinum group elements]

PGE deposit models	Example/locations	References
PGE ore deposit models considered in mineral potential evaluation		
Alaska-Ural type	Goodnews Bay, southwestern Alaska; Union Bay, southeastern Alaska	Himmelberg and Loney (1995); Foley and others (1997)
Ophiolites	Angayucham and Tozitna terranes, northern Alaska	Loney and Himmelberg (1989); Patton (1992)
Layered magmatic PGE	Stillwater, Montana	Zientek and others (2002)
Magmatic-sulfide PGE	Wellgreen, Yukon and Fish Lake Complex, Alaska, both in the Wrangellia terrane	Hulbert (1997)
Synorogenic Ni-Cu-PGE	Brady Glacier, Mount Fairweather trend, southeastern Alaska	Czamanske and others (1981); Himmelberg and Loney (1981)
Large-igneous-province/flood-basalt and feeder-zone Ni-Cu-PGE	Norilsk, Russia	Li and others (2009)
	Duluth Complex, Minnesota	Miller and others (2002)
Troctolite-anorthosite-granite-hosted Ni-Cu-Co±PGE	Voisey's Bay, Newfoundland and Labrador, Canada	Naldrett and others (2000)
PGE found with chromite in island-arc crustal sections	Red Mountain, Kenai Peninsula, Alaska	Foley and Barker (1984)
Fe-Ti±V-rich MUM rocks that have PGE	Klukwan, Snettisham, southeastern Alaska	Still and others (1991)
PGE ore deposit models known in Alaska but not factored into mineral potential assessment		
PGE-enriched porphyry Cu-Mo-Au deposits	Pebble, Alaska	Ghaffari and others (2011); Kelley and others (2013)
PGE-enriched composite plutons	Butte Creek, Alaska	Keith and others (1987)
Differentiated igneous complexes	Mentasta Pass, Alaska Range, Alaska	Richter (1967)
PGE-enriched skarns adjacent to PGE-bearing MUM intrusions	Unnamed skarn occurrence, West Fork Rainy Creek, Mount Hayes quadrangle, Alaska	Bittenbender and others (2007)
PGE-bearing placer deposits in unconsolidated sediments	Goodnews Bay, Alaska	Tolstykh and others (2002)
PGE ore deposit models not presently known in Alaska and not optimized for this assessment		
Hydrothermal PGE deposits	New Rambler, Wyoming; Kupferschiefer, Germany	Nyman and others (1990); Piestrzyński and others (2002)
Black shale-hosted PGE	Nick Property, Yukon	Hulbert and others (1992)
Unconformity-related U±Au±PGE	Rum Jungle, Australia	Mernagh and others (1998)
Supergene PGE	Serra Pelada, Brazil	Moroni and others (2001)
Meteorite impacts	Sudbury, Ontario	Ames and others (2008)
Komatiites	Kambalda, Australia	Barnes and others (2013)

Table 7. Scoring template for analysis of PGE(-Co-Cr-Ni-Ti-V) potential within each HUC in Alaska.

[Abbreviations: ADGGS, Alaska Division of Geological & Geophysical Surveys database; AGDB2, Alaska Geochemical Database, Version 2.0; ARDF, Alaska Resource Data File; HUC, hydrologic unit code; MUM, mafic to ultramafic; pct, weight percent; PGE, platinum group elements; ppm, concentration in parts per million;]

Category	Dataset/layer	Component	Selection and score
Lithology[1]	Geologic map of Alaska (Wilson and others, 2015)	MUM rocks, major component	2 points if present
		MUM rocks, minor or incidental component	1 point if present
ARDF records[2]	ARDF	PGE model keywords[3]	3 points if PGE reported as major or minor commodities 2 points if chromite is present and favorable geologic keywords point if permissible geology but no direct evidence for PGE
Heavy-mineral-concentrate-sample mineralogy[2]	AGDB2 + ARDF	ARDF-record placers	3 points if PGE reported as major or minor elements 2 points if chromite or other PGE-related minerals are reported, or uncertain PGE identifications 1 point if mineralogy for MUM rocks is reported in a drainage, but no direct evidence for PGE
		Ore-related mineral	2 points if chromite is present
			2 points if copper cobalt sulfide is present
			2 points if nickel cobalt sulfide is present
			2 points if nickel sulfide is present
		Rock-forming mineral	2 points if chromium nickel silicate is present
			1 point if serpentinite is present
			1 point if chrome diopside is present
		Chalcopyrite	1 point if chalcopyrite is present
Heavy-mineral-concentrate-sample geochemical data[2]	AGDB2	PGE and Co, Cr, Ni, Ti, V	3 points if Ir ppm >0
			3 points if Os ppm >0
			3 points if Pd ppm >0
			3 points if Pt ppm >0
			3 points if Rh ppm >0
			3 points if Ru ppm >0
			2 points if Co ppm >500 1 point if Co ppm >150 *and* ≤500
			2 points if Cr ppm >5,000 1 point if Cr ppm >1,500 *and* ≤5,000
			2 points if Ni ppm >700 1 point if Ni ppm >200 *and* ≤700
			1 point if TiO_2 pct >5.0
			2 points if V ppm >1,500 1 point if V ppm >700 *and* ≤1,500
Sediment-sample geochemical data[2]	AGDB2 + ADGGS + NURE	PGE and Co, Cr, Ni, Yi, V	2 points if Co ppm ≥70 (98th percentile) 1 point if Co ppm ≥36 *and* ≤70 (91st percentile)
			2 points if Cr ppm ≥500 1 point if Cr ppm ≥200 *and* <500
			2 points if Ni ppm ≥150 (98th percentile) 1 point if Ni ppm ≥81 *and* <150 (91st percentile)
			2 points if TiO_2 pct ≥1.11 (98th percentile) 1 point if TiO_2 pct ≥0.7 *and* <1.11 (91st percentile)
			2 points if V ppm ≥455 (98th percentile) 1 point if V ppm ≥269 *and* <455 (91st percentile)
			3 points if Os ppm ≥0.016 (91st percentile)
			3 points if Pd ppm ≥0.009 (91st percentile)
			3 points if Pt ppm ≥0.006 (91st percentile)

Category	Dataset/layer	Component	Selection and score
Rock-sample geochemical data[2]	AGDB2	PGE and Co, Cr, Ni, Ti, V	2 points if Co ppm >200 1 point if Co ppm >100 *and* ≤200
			2 points if Cr ppm >2,000 1 point if Cr ppm >700 *and* ≤2,000
			2 points if Ni ppm >1,500 1 point if Ni ppm >500 *and* ≤1,500
			2 points if TiO_2 pct >3.0 1 point if TiO_2 pct >2.0 *and* ≤3.0
			2 points if V ppm ≥1,000 1 point if V ppm >500 *and* <1,000
			3 points if Ir ppm >0
			3 points if Pd ppm >0.005
			3 points if Pt ppm >0.004
			3 points if Rh ppm >0
			3 points if Ru ppm >0
	ADGGS	PGE and Co, Cr, Ni, Ti, V	2 points if Co ppm >70 1 point if Co ppm >30 *and* ≤70
			2 points if Cr ppm >2,000 1 point if Cr ppm >700 *and* ≤2,000
			2 points if Ni ppm >500 1 point if Ni ppm >50 *and* ≤500
			2 points if TiO_2 pct >3.0 1 point if TiO_2 pct >2.0 *and* ≤3.0
			2 points if V ppm ≥100 1 point if V ppm >50 *and* <100
			3 points if Ir ppm >0
			3 points if Pd ppm >0
			3 points if Pt ppm >0
			3 points if Rh ppm >0
			3 points if Ru ppm >0

[1]Maximum possible score is 2 points.

[2]Maximum possible score is 3 points.

[3]See appendix C for a list of PGE model keywords and the scoring template for ARDF records; maximum possible score is 3 points.

Table 8. Mineral resource potential versus certainty classification matrix for PGE(-Co-Cr-Cu-Ni-Ti-V) deposits in Alaska.

[Abbreviations: ARDF, Alaska Resource Data File; c, certainty; HUC, hydrologic unit code; p, potential; PGE, platinum group elements]

PGE(-Co-Cr-Cu-Ni-Ti-V)	Estimated certainty[1]				
	Low	Medium	High		
Unknown (Total score = 0 *and* no sediment samples in HUC)	Total score >4 1–3 datasets not null (c)	Total score >4 (p) 4–5 datasets not null (c)	ARDF-record score ≥3 *or* Total score >4 (p) ARDF-record score ≥3 *or* 6 datasets not null (c)	High	Estimated potential[1]
	Total score 3–4 (p) 1–2 datasets not null (c)	Total score 3–4 (p) 3–4 datasets not null (c)	Total score 3–4 (p) 5–6 datasets not null (c)	Medium	
	Total score <3 (p) 1–2 datasets not null (c)	Total score <3 (p) 3 datasets not null (c)	Total score <3 (p) 4–6 datasets not null (c)	Low	

[1]Abbreviations (p) and (c) in cells denote which components contribute to assignment of *potential* and *certainty*, respectively.

Table 9. Scoring template for analysis of carbonate-hosted Cu(-Co-Ag-Ge-Ga) potential within each HUC in Alaska.

[Abbreviations: ADGGS, Alaska Division of Geological & Geophysical Surveys database; AGDB2, Alaska Geochemical Database, Version 2.0; ARDF, Alaska Resource Data File; HUC, hydrologic unit code; ppm, concentration in parts per million]

Category	Dataset/Layer	Component	Selection and score
Lithology[1]	Geologic map of Alaska (Wilson and others, 2015)	Carbonate rocks, major component	5 points if area >5 km^2 1 point if area ≤5 km^2
		Carbonate rocks, minor or incidental component	1 point if present
ARDF records[2]	ARDF	Cu-carbonate model keywords[2]	3 points if keyword total score ≥4 1 point if keyword total score >0 *and* <4
Heavy-mineral-concentrate-sample mineralogy[3]	AGDB2	Ore-related mineral	2 points if copper cobalt sulfide minerals are present
			2 points if copper silicate minerals are present
			2 points if copper sulfide and (or) copper oxide minerals are present
			2 points if cuprite is present
			2 points if enargite is present
		Chalcopyrite	1 point if chalcopyrite is present
Sediment-sample geochemical data[4]	AGDB2 + ADGGS + NURE	Cu	2 points if Cu ppm ≥150 (≥98th percentile) 1 point if Cu ppm ≥50 *and* <150 (≥75th percentile *and* <98th percentile)
Sediment-sample trace-element geochemical data	AGDB2 + ADGGS + NURE	Ag, Co, Ge, Ga	1 point if Ag ppm ≥0.4 (≥91st percentile)
			1 point if Co ppm ≥36 (≥91st percentile)
			2 points if Ge ppm ≥3 (≥91st percentile)
			2 points if Ga ppm ≥30 (≥91st percentile)
Rock-sample geochemical data	AGDB2 + ADGGS	Cu in sedimentary or metamorphic rocks	2 points if Cu ppm ≥5,000 1 point if Cu ppm ≥1,000 *and* <5,000
Rock-sample trace-element geochemical data	AGDB2 + ADGGS	Ag, Co, Ge, Ga in sedimentary or metamorphic rocks	1 point if Ag ppm ≥1
			1 point if Co ppm >45
			2 points if Ge ppm ≥3
			2 points if Ga ppm ≥35

[1]Maximum possible score is 5 points.

[2]See appendix C for a list of Cu-carbonate model keywords and the scoring template for ARDF records; maximum possible score is 3 points.

[3]Maximum possible score is 11 points.

[4]Maximum possible score is 2 points.

[5]Maximum possible score is 6 points.

[6]Maximum possible score is 2 points.

[7]Maximum possible score is 6 points.

Table 10. Mineral resource potential versus certainty classification matrix for carbonate-hosted Cu(-Co-Ag-Ge-Ga) deposits in Alaska.

[Abbreviations: c, certainty; HUC, hydrologic unit code; p, potential]

Cu(-Co-Ag-Ge-Ga)	Estimated certainty[1]				
	Low	Medium	High		
Unknown (Total score = 0 *and* no sediment samples in HUC)	Total score ≥8 (p) 1–3 datasets not null (c)	Total score ≥8 (p) 4–5 datasets not null (c)	Total score ≥8 (p) 6–7 datasets not null (c)	High	Estimated potential[1]
	Total score 5–7 (p) 1–3 datasets not null (c)	Total score 5–7 (p) 4–5 datasets not null (c)	Total score 5–7 (p) 6–7 datasets not null (c)	Medium	
	Total score 1–4 (p) 1–3 datasets not null (c)	Total score 1–4 (p) 4–5 datasets not null (c)	Total score 1–4 (p) 6–7 datasets not null (c) *or* Total score = 0 *and* sediment data points in HUC (p,c)	Low	

[1]Abbreviations (p) and (c) in cells denote which components contribute to assignment of *potential* and *certainty*, respectively.

Table 11. Scoring template for analysis of sandstone-hosted U(-V-Cu) potential within each HUC in Alaska.

[Abbreviations: ADGGS, Alaska Division of Geological & Geophysical Surveys database; AGDB2, Alaska Geochemical Database, Version 2.0; ARDF, Alaska Resource Data File; HUC, hydrologic unit code; NURE, National Uranium Resource Evaluation database; ppm, concentration in parts per million]

Category	Dataset/layer	Component	Selection and score
ARDF records	ARDF	ssU model keywords[1]	2 points if ssU model is 'maybe' or 'placer' 4 points if ssU model is 'yes'
Lithology[2]	Geologic map of Alaska (Wilson and others, 2015)	Arkosic sandstone	4 points if present
		Cretaceous to Tertiary sandstone	3 points if present
		Sandstone	2 points if present
		Unconsolidated geologic units within 3-km buffer around sandstone map units	1 point if present
Coal	Map of Alaska's coal resources (Merritt and Hawley, 1986)	Upper Cretaceous to Tertiary coal	2 points if present
		Lower Cretaceous and older coal	1 point if present
Sedimentary-rock-sample geochemical data[3]	AGDB2 + ADGGS + NURE	U	5 points if U ppm ≥40 (98th percentile)
			3 points if U ppm ≥11 *and* <40 (91st percentile)
		V	2 points if V ppm ≥1,500 (98th percentile)
			1 point if U ppm ≥390 and <1,500 (91st percentile)
Sediment-sample geochemical data[3]	AGDB2 + ADGGS + NURE	U	5 points if U ppm ≥21.8 (98th percentile)
			3 points if U ppm ≥6.3 *and* <21.8 (91st percentile)
			1 point if U ppm ≥3.6 *and* <6.3 (75th percentile)
Aeroradiometric data[4]	Aerial gamma-ray survey data	eU (equivalent U in ppm)	2 points if mean U ppm value >5 1 point if mean U ppm value >2 *and* ≤5

[1] See appendix C for a list of ssU keywords and the scoring template for ARDF records.

[2] Lithology scores are for the highest ranking sedimentary lithology present anywhere in a HUC.

[3] Maximum single score for each element in a HUC is used.

[4] Score is based on mean equivalent Uranium (eU) value. Data from Duval (2001).

Table 12. Mineral resource potential versus certainty classification matrix for sandstone-hosted U(-V-Cu) deposits in Alaska.

[Abbreviations: ARDF, Alaska Resource Data File; c, certainty; HUC, hydrologic unit code; p, potential]

ssU	Estimated certainty[1, 2]				
	Low	Medium	High		
Unknown (No sediment-sample- or rock-geochemical data, aeroradiometric data, or ARDF-record data in HUC *or* lithology and coal are only data available)	Total score ≥11 (p) 1–3 datasets not null (c)	Total score ≥11 (p) 4 datasets not null (c)	Total score ≥11 (p) 5–6 datasets not null (c)	High	Estimated potential[1]
	Total score 5–10 (p) 1–3 datasets not null (c)	Total score 6–10(p) 4 datasets not null (c)	Total score 6–10 (p) 5–6 datasets not null (c)	Medium	
	Total score 0–5 (p) 1–3 datasets not null (c)	Total score 0–5 (p) 4 datasets not null (c)	Total score 0–5 (p) 5–6 datasets not null (c)	Low	

[1]Abbreviations (p) and (c) in cells denote which components contribute to assignment of *potential* and *certainty*, respectively.

[2]Certainty scores for HUCs that have high *potential* were reduced by 1 if ARDF-record score = 0.

Table 13. Scoring template for analysis of Sn-W-Mo(-Ta-In-fluorspar) potential within each HUC in Alaska.

[Abbreviations: ADGGS, Alaska Division of Geological & Geophysical Survey database; AGDB2, Alaska Geochemical Database, Version 2.0; AM, analytical method; ARDF, Alaska Resource Data File; ES_SQ, semiquantitative emission spectroscopy; HFSE, high field strength elements; HUC, hydrologic unit code; NURE, National Uranium Resource Evaluation database; pct, weight percent; ppm, concentration in parts per million]

Category	Dataset/Layer	Component	Selection and score
ARDF records	ARDF	Sn-W-Mo-In-Ta-F keywords[1]	3 points if keyword total score ≥20 1 point if keyword total score ≥4 *and* <20
Lithology	Geologic map of Alaska (Wilson and others, 2015)	Granitic rocks	1 point if present
Igneous-rock-sample geochemical data[2]	AGDB2 + ADGGS + literature	Peraluminous[3]	2 points if classified as peraluminous *and* SiO_2 pct >65
		10,000×Ga/Al[4]	2 points if 10,000Ga/Al ≥2.6 *and* SiO_2 pct >65
		High-silica granitic rocks	1 point if SiO_2 pct ≥73
Sediment-sample geochemical data[5]	AGDB2 + ADGGS + NURE	In	1 point if In ppm ≥0.08 (≥91st percentile)
		Mo	3 points if Mo ppm ≥10 (≥98th percentile) 2 point if Mo ppm ≥5 *and* <10 (≥91st percentile and <98th percentile)
		Sn	3 points if Sn ppm ≥19 (≥98th percentile) 2 points if Sn ppm ≥5 *and* <19 (≥91st percentile and <98th percentile)
		Ta	1 point if Ta ppm ≥1 (≥91st percentile)
		W	1 point if W ppm ≥6 (≥91st percentile)
Heavy-mineral-concentrate-sample mineralogy[6]	AGDB2	Sn- or Mo-bearing mineral	3 points if molybdenite, wulfenite, powellite, or cassiterite present
		W-, F-, or In-bearing mineral	2 points if scheelite, wolframite, fluorescent mineral, or fluorite present
		HFSE(Ta)-bearing mineral	1 point if columbite, thorite, or uranothorite present
Heavy-mineral-concentrate-sample geochemical data[7]	AGDB2	In	3 points if In ppm >0.2 (AM ≠ ES_SQ) *or* if In ppm >0 (AM = ES_SQ)
		Mo	3 points if Mo ppm >4 (AM ≠ ES_SQ) *or* if Mo ppm >20 (AM = ES_SQ)
		Sn	2 points if Sn ppm >275(AM ≠ ES_SQ) *or* if Sn ppm >1,000 (AM = ES_SQ)
		Ta	3 points if Ta ppm >29
		W	1 point if W ppm >45 (AM ≠ ES_SQ) *or* if W ppm >500 (AM = ES_SQ)
Aeroradiometric data[8]	Aerial gamma-ray survey data	Thorium[9]	1 point if Th value ≥6 (75th percentile)

[1]See appendix C for a list of Sn-W-Mo-F keywords and the scoring template for ARDF records; maximum single score for a HUC is used as the total score.

[2]Igneous-rock-sample geochemical data scores are additive.

[3]Score applied only to igneous-rock samples that have SiO_2 weight percent >65.

[4]10,000Ga/Al scores applied only to igneous-rock samples that have SiO_2 weight percent >65.

[5]Maximum single score for each element in a HUC is used. Element scores are additive, for a possible total score of 9.

[6]Maximum possible total score is 3.

[7]Maximum possible total score is 3.

[8]Data from Duval (2001).

[9]Apparent Th as ^{208}Thallium (parts per million equivalent thorium).

Table 14. Mineral resource potential versus certainty classification matrix for Sn-W-Mo(-Ta-In-fluorspar) deposits in Alaska.

[Abbreviations: c, certainty; HUC, hydrologic unit code; p, potential]

Sn-W-Mo(-Ta-In-fluorspar)	Estimated certainty[1]				
	Low	Medium	High		
Unknown (Total score = 0 *and* no sediment-sample data points in HUC)	Total score ≥8 (p) 0–2 datasets not null (c)	Total score ≥8 (p) 3–4 datasets not null (c)	Total score >8 (p) 4–5 datasets not null (c)	High	Estimated potential[1]
	Total score 3–7 (p) 0–2 datasets not null (c)	Total score 3–7 (p) 3–4 datasets not null (c)	Total score 3–7 (p) 4–5 datasets not null (c)	Medium	
	Total score 0–2 (p) 0–2 datasets not null (c)	Total score 0–2 (p) 3–4 datasets not null (c)	Total score 0–2 (p) 4–5 datasets not null (c)	Low	

[1]Abbreviations (p) and (c) in cells denote which components contribute to assignment of *potential* and *certainty*, respectively.